Isaac Newton Group, La Palma

OBSERVERS' GUIDE

General Editors: D. Carter, U. Sharan & R.E.S. Clegg

With contributions from:
C.R. Benn, P.S. Bunclark, S.M. Hughes, P.R. Jorden, R.A. Laing S.J. Maddox, W.L. Martin, R.F. Peletier, M. Pettini, D.L. King, R.G.M. Rutten, E. Terlevich, K.P. Tritton, S.W. Unger, N.A. Walton, F.G. Watson & S.P. Worswick

August 1995

The Isaac Newton Group of Telescopes at the Observatorio del Roque de los Muchachos del Instituto de Astrofisica de Canarias is operated by the Royal Greenwich Observatory on behalf of the Particle Physics & Astronomy Research Council (UK) and the Nederlandse Organisatie voor Wetenschappelijke Onderzoek (Netherlands).

Contents

List of Figures

List of Tables

Chapter 1

General information

1.1 Introduction

This guide is about the Isaac Newton Group of Telescopes at the Observatorio del Roque de los Muchachos on the island of La Palma. It describes the telescopes and instruments available, explains how to apply for observing time, how to communicate with and travel to the observatory, and shows what support you can expect before, during and after an observing run.

If you are preparing an application to observe on La Palma or if you have already been allocated observing time, read this manual first. The telescopes and instruments are described in Chapters 2–8. If you need further details consult the user manual for the instrument you have in mind (see section 1.6.2). For up-to-date information and advice, consult the appropriate scientific or technical specialist at Cambridge or La Palma. A list of contact people (Telescope Managers, Instrument and Detector specialists) is kept up to date on the ING information pages of the World-Wide Web. If you have any trouble finding the right person or information you need, contact the La Palma Support Group at Cambridge (see section 1.4.4) whose staff will steer you in the right direction.

Although this guide was up to date when published, more recent documentation may be available — see section 1.6.3 below for a guide to sources of up-to-date information. The LaTeX source of this Guide is available by anonymous ftp from the Cambridge Sun cluster (*ftp.ast.cam.ac.uk*) in the directory */pub/lpinfo/lpguide*.

Any comments on this guide should be sent to the editors at the Royal Greenwich Observatory, Cambridge.

1.2 El Observatorio del Roque de los Muchachos

The Isaac Newton Group of Telescopes (ING) consists of the 4.2-m William Herschel Telescope (WHT), the 2.5-m Isaac Newton Telescope (INT) and the 1.0-m Jacobus Kapteyn Telescope (JKT). The 2.5-m and the 1.0-m telescopes and associated instrumentation began scheduled use by the astronomical community in May 1984, and the 4.2-m telescope in August 1987. This group of telescopes forms part of the Observatorio del Roque de los Muchachos, which also includes the Carlsberg Automatic Meridian Circle (CAMC), the 2.5-m Nordic Optical Telescope, the 50-cm vacuum tower solar telescope and 0.6-m reflector of the Swedish Royal Academy of Sciences and the German gamma-ray array HEGRA. These will be joined by the Italian National Telescope (GALILEO), currently under construction.

The observatory occupies an area of 1.89 square kilometres of the district of Garafía at approximately 2350 m above sea level on the highest peak of the Caldera de Taburiente, an extinct volcano on the island of La Palma. La Palma is one of the westerly islands in the Canary archipelago (see Figures 1.1, 1.2, and 1.3) and the Canary Islands are an autonomous region of the Kingdom of Spain. New geodetic positions for the telescopes, determined in 1993 using a GPS receiver, are given in Table 1.1.

Table 1.1: Geographical coordinates

Telescope	Latitude	Longitude	Ground Floor Height (m)
WHT	28° 45' 38.3" N	17° 52' 53.9" W	2332
INT	28° 45' 43.4" N	17° 52' 39.5" W	2336
JKT	28° 45' 40.1" N	17° 52' 41.2" W	2364
CAMC	28° 45' 36.0" N	17° 52' 56.7" W	2326(*a*)
a (Telescope axis)			

Facilities on site include mechanical and electronic workshops, a VAX cluster running the Starlink software collection, SUN workstations running the Starlink software collection and IRAF, a library and chartroom, dining and catering facilities and comfortable sleeping accommodation. A set of offices is maintained at sea level in the city of Santa Cruz de La Palma, approximately 40 km distant by road.

The observatory site (and its sister on Tenerife, the Observatorio del Teide) is operated by the Instituto de Astrofísica de Canarias. The Isaac Newton Group is operated by the Royal Greenwich Observatory on behalf of the UK Particle Physics & Astronomy Research Council (PPARC) and the Nederlandse organisatie voor wetenschappelijk onderzoek (NWO). A fuller description of the two observatories can be found in a special issue of *Astrophysical Letters and Communications, vol 28, p 45, 1991.*

Figure 1.1: Map of the Canary Islands

Figure 1.2: Map of the island of La Palma

Figure 1.3: Plan of the observatory site

1.3 Weather and Observing Conditions

1.3.1 Weather and Climate

La Palma lies in both the cool northeasterly Canary Current and the northerly trade winds, giving it a sunny climate with year-round moderate temperatures. The sea level climate is Atlantic, with temperatures varying rather little during the year. The average temperature at sea level is approximately 22° C in August and 15° C in January. The average temperature at the Roque is approximately 18° C in summer, 3° C in winter, with a typical daily range of 7° C. Precipitation occurs almost entirely in the winter months (October–April), with snow and ice being common between January and March. Rarely, snowstorms can cause drifts of one metre or more. In the worst conditions there may be delays of several hours or even days in reaching the site while roads are closed.

La Palma occasionally comes under the influence of winds from the Sahara (see La Palma Technical Note 41), bringing very fine clouds of dust in suspension. The months most affected are July and August.

Warm clothing is advisable in all seasons. Lip balm and sunglasses are strongly recommended for the mountain top because of the low humidity and amount of glare from sunlight.

1.3.2 Observing conditions

The results of the original site campaign testing carried out at Fuente Nueva (near the current site of the JKT) for twelve months in 1974-1975 showed that the Observatorio del Roque de los Muchachos is one of the best astronomical sites in the world. Meteorological observations made at every hour of the night indicated that during the testing period 59% of dark hours were photometric and 71% spectroscopic. A photometric hour was defined as an hour within astronomical darkness for which the relative humidity was less than 90 per cent, the average wind speed less than 15 m/s, the zenith extinction in V less than 0.3 magnitudes, and obscuration by cloud less than 5 per cent above 30° elevation and less than 15 per cent above 10° elevation. Hours meeting the above humidity and wind speed restrictions, but with zenith extinction less than 0.5 magnitudes and obscuration less than 50 per cent above 30° elevation, were classified as spectroscopic hours. Other hours were termed unusable.

Analysis of Polar Trail films showed that for 40 per cent of usable hours the seeing was less than or equal to 1 arcsec. Such stable conditions are related to local topography: the mountain has a smooth convex contour facing the prevailing northerly wind and the airflow is comparatively undisturbed. Microthermal tests over a period of six months indicated that seeing conditions are relatively uniform over the whole site. A summary of the results of site testing can be found in an article by Bennet McInnes *(Quarterly Journal of the Royal Astronomical Society, vol 22, p266, 1981)*, and a review of the properties of the site has been published by Paul Murdin *(Vistas in Astronomy, vol 28, p449, 1985)*.

The site testing results have been confirmed by the experience of the first ten years operation of the Isaac Newton Group. In the period 1984-1993, 76 per cent of the dark hours were spectroscopic. Measurements through the INT (which include dome and instrumental effects) indicate that the seeing is subarcsecond for about 50 per cent of the spectroscopic hours: however, no large body of data yet exists of direct measurements of the intrinisic site properties. Occasional measurements of image profiles in very good conditions have yielded typical values of 0.5 - 0.7 arcseconds. The most detailed meteorological records (including extinction) are from the Carlsberg Meridian Circle site. These are available continuously from June 1984 and are published every six months by the Copenhagen University Observatory, the Royal Greenwich Observatory and the Real Instituto y Observatorio de la Armada, San Fernando; they are also stored in the ING information section on the World-Wide Web.

As part of the "half-arcsecond programme", a Differential Image Motion Monitor (DIMM) has been installed on a tower near the WHT. A programme of systematic measurments of seeing inside and outside the WHT dome, combined with improved metorological information will be used to search for the most important internal end external influences on seeing. In order to reduce the internal seeing active cooling of the telescope mirrors and of the oil supply to the telescopes will be undertaken.

Table 1.2 is a summary of clear weather statistics taken from the INT observing log, 1984–1993. Clear weather is expressed as usable (spectroscopic) time as a percentage of astronomical dark hours. Although the number of good nights per month shows a seasonal variation, the greater length of the winter nights means that the number of spectroscopic hours per month is rather uniform throughout the year (see fig 1.4).

Table 1.2: Clear weather and seeing statistics

January	70%	May	81%	September	74%
February	67%	June	94%	October	66%
March	70%	July	95%	November	60%
April	74%	August	95%	December	57%

Typical values of the night sky brightness measured by the JKT are given below. They were measured in good conditions on moonless nights, in magnitudes per square arcsecond. The variation between 1984 and 1989 may be partly due to a correlation with the 11-year Solar cycle.

U: 21.4, *B:* 22.3, *V:* 21.4, *R:* 20.4, *I:* 19.3 (June 1984)
U: 21.0, *B:* 21.8, *V:* 20.8, *R:* 20.4, *I:* 19.4 (Sept 1989)

A flux–calibrated, low resolution night sky (airglow) spectrum is shown in Figure 1.5.

Observing conditions for astronomy on La Palma are protected from artificial light pollution by Parliamentary law according to standards that conform to the recommendations of the IAU. However, emission lines of Hg I

Figure 1.4: Distribution of clear (spectroscopic) hours by month

do appear in the sky spectrum, especially if some dust is present.

Measurements of the distribution of extinction in the *V* band, taken from CAMC observations of 1984–1986, are given in Table 1.3.2.

Table 1.3: V band extinction

		V	<	0.10	2%
0.10	<	V	<	0.20	66%
0.20	<	V	<	0.30	13%
0.30	<	V	<	0.40	8%
0.40	<	V	<	0.50	3%
0.50	<	V			8%

Extinction coefficients remain essentially constant on clear and dusty nights, and colours (*U-B*, *B-V*, *V-R* and *V-I)* are unaffected at the one per cent level. About 2 per cent of the dark hours of the year are rendered unusable because of Sahara dust. There can be temporary anomalies due to volcanic eruptions – see for example *Gemini*, **41**, p8 and **35**, p19 for the effect of the 1991 Mount Pinatubo eruption on La Palma extinction.

Figure 1.5: Flux calibrated night sky spectrum, La Palma

1.4 Communications

1.4.1 Telephone and Telefax (La Palma)

Table 1.4 lists a number of useful telephone numbers on La Palma. The dialling codes required to reach La Palma are as follows:

From outside Spain:	34 22
From inside Spain:	922
From Tenerife province:	Just dial number

For example, to dial the ING's La Palma sea level office from the UK, dial 010-34-22-411005.

There is normally no time-difference between the UK and the Canary Islands, apart from a brief period (usually four or five weeks) in the autumn when a one-hour difference occurs because Britain and Spain do not change from daylight saving time on the same day. The Canary Islands are one hour behind mainland Spain.

Table 1.4: Useful telephone numbers on La Palma

	Telephone No.
Sea level:	
RGO Office (office hours)	41 10 05/48/49
Telefax	41 42 03
Out of hours (emergencies	41 39 45
only: try INT first)	41 65 23
Mountain Top:	
Residencia/Switchboard	40 55 00
JKT control room	40 55 85
INT control room	40 56 40
WHT control room	40 55 59
CAMC Building	40 56 80
Telefax (INT)	40 56 46
Telefax (Residencia)	40 55 01
Hotels:	
Hotel Castillete	42 08 40
Hotel Maritimo	42 02 22
Parador (Hotel)	42 23 40
Hostal Residencia Canarias	41 31 82

1.4.2 Post

The sea level offices in Santa Cruz are in Edificio Tinabana on Calle José Lopez at the corner with Avenida el Puente. They are normally open to visitors from 0830 to 1700 Monday to Thursday and 0830 to 1630 on Friday, but are closed for lunch from 13:00 to 14:00.

The normal postal address is a post office box cleared every working day by office staff; there is a courier service every weekday between the mountain top and the RGO offices at sea level:

Royal Greenwich Observatory
Apartado 321
38780 Santa Cruz de La Palma
Tenerife
Spain

Use the above address for all normal postal services. Certain special services (e.g. courier services) require a street address. Only in these cases, use:

Royal Greenwich Observatory
Edificio Tinabana
Calle José Lopez
38700 Santa Cruz de la Palma
Tenerife
Spain

Letters of a standard size take 7–10 days between the UK and La Palma, and packages that cannot be handled by machine can take months.

1.4.3 Electronic mail

The *INTERNET* site address for the ING is *ing.iac.es* for the Sparc server, and *lpve.ing.iac.es* for the data reduction Vax. The *SPAN* site code is 29146.

1.4.4 Cambridge

UK support for the operation of the Isaac Newton Group of Telescopes is from the Royal Greenwich Observatory headquarters in Cambridge. The postal address is:

Royal Greenwich Observatory
Madingley Road
Cambridge
CB3 0EZ
UK

Telephone: +44 1223 374000; Telefax +44 1223 374700.

Electronic mail: (Internet): *username@ast.cam.ac.uk*
Faxes relating to La Palma support may also be sent to +44 1223 374871.

The La Palma Support Group at Cambridge is the main contact point for all information about La Palma Operations. Current (1995) key members and their usernames are:

Dave Carter	(overall coordination)	Tel 374725	*dxc*
Bill Martin	(schedules & observing)	Tel 374870	*wlm*
Ed Zuiderwijk	(archive)	Tel 374868	*ejz*

1.5 Applying for Observing Time

1.5.1 Apportionment of telescope time

Telescope time on the three Isaac Newton Group Telescopes is shared between two institutions: the UK Particle Physics & Astronomy Research Council (PPARC) and the Instituto de Astrofísica de Canarias of Spain (IAC). These institutions meet formally with other users of the Observatorios del Roque de los Muchachos and del Teide as the International Scientific Committee (Comité Científico Internacional, or CCI). PPARC has made further collaborative arrangements with the Nederlandse organisatie voor wetenschappelijk onderzoek (NWO), The National Board of Science and Technology of Ireland (NBST) and the Dublin Institute for Advanced Studies (DIAS). The way the available observing time is shared between these international partners is the subject of a series of agreements, protocols and minutes summarized below. Figure 1.6 shows the shares of telescope time available to each country.

Spain has at its disposal 20 per cent of the observing time on each of the three telescopes; it is the responsibility of the IAC to make this time available to Spanish institutions and others, via the Comisión para la Asignación de Tiempo (CAT), as described below.

A further 5 per cent of the observing time is for international collaborative programmes between member institutions of the CCI. It is intended that this time shall be used for the study of one, or a few, broad topics each year by several telescopes. This time is allocated annually by the CCI. Further information is available from the secretary of the CCI, currently Campbell Warden at the IAC, La Laguna.

The remaining 75 per cent of the time is at the disposal of the UK. The PPARC has agreed to share this time with foreign institutions under two separate agreements, one with the NWO, the other with the NBST and DIAS. Under the first agreement PPARC and NWO agreed to share this 75 per cent of observing time on all three telescopes in the proportions: 80 per cent PPARC - 20 per cent NWO. The Anglo-Dutch Joint Steering Committee has decided that time should be allocated to astronomers from the two countries by the PPARC Panel for the Allocation of Telescope Time (PATT). However the current procedure is that the Dutch share of this time is allocated by a separate committee, which meets about two weeks before the UK PATT, and the allocations are combined and ratified at the PATT meeting. For this reason the deadline for Dutch applications (an application with a Principal Applicant from a Dutch institution, or who is an Dutch employee under the Joint Programme, or an application with

Figure 1.6: Time allocation on the Isaac Newton Group of Telescopes

Dutch applicants and no UK or Irish applicants) is often some two weeks before that for UK applications.

Under the second agreement, PPARC has made available 27 nights per year of its share on the JKT to the NBST/DIAS. The Irish Advisory Committee for La Palma (AC) set up by the two Irish institutions has decided that proposals by Irish astronomers to take up this allocation of 27 nights per year should also be submitted to PATT. Irish astronomers are not however discouraged from applying for use of the other telescopes of the ING. PATT includes members from institutions in the Netherlands and Ireland; details concerning PATT applications are given below.

All the above agreements envisage that observing time shall be shared equitably over the different seasons of the year and phases of the moon.

1.5.2 Applications for telescope time

Time on the JKT and INT will be offered in units of one week; time on the WHT will be offered in units of one night.

Any astronomer, irrespective of nationality or affiliation, may apply for observing time on the Isaac Newton Group of Telescopes. Astronomers who are working at an institute in one of the partner countries should apply through the route appropriate to the nationality of the institute.

Applications to be considered by the PPARC Panel for the Allocation of Telescope Time (as explained in section 1.5.1, this includes all UK and Irish shares of available telescope time) can be submitted at any time to:

The Executive Secretary
Panel for the Allocation of Telescope Time
Particle Physics & Astronomy Research Council
Polaris House
North Star Avenue
Swindon
SN2 1SZ
UK

Telephone: +44 1793 442027
Telefax: +44 1793 442002

At present PATT allocates time on all PPARC supported telescopes in two semesters, from 1 February to 31 July and from 1 August to 31 January. The corresponding closing dates, by which application forms must have reached Swindon, are the end of September and March respectively. Decisions on time allocations are made on the basis of scientific merit and technical feasibility of the proposed observations, and are normally communicated to the principal investigator 10 to 12 weeks after the closing date. Further details of current arrangements regarding applications are given in the *PATT Newsletter* which is issued twice a year, in September and March. Application forms and related instructions may be obtained from SUN Starlink sites from the directory /star/etc/formload or by writing to the above address.

Irish astronomers should send copies of their applications by the closing dates for PATT proposals, to:

The La Palma Advisory Committee
School of Cosmic Physics
5 Merrion Square
Dublin 2

Telephone +353 1 774321
Telefax: +353 1 682003
E-mail: lpac@dias.ie (Internet)

Dutch astronomers should send one copy of their proposals to:

The Secretary, Programme Committee
NFRA
P.O. Box 2
7990 AA DWINGELOO
The Netherlands

The deadline for Dutch applications is usually two weeks before the PATT deadline, and the form is the same as the PATT form.

Applications to take up the 20 per cent share of telescope time at the disposal of Spain should be submitted to:

Comisión para la Asignación de Tiempo
Instituto de Astrofisíca de Canarias
C/Via Lactea S/N
La Laguna
38200 Tenerife
ISLAS CANARIAS

Telephone number: +34 22 605200
Telefax: +34 22 605210

CAT, like PATT, allocates time on the Isaac Newton Group of Telescopes in two semesters. Its closing dates are similar, namely the last weeks of September and March. Application forms and details of arrangements may be obtained from the above address.

1.5.3 Preparing an application

Formal announcements of the status and availablity of ING telescopes and instruments are made in the PATT Newsletter (see above). Check in the most recent issue, and in the RGO's house journal *Spectrum* for the latest information (see section 1.6.3).
It is possible obtain detailed information about instruments and telescopes from the paper and on-line documentation described in section 1.6.2.
If in any doubt, you are encouraged to discuss your application with the appropriate instrument or detector specialist; lists of these are published occasionally in *Spectrum* and kept up to date via the ING e-mail bulletin and on the ING Information page on the World-Wide Web.

1.5.4 Service Observing Scheme

A service observing scheme is currently operated jointly by PATT and CAT for these instruments:

WHT: ISIS, FOS, UES, LDSS, CCD Imaging

INT: IDS, FOS, CCD imaging

JKT: CCD imaging.

The service scheme is primarily intended for small programmes, e.g. single objects or targets of opportunity, though it may also be appropriate for projects requiring infrequent observations such as long term photometric monitoring. Proposals should be for observations lasting no longer than 3 hours in total. Anything larger should be submitted through the normal PATT or CAT procedure. Service observations will be carried out by a support astronomer, and the data will be sent to the applicant after the observations have been made.
Service requests should be sent to the account *service@mail.ast.cam.ac.uk*. A service proposal form can be obtained by anonymous ftp from the Cambridge

SUN cluster *ftp.ast.cam.ac.uk* where it is held in the directory */service.*

1.6 Preparation for Observing

1.6.1 Support Astronomers

All visiting astronomers are assigned a staff support astronomer to advise them on the optimal way of carrying out their scientific programme. When you are assigned time on La Palma wait for the detailed schedule to be published to see who your support astronomer is. If you are a principal applicant you will get a letter from the La Palma Support Group identifying your support astronomer. It is very important to discuss your observing programme with the support astronomer in advance of your run and confirm the instrumental configuration required; note however that major changes from the programme proposed will not in general be possible.
It is essential that all visiting astronomers discuss their observing requirements with ING or RGO staff well in advance of an observing run, so as to use to the best advantage the facilities available. Users of the ING Telescopes have available a wide range of options in the details of the instrumental set-up. For example, optical elements may be offered with a choice of coatings which maximise efficiency in the wavelength range of interest, CCD systems are offered with a choice of chips with different characteristics, and so on.

1.6.2 Documentation

A complete description of the user documentation system is given in the "La Palma Users' Documentation Guide". In summary, the documentation consists of
a) this Observers' Guide
b) a series of User Manuals
c) a series of Technical Notes

Copies of all the above can be obtained from Bill Martin *(wlm@mail.ast.cam.ac.uk)* at the RGO. The User Manuals provide detailed information on the operation of the telescopes, instruments and detectors, whereas the Technical Notes contain information on a wide range of topics. A full list of current Manuals and Technical Notes is given in Appendix A. Much of the documentation, including manuals for the major instruments is available to users of the World-Wide Web. The documents are held in *Hypertext Markup Language (html)* on the Cambridge and ING Sun clusters. The *Uniform Resource Locator (URL)* for the ING information system on the Cambridge cluster is *http://www.ast.cam.ac.uk/%7Elpinfo/*, and on the ING cluster it is *http://ing.iac.es/*.

1.6.3 Newsletters and up-to-date information

Announcements of the status and availablity of ING telescopes and instruments are made in the PATT Newsletter.

Spectrum, the newsletter of the Royal Observatories, contains up-to-date information on ING telescopes and instruments, as well as highlights of recent results and other topical items. *Spectrum* is published every three months and is distributed widely within the community. If you would like to be included in the mailing list, contact the editor at the RGO, Cambridge.

Up-to-date information is available electronically: the *ING Bulletin* is issued by email only, from La Palma; to receive these bulletins, mail *bulletin@ing.iac.es* or *dxc@ast.cam.ac.uk* to be included in the mailing list for it. The most recent information is kept in the ING information page on the Cambridge World-Wide-Web server, the URL is *http://www.ast.cam.ac.uk/%7Elpinfo/*, or on the ING World-Wide-Web server *http://ing.iac.es/*, or the La Palma Gopher server *gopher://ing.iac.es/*. The information which used to be in the LPINFO account on the Cambridge and La Palma Vax computers has all been transferred to the World-Wide-Web servers.

Your support astronomer will be able to advise you. If in doubt, contact the support astronomy group at Cambridge or La Palma.

1.6.4 Facilities at RGO

Good finding charts and accurate positions of targets and corresponding guide stars (autoguiding facilities are available with most instruments) invariably result in more efficient and trouble-free observing. A range of facilities are available at the RGO Cambridge to assist visiting astronomers in preparing for their observations. Paper and glass copies of the first epoch Palomar Sky Survey and film copies of the ESO and PPARC Schmidt surveys of the southern sky and the second epoch Palomar sky survey are located in a chart room which also houses Starlink terminals, Polaroid cameras, light tables and an extensive set of star catalogues and celestial atlases. Programs are available to produce overlays to aid target identification on the sky survey plates or give offsets and guide star information for individual telescopes and instruments. A Coradograph measuring machine with interfaced microcomputer is available to measure accurate positions (typically to better than 1 arcsec) of objects of interest relative to a grid of reference stars suggested by the programs. Glass and film copies of the sky survey plates are used for this purpose.

A copy of the NASA/STSCI Digitised Sky Survey on CD-Rom is available, together with software to access it on a Sparcstation.

Lastly, the important APM facility (operated by the RGO) has an accurate plate-scanning machine and can on request produce finding charts and measure positions off Sky Survey plates. The APM stored Catalogues contain stellar and non-stellar objects, with for example stellar magnitude limits of about $B = 21.5$ & $R = 20$ for the North (from Palomar O & E plates) and $B = 22.5$ & $R = 21$ for the South (from UK Schmidt plates). Typical internal accuracy is 0.1–0.25 arcsec but about 0.5 arcsec in the external reference frame. The Catalogues can be accessed over the *INTERNET* network. Fuller details are in *Spectrum*, **2**, p14 (1994).

1.7 Travel

Although you are responsible for making your own travel arrangements to and from La Palma, advice is available from the RGO's travel section at Cambridge (Belinda Rowlands, Tel 374888). You must, however, contact Montse Lorenzo on La Palma (Tel 405655; e-mail bookings@ing.iac.es) to book your transport up the mountain and accommodation for your stay on La Palma. Before your departure make sure you have received an information pack (from Bill Martin) that gives practical advice about your journey to La Palma and the working environment at the Observatorio.

1.7.1 Visas

A visa is not required for EC nationals visiting Spain for less than 90 days; astronomers of other nationalities should enquire about visa regulations from the RGO travel section, Cambridge or directly at their local Spanish Consulate. The London Consulate General is at 20 Draycott Place, SW3 2RZ, telephone number 0171 581 5925. No other special arrangements (e.g. work permits) need to be made by astronomers visiting La Palma for less than 90 days. UK residents should remember to bring their form E111, plus a photocopy, which entitles them to free medical treatment in Spain.

1.7.2 Which La Palma?

The Canary island of La Palma (San Miguel de La Palma) is not to be confused with the town of Palma de Mallorca on the Balearic island of Mallorca in the Mediterranean, nor with Las Palmas, the main town on the island of Gran Canaria. Similarly, the main town on the island of La Palma, Santa Cruz de La Palma, is not to be confused with Santa Cruz de Tenerife, the main town on Tenerife. Obviously, confusion between these different localities can lead to serious difficulties.

1.7.3 Air Travel between the UK and La Palma

The airport on La Palma is called Santa Cruz de La Palma (IATA code SPC). There are currently no daily direct flights between the UK and La Palma. An intermediate stop will be necessary in either Tenerife or Las Palmas (Gran Canaria) to change to an inter-island flight (see Figure 1.1). There are several airlines which operate charter flights directly from UK airports (e.g. Gatwick, Luton, Birmingham, Glasgow, Newcastle, Bristol and Manchester) to Tenerife or Las Palmas. Charter flights are usually the most convenient way of travelling to and from the Canary Islands, because they are direct (hence fast), cheap and available from many northern European locations.
Iberia operates a number of scheduled flights every day to Spanish mainland destinations from where it is possible to connect onto an internal flight to the Canaries. Most charter flights between Gatwick and the Canaries take just over four hours; the Iberia flights (from Heathrow) take six or seven hours because of the change of plane on the Spanish mainland. There are a few direct flights each week between Madrid and La Palma.

Flights between Tenerife and La Palma take half an hour; between Las Palmas and La Palma about three quarters of an hour. There are several flights a day between the islands. Even so, there may not be sufficient connection time in Tenerife or Las Palmas to complete the journey between the UK and La Palma in one day. In this case it will be necessary to stay overnight in a hotel on Tenerife or in Las Palmas.
Tenerife has two airports linked by taxi (about 1 hour) and bus services (about 2 hours). All international flights arrive and depart from the southern airport (TFS); a few inter-island flights use TFS but most use the northern airport (TFN). There are hotels in the towns of Los Cristianos and El Medano which are close to the international airport (15 minutes by taxi), or in La Laguna, a similar distance from the northern airport. There are a large number of hotels in the main city of Santa Cruz de Tenerife, about 30 minutes from the north airport and an hour from the south.
There are several hotels in the city of Las Palmas, which is about half an hour away from the airport by taxi. A good bus service operates between the city and the airport. There is a hotel (Bahia Mar) between the airport and the city of Las Palmas, and many hotels in the resort towns to the south.
An inter-island ferry operates between Santa Cruz de Tenerife and Santa Cruz de La Palma three times per week. The direct crossing takes eight hours, but some journeys operate via other islands.
When you arrive on La Palma, you may have arranged to be met by the observatory official taxi for transport to site (see section 1.7.5). Alternatively, go directly by taxi from the airport to your hotel in Santa Cruz de La Palma and follow the arrangements that have been made for you.
Travel and accommodation can be difficult at certain times of the year, for example at Christmas and carnival (February). Inter-island travel is also heavily booked at the start and end of school and university vacations.

1.7.4 Air Travel between the Netherlands and La Palma

There are several options at the moment.

- From Amsterdam directly to La Palma. There is currently one flight per week (on Mondays) but rumours are that there will be more.

- From Amsterdam with Iberia or KLM to Madrid, and on to La Palma directly. This option exists twice a week.

- From Amsterdam directly to Tenerife South (TFS) or Gran Canarias (Las Palmas), and then with an inter-island flight to La Palma. Transavia has 6 flights a week that go either to TFS or Las Palmas, and are scheduled flights. There are also charter-flights on this route. There are 2 (3 in summer) flights per day from Las Palmas to La Palma, and about 8 flights a day from Tenerife North (TFN) to La Palma. There are only 3 flights a week from TFS to La Palma. It takes 1 hour by taxi or 2 hours by bus to go from TFS to TFN.

- From Amsterdam via Madrid and Tenerife North to La Palma with Iberia. This avoids changing airports in Tenerife.

The costs of all these options are similar. In the summer it is generally easy to reach La Palma in one day, but in winter this is mostly impossible and people will have to spend the night in either Tenerife or Gran Canaria.

1.7.5 Transportation on La Palma

The ING is happy to transport visitors up and down the mountain free of charge as part of its normal transport arrangements. These are that on weekdays transport leaves the Santa Cruz office at 07:45 to make the upward journey and leaves the site at 16:00 (15:30 on Fridays) to make the downward journey. There is frequently official transport at weekends but it is not guaranteed and would-be travellers should check well in advance. The journey takes about 1 hour (via Mirca). There is an alternative route via Garafia that may need to be used in some circumstances; this journey takes two hours.

At other times (weather permitting) it is possible to travel up or down by taxi (booked via the ING receptionist at least 3 working days in advance) but such journeys must be paid for by the visitors concerned (current cost 4500 Ptas via Mirca). Visitors being met at the airport by a taxi booked in advance should look for a driver who will identify himself. Visitors should remember that the road is only negotiable by ordinary cars when the surface is free from snow and rocks. In the event of bad road conditions ING will make other, ad hoc, arrangements.

The ING transport consists of a fleet of saloon cars. Members of the permanent staff often drive straight from their homes to the telescopes in the morning and vice-versa in the evening without visiting the Santa Cruz office. Others call in at the office for administrative purposes or to receive visitors and drive them to the mountain top. On weekdays you should report to the office before 07:45 in order to catch the transport. At weekends, when prior arrangements have been made with the receptionist, you will be met at your hotel or the Santa Cruz office at a pre-arranged time.

Never make your own arrangements to travel up to or down from the site (e.g. by hire car or unofficial taxi) unless you have contacted a staff member and made sure that weather and road conditions are safe.

1.7.6 Accommodation on site

A well-appointed Residencia provides accommodation and related facilities for all astronomers and mountain-based personnel at the observatory. This Residencia, which is operated by the Instituto de Astrofísica de Canarias, is located near the observatory entrance (see Figure 1.3). There is a Residencia receptionist to deal with room allocation, room key, meals, etc. (The ING receptionist or duty officer will deal with things like transport, mail, etc). The Residencia bedrooms are mostly single (with some twin bedrooms and one double bedroom suite) and are fully furnished together with their own showers, telephones and window blinds. There are also very comfortable lounge and recreation areas, and some computer terminals are now available too. A limited transport service operates between the Residencia and the telescope buildings. If the weather permits, cars can be made available to the scheduled observers, one for each observing team, during their run only.

1.7.7 Freight

RGO can advise on freighting of equipment between the UK and La Palma. The Freight Officer at Cambridge (Ext 4835) and Manuel Acosta at the ING Sea Level Office will be pleased to provide any information required. The following notes are included for general guidance. Santa Cruz de La Palma has a port for sea freight, but no commercial air-freight facilities. It is possible, nevertheless, to fly equipment to La Palma (via Germany) in passenger aircraft provided the individual items are not too large or unacceptable for other reasons (e.g. hazardous materials).

Past experience has shown that cases smaller than one cubic metre in volume and weighing less than about 150 kg can be air-freighted to La Palma in this way. Larger items may be air-freighted to Tenerife, where commercial cargo services are available, but have to complete the journey to La Palma by ferry. This is an important point to keep in mind, as packing requirements may be different if sea travel is involved. The minimum transit time for air freight from the UK to La Palma is five days after leaving RGO, probably due in part to the formalities required to clear customs at La Palma airport. *N.B:* do not send goods via Madrid or Gran Canaria.

Alternatively, it is possible to send equipment to La Palma by sea freight, again via Tenerife. The time between acceptance of a consignment at the UK port of departure and arrival in La Palma is two weeks approximately. Mark freight for customs clearance in La Palma, not Tenerife, else further delays are likely to result. It is sometimes possible to get a sailing direct to La Palma, though these are less frequent.

There are port dues payable at La Palma docks, which are currently 2 per cent of the value of the goods shipped. Handling fees are charged at the airport at a similar rate.

RGO normally uses a shipping agent in the UK to arrange both air and sea freight. A minimum of 24 hours notice is required for collection and delivery to the appropriate UK airport; goods must reach the airport at least 24 hours before flight departure. For sea-freight, the consignment must arrive at the port of embarkation at least three days in advance of the sailing date. All cases must be clearly marked with the full Observatorio address and name of recipient. Details of the documentation required to ship equipment between the UK and La Palma and of the regulations regarding air and sea transport of hazardous items (such as chemicals, aerosols, compressed gases etc.) may be obtained from the Freight Officer at RGO. It may be possible to include items with RGO freight (cost to be recharged): contact the Officer before arranging freight to see if this is possible.

Paperwork must include a description (in English and Spanish) and the value of each item, also dimensions, gross and net weights of each case. Dimensions and weights must be marked on the outside of each case. Descriptions need not be very detailed (e.g. “Telescope spectrograph with associated equipment”). Dimensions are in centimetres (L $\times$ W $\times$ H) and weights in kilograms. Paperwork can therefore only be completed after packing, so sufficient time must be allowed for both before shipment. Small items can be packed in almost any available case but larger items may require specially made casing made by a packaging firm. Around one week is needed to arrange purchase and supply of this casing (2 weeks would be safer).

If export is only temporary then customs are far happier if they can be shown recognisable marks such as serial numbers etc. Temporary exports must be returned to the UK within 3 years and be packed in the same way as when they left the UK. UK customs are not interested in permanent exports; only Spanish customs are concerned.

Written instructions for shipments to La Palma are available from RGO. These instructions give examples of certificates of origin, forms and names of people who would require notification of any shipment and their addresses.

Some hi-tech equipment may need an export licence before it can be shipped abroad. Computers with over 128 kbyte of memory and CCDs are examples. Advice should be obtained from the Department of Trade (enquiries telephone number 0171-215-8032 or 0171-215-8033) well in advance. Two to three weeks should be allowed to get the licence once the need is determined and the appropriate form obtained (from the Department of Trade, using telephone number 0171-211-6611).

Where an instrument is described under one heading (e.g. “CCD Based Photon Counting System”) and one or more of the components of the instrument requires an export licence then it is advisable to list all of the components on the export licence application form, even though some of the individual items do not require a licence. If there is any doubt at all that a licence may be needed then an application for a licence should be made.

For shipping purposes, note that the Canary Islands, although part of Spain, are not in fact part of the EC Customs Union.

1.8 Observing and after

1.8.1 Facilities on site

Observers should contact their support astronomer as soon as possible after arrival for a briefing on the current performance of the instrument and telescope. Note that the astronomer scheduled for support may not be on the mountain-top until the day of the observing run.

The library on the first floor of the INT building houses paper copies of the Palomar Sky Surveys I and II (the latter still arriving), film copies of the SERC J and ESO B surveys, and copies of various other atlases and charts e.g. the SAO and Papadopoulos charts. There is a light table, and a Polaroid camera for making finding charts. The STSCI/NASA digitised sky survey is at the time of writing (Feb 95) on order.

The library takes about 50 journals, including all the major titles, with significant back runs (mostly not before 1950) of AJ, ApJ, MNRAS, PASP, A&A and others. Further details of these, and of books held on site can be obtained from *librarian@lpve.ing.iac.es*.

There are currently two data-reduction clusters, comprising Dec VAX and SUN SPARC computers respectively. The VAX cluster comprises a VAX 3500, 4 VAXstations, SCSI disk drives and tape drives for DATs, Exabytes and half-inch 9-track tapes. The cluster runs the VMS operating system, and has Starlink software, MAIL, EDT, LaTeX, Fortran compiler etc.

The SUN cluster comprises 6 SPARCstations, with SCSI disks and drives for DAT and Exabyte tapes. There is a SPARCstation for data reduction in each of the telescope control rooms. Software provided includes the Starlink UNIX collection, IRAF, LaTeX, GNU Emacs, the Mosaic information browser, a number of editors and mailers, and Fortran (f77) and C (gcc) compilers. The Sun cluster runs SunOS 4.1.3, but is due to be upgraded to Solaris 2.4 during 1995.

Guest accounts on the VAX and SUN clusters may be obtained by running a captive account whose name and password are known to local staff.

Information on the current status of the computing facilities is included in the Visitor's Pack which awaits each observer on arrival.

1.8.2 Observing protocol

The 4.2-m WHT and 2.5-m INT are worked by telescope operators, to the instruction of the observer. The telescope operator is responsible for the safety of the telescope, and will restrict its use and/or close the dome in unsuitable conditions, such as rain, snow, excessive wind speed, etc. He or she will also maintain observing records and attempt to repair any faults which may occur during the night, calling out the duty technician if unable to fix the fault. The duty technician is present each night until 2300 and on call thereafter to attend to instrumental faults.

The operation of the 1.0-m JKT and associated instrumentation is sufficiently straightforward that it is normally worked by the scheduled observer (after suitable training) without the help of a telescope operator.

Each scheduled observer will be supported both before and possibly during his observing run by a support astronomer assigned to him well in advance of his observing time. Support astronomers will be active research workers who have experience of the instrumentation requested. Support astronomers will be drawn from staff on the island, from the UK, from the Netherlands and from the IAC on Tenerife. The Head of the Astronomy Group resident on the island is currently (1995) Chris Benn.

On the INT and JKT data are dumped to exabyte or DAT tape in FITS format (D-Tape). These D-Tapes are shipped to the UK about once per week, where they are stored in the tape archive. The Observer may take the data home by either making a copy of the data himself from D-Tape or disk, or by having the tape copied to DAT or exabyte by the Observatory tape copying service. If the latter is required then the Observer should ensure that copy requests are submitted after each night's observing.

On the WHT the D-tape is also written in FITS format, and the observer can make a separate FITS tape by running two FITS writing jobs simultaneously, or request a copy to be made of the D-tape, of make a VMS backup tape from the data files stored on the Vax discs. Automatic writing of FITS tapes is currently being implemented, and should be available by mid-1995.
Observers are entitled to sufficient magnetic tapes to make one copy of all their data. If any further tapes are required they may be purchased from the Tape Copier (or Duty Officer outside daytime hours).
A duty officer is always present at the observatory, and will take charge in any emergency. You must obey the duty officer's instructions if an emergency arises.

1.8.3 Data ownership

The PPARC-NWO Joint Steering Committee and the International Scientific Committee have decided that ING policy is that data belongs exclusively to those who collected it for a period of one year, after which it is available in a common archive for all astronomers. It may be used at any time for engineering or instrumental investigations in approved programmes carried out to improve facilities provided at the observatory.
Service observations which are made by support astronomers at the request of others are similarly treated. However, calibration data may well be used for more than one observation and may therefore be available in common for several groups. It may happen that identical or similar service observations are requested by two or more groups. Requests which are approved before the data are taken may be satisfied by requiring the data to be held in common by the several groups. It is up to them how they organise themselves to process it, analyse it, relate it to other work, and eventually, presumably, publish it.
Requests for observations from programmes already executed on the telescopes should be referred to the original owners of the data, and/or to the data archive. This is the policy whether or not the data were obtained by PATT or CAT scheduled astronomers, or by service requests.

1.8.4 The data archive

Astronomical data collected with telescopes of the Isaac Newton Group are held in an archive at the RGO at Cambridge. Data tapes are normally copied on site before the observer leaves; the copy tape (C-tape) is taken by the observer, while the original is sent off (after observer and C-tape have arrived safely at his or her home institute) to be added to the archive.
The catalogue of observations, including details of telescope and instrumental setup, is kept on disc on the VAX node GXVG at Cambridge. This is accessible through INTERNET, JANET and STARLINK networks. Catalogue query software can be run from a captive account, ARCQUERY, or by using a mailserver access mode. Query functions are available to search the catalogue and make requests for the release of observations. For further information see La Palma User Manual No XXVI, *La Palma Data Archive*

User Manual. If you are interrogating the catalogue for the first time, please register as an archive user with the `ADDRESS_INFO` command.
The proprietary period of the data is 1 year. During this time data will be released only with the explicit consent of the original principal investigator. Thereafter, the observations are in the public domain. However, observations remain the property of the observatory throughout.
Archive-related operations during the actual data acquisition are kept to a minimum, so as not to interfere with an efficient observing procedure. However, observers are requested to assign sensible names to their observing targets, in order to enable archive users later on to judge what the observations are about. Further, it is recommended that the initials of the principal investigator are used when logging on to the data acquisition computer, even if this is not the actual observer.
Apart from the "electronic" archive on the VAX, the collection of photographic plates from the ING telescopes is also kept at Cambridge.

1.8.5 Publication of data

The CCI asks users of the facilities offered by the Isaac Newton Group of Telescopes to give proper acknowledgement to this effect in papers that they publish. This may be done in either of two ways:
(i) (preferably) as a footnote to the title:
"Based on observations made with (name of telescope) operated on the island of La Palma by the Royal Greenwich Observatory in the Spanish Observatorio del Roque de los Muchachos of the Instituto de Astrofisica de Canarias."
(ii) (if the editors will not allow a footnote) in the acknowledgements section:
"The (named telescope) is operated on the island of La Palma by the Royal Greenwich Observatory in the Spanish Observatorio del Roque de los Muchachos of the Instituto de Astrofisica de Canarias."
Authors are asked to send a preprint, and eventually three reprints, of such papers to the RGO librarian at Cambridge and the IAC at La Laguna.

Chapter 2

Telescopes, acquisition and guiding

2.1 The 4.2-m William Herschel Telescope (WHT)

2.1.1 General description

The William Herschel Telescope (WHT) has an altazimuth mount with a 4.2-m diameter f/2.5 parabolic primary mirror. At present, the Cassegrain and two Nasmyth focal stations (all f/11), and the corrected Prime focus (f/2.8) are in use. The three f/11 stations are all fed by the same secondary mirror, and they can be selected by the motion of the Nasmyth flat mirror. One Nasmyth focus is occupied permanently by the Utrecht Echelle Spectrograph; the other is used by the Ground-Based High-resolution Imaging Laboratory (GHRIL: see section 4.4.1), which also contains the optical table for the WYFFOS spectrograph (section 5.10). Schematic drawings of the telescope are shown in Figure 2.1.

The altazimuth design of the telescope means that the field of view rotates as the telescope tracks. In order to compensate for this, it is possible either to mount instruments on a turntable or to place image derotation optics in the beam. The former option is used at the Cassegrain and prime foci, but at Nasmyth, only light instruments may be mounted directly on the turntables and heavy apparatus, which must be kept stationary, is used with image derotators. There are currently two types of image derotators:-

- Optical image derotator, which consists of a flat mirror, and a pair of fused silica prisms, each with lens surfaces (see La Palma Technical Note 9). These have a 2.5 arcminute diameter unvignetted field of view. The optical image derotator is standard on the UES Nasmyth focus, and an option on the GHRIL Nasmyth focus.
- Infrared image derotator, which is all reflecting design with three mirrors. This has a 2.9 arcmin unvignetted field of view, and is an option on the GHRIL Nasmyth focus.

The appropriate unit is mounted on one of the Nasmyth turntables and is rotated under computer control at an appropriate rate to keep the final image at a fixed orientation. This allows the instrument to remain stationary, at the cost of a reduced field, and a 30% reduction in throughput

2.1.2 Summary of mechanical performance

- **Telescope limits:** $-175° < Azimuth < 355°$; $10° < Altitude < 90°$

  An additional effective upper limit to the altitude of the telescope of 89.8° is imposed by the speed limit in azimuth — see Section 2.1.5.

  The telescope is partially obscured at elevations below 12°.

  The area of the sky accessible to the WHT is shown in Figure 2.2.

- **Cassegrain turntable limits:** $-270° < mountPA < 255°$.

  Constraints on sky position angle depend on instrument mounting.

- **Nasmyth turntable limits:** These are instrument-dependent. There are no Nasmyth turntable limits if the instrument is stationary (i.e. if derotation optics are used or if an on-axis point source is observed and the field is allowed to rotate). This is always the case for the Utrecht Echelle Spectrograph. If instruments are attached directly to the GHRIL turntable, then limits may be imposed by the twisting of their cables.

- **Prime focus turntable limits:** $-85° < mountPA < 273°$.

- **Speed limits:** Maximum speeds and accelerations for altitude, azimuth and turntables are $1°\ s^{-1}$ and $0.3°\ s^{-2}$, respectively.

- **Switching between focal stations:** Cassegrain to Nasmyth: 4 minutes; Nasmyth to Nasmyth: 1 minute. Switching between Cassegrain/Nasmyth and prime foci requires a daytime top-end change.

- **Tracking and pointing at Cassegrain and Nasmyth:**

  Pointing accuracy: rms residual of a global fit = 1.1 arcsec (Cass)
  Pointing accuracy: rms residual of a global fit = 1.5 arcsec (Nasmyth)
  Tracking accuracy:
  (unguided) < 0.3 arcsec in 3 minutes; < 1.0 arcsec in 10 minutes
  (guided) < 0.2 arcsec
  Rotator tracking: < 0.2 arcsec over the whole field
  Offsetting accuracy: < 0.2 arcsec over 10 arcmin

2.1.3 Optics

The optical layout of the WHT is shown in Figure 2.3. Tables 2.1 and 2.2 give the optical characteristics of the Prime, Cassegrain and Nasmyth foci. Spot diagrams and vignetting curves for the f/11 focal stations of the WHT are given in Figures 2.5 and 2.6. Spot diagrams for prime focus at various positions of the Atmospheric Dispersion Compensator are given in the *WHT Prime Focus and Imaging Manual*. A more detailed optical description is given in La Palma Technical Note 9.

Table 2.1: Summary of mirror characteristics for the WHT

Element	Shape	Asphericity	Working Diameter (mm)	Focal length (mm)	Separation from primary (mm)	Material
Primary	Concave parabaloid	-1	4180	10439.6		Cervit
Secondary	Convex hyperboloid	-2.5329	1001	-3115.7	8035	Zerodur
Nasmyth	Flat	0	616×432		1750	Cervit

2.1.3.1 Prime Focus Corrector

At Prime Focus a four-element field corrector and a two-element atmospheric dispersion compensator are provided, the layout of these elements is shown in Figure 2.4. The field corrector provides good images over an unvignetted field 40 arcmin in diameter, and 45% vignetting at 1 degree diameter. The atmospheric dispersion corrector is specified to compensate for atmospheric dispersion over a wavelength range of 3300 to 11000Å, at zenith distances up to 73°.

2.1.4 Telescope control

The WHT is controlled by a MicroVAX 4000 computer interfaced through CAMAC. The mechanisms currently under computer control are altitude, azimuth and instrument rotator drives, focus and dome rotation. The primary mirror cover, shutters and Nasmyth flat are controlled manually. The telescope control system may be run in a stand-alone mode from its own terminal or from the system computer, which allows access to almost all of the same commands. The user interface is divided into two mutually exclusive parts: one for typed commands, the other a "handset" for guiding and focussing. Both of these are controlled from the same terminal. In addition, there is a display of telescope parameters, updated once a second. The telescope may be operated from the control room or from the GHRIL enclosure. Commands can also be issued to the TCS through the D-task from the ICL interface to the Instrument Control Computer, but the handset cannot be used this way. The control system is described in detail in the "William Herschel Telescope Users' Manual".

For the purposes of preparation, the observer will need to consider: positions, finding charts, guide stars, catalogue formats, the need for blind offsetting and the restrictions imposed by the altazimuth mount (Section 2.1.5).

Figure 2.1: Schematic views of the WHT (a) in perspective (b) looking orthogonally to the altitude and azimuth axes

Figure 2.2: The area of sky accessible to the WHT. Lines of equal zenith distance are given on a plot of declination against hour angle. The limits corresponding to partial obscuration of the telescope by the dome rail (Zenith distance <78 degrees) and the zenith blind spot (Zenith distance $>$ 0.21 degrees; see text) are shown.

Figure 2.3: Optical layout of the WHT

Figure 2.4: Layout of the WHT Prime Focus Corrector and Atmospheric Dispersion Compensator

Figure 2.5: Spot diagrams for the f/11 Cassegrain and Nasmyth foci of the WHT. (a) Aberrations on a flat focal surface passing though the nominal focus on-axis. (b) Aberrations on a concave surface with radius of curvature 2.2 m. This illustrates the image quality available at the edge of the field for a suitably focused autoguider. (c) Aberrations on a flat surface which is focused for a compromise over the field.

Figure 2.6: Spot diagrams in a single plane for the Nasmyth foci of the WHT when used with the image derotation optics. Images for wavelengths from 330 - 1000 nm and distances of up to 2.5 arcmin from the axis are shown.

Figure 2.7: Vignetting at various foci of the WHT. The curves show the percentage transmission as a function of field radius. For accurate photometry, they should be interpreted with caution. The diagram refers to the area outside the constant central obstruction (8.4%) and secondary vane obstruction (0.6%). (a) f/11 Cassegrain and Nasmyth foci (b) prime focus.

Table 2.2: Optical characteristics of WHT foci

Focal station	Prime (without corrector)	Prime (with corrector)	Cassegrain	Nasmyth (without image derotator)	Nasmyth (with optical derotator)	Nasmyth (with infrared derotator)
Focal length (mm)	10440	11739	45738	45738	46419	45738
Focal ratio	f/2.498	f/2.81	f/10.94	f/10.94	f/11.11	f/10.94
Field diameter (arcmin)						
(no vignetting)		40	15	7	2.5	2.9
(50% vignetting)		60	19	23	5	
Scale (arcsec/mm)	19.76	17.55	4.51	4.51	4.44	4.51
Diameter of central obstruction(**1**) (mm)	1210	1210	1210	1210	1210	1210
Focus/mirror shift(**2**)			20	20	21	20

1) Theoretical obscuration (baffles + vanes) = 9.083%
2) Movement of focus position for unit movement of secondary mirror

2.1.5 Planning observations

2.1.5.1 Positions, finding charts and offsets

In order to take advantage of the good pointing of the WHT to speed up acquisition, it is essential that object positions be measured as accurately as possible, preferably to better than 1 arcsec for slit spectroscopy. In such cases, acquisition to within 3 arcsec is usually possible and even objects close to the limit of the integrating TV can be identified unambiguously. Obviously, less accurate positions will suffice for imaging observations and for bright objects which are immediately recognisable, but errors comparable with the size of the TV field (1.6 × 1.1 arcmin) will inevitably cause delays (recall that there is no finder telescope).

Given accurate positions, it is often possible to do without a finding chart, even for slit spectroscopy, but it is vital to ensure that either the target object or a suitable offset star will be visible on the integrating TV system. The approximate limit for a stellar object, under perfect conditions, at new moon and with maximum integration is roughly $m_v = 21.5$, but under many circumstances, this is a gross overestimate. If the object itself is fainter than $m_v = 17 - 18$ (and especially if it is diffuse), then a suitable offset star brighter than this limit should be found. The recommended procedure for blind offsetting is to slew to the reference star, centre it on a defined position using the handset and then to use the BLIND command to move to the target object. This requires the RA and Dec of both objects, rather than one position and an offset.

A finding chart is obviously essential for very crowded fields or if positions

are poorly known. The chart should cover somewhat more than the TV field (say 3 – 5 arcmin square) and should reach to the limit of the Palomar or Southern IIIaJ survey. Directions and scale should be clearly marked.
The telescope computer accepts coordinates in three systems: mean pre-IAU76 (FK4; default B1950), mean post-IAU76 (FK5; default J2000) and geocentric apparent of the date and time of observation. Neglect of the distinction between the two mean coordinate systems can lead to errors of up to 1 arcsec, comparable with the absolute pointing error of the telescope. For most purposes, it is enough to know that published coordinates with equinoxes earlier than 1975 are usually in the pre-IAU76 system (most are B1950) and that modern astrometric measurements use the post-IAU76 system (J2000). Optional parameters are proper motions (any epoch), parallax and radial velocity. For solar-system objects, differential tracking rates in RA and Dec may be specified. A list of conventions and units is given in the section on catalogues (see below). Very few observers will need to bother with parallax or radial velocity, and most will also be able to ignore proper motions. There are cases, however, where neglect of the proper motions will lead to severe difficulties, the most common trap being set by white dwarfs, which are often used as spectrophotometric standards, and which have large proper motions.

2.1.5.2 Catalogues

Catalogues of objects may be entered through the user interface of the telescope computer or using an editor on the data-reduction computers. Alternatively, the observer may bring a catalogue on half inch tape, DAT or exabyte cartridge or transfer it via ftp to an account on the cluster, whence it can be accessed by the telescope computer. Catalogues are text files, which can be transferred using any tape format acceptable to a VAX. BACKUP is recommended, with COPY as the second choice. Tape densities of 1600 and 6250 BPI, DATs and exabytes are supported. Those wishing to transfer files from computers other than VAXs or Suns should contact the La Palma computing staff well in advance of their visit.
Catalogues are simply lists of source parameters in free format with spaces separating the fields. All data for an entry should be on one line of the file. Anything following an asterisk is treated as a comment and is ignored. Do not use tab, control or other peculiar characters. The parameters must be in the order: Name, RA, Dec, Equinox, RA proper motion, Dec proper motion, Epoch, Parallax, Radial velocity. The first four parameters are mandatory and the remainder are optional with sensible defaults.
The formats and units of the necessary parameters are as follows:

- **Name** — up to 20 characters. Embedded spaces are allowed, but if they are used, then the name must be enclosed in double quotes (e.g. “NGC 7027”).
- **Right ascension** — hours, minutes, seconds, separated by spaces.
- **Declination** — degrees, minutes, seconds, separated by spaces.

- **Equinox** —

  for mean positions, a leading letter indicates the coordinate system:
  B implies mean pre-IAU76 or FK4
  J implies mean post-IAU76 or FK5

  A number indicates the epoch of the mean equator and equinox of that system (e.g. B1950.0, J1987.5).

  The remaining option is APPARENT (abbreviable to A), for which no number is required or indeed accepted.

The formats, units and defaults of the optional parameters are as follows:

- **Proper motions** — in RA (seconds of time per year) and Dec (arcseconds per year). Defaults to zero if not specified.
- **Epoch of position** — (year). This should not be confused with the equinox. The epoch of observation is used in conjunction with the proper motions to correct for the space motion of the object. If the epoch is not specified, then it is assumed to be the same as the equinox.
- **Parallax** — (arcsec). Generally negligible. Defaults to zero if not specified.
- **Radial velocity** — (km/s, positive for a receding object). Generally unimportant. Defaults to zero if not specified.

Although not part of a catalogue entry, differential tracking rates may also be specified. These are in seconds of time per second for RA and arcseconds per second for Declination.
Examples of catalogue files are:

1. The simplest possible catalogue, containing name, RA, Dec and equinox:

   3C567 12 34 56.78 -01 23 45.6 B1950
   NGC123 00 12 46.6 05 34 56 J1987.5
   COMET 12 12 12.12 12 12 12.1 A

2. A more complicated entry, including proper motions:

   SP1 00 31 22.2 -12 24 21 B1950.0 0.011 -0.17

2.1.5.3 System catalogues

The WHT telescope computer has a standard catalogue containing accurate positions and proper motions for astrometric, photometric and spectrophotometric standards. This is described in detail in La Palma Technical Note 85, which is updated periodically. The main elements of the catalogue are:

- A grid of bright stars with extremely accurate positions, selected from the FK5 catalogue and used to check the pointing of the telescope.

- A similar grid of fainter stars (V $\approx$ 9) from AGK3 and CPC2, with slightly less accurate positions, but suitable for detectors which saturate on the bright grid.
- Spectrophotometric standards, selected from the literature. All have accurate positions and the flux distributions and references to original measurements are collected in La Palma Technical Note 65.
- UBVRI photometric standards selected from Landolt (*Astronomical Journal* **88**, *439*, 1983, and *Astronomical Journal* **104**, *340*, 1992), again with accurate positions.
- A few useful photometric sequences for calibration of CCD frames.
- Some fields with a paucity of bright stars, to be used for sky flat fields.
- Astrometric fields for calibration of detector geometry.

Use of the catalogue positions will speed up acquisition and avoid potential difficulties with inaccurate positions and proper motions given in the literature.

2.1.5.4 Altazimuth problems

Observers who have not previously used an altazimuth telescope may find some aspects of the operation of the WHT to be counter-intuitive. The two main problems are long slews in azimuth and the rotation of the field of view.
The WHT has to move through a large angle in azimuth as it tracks close to the zenith. In fact, the velocity in azimuth exceeds the mechanical speed limit within 0.21° of the zenith, so objects in this area (the "zenith blind spot") cannot be observed. Only objects between declinations of 28°30' and 29° are affected, but time may also be wasted by alternating between northern (Dec > 28° 45' , roughly speaking) and southern (Dec < 28° 45') objects . The WHT can only move in elevation by about 78° (between horizon and zenith) — it cannot move through the zenith. Consequently, moving between objects on the meridian but north and south of the zenith takes three minutes (180° in azimuth at 1° s^{-1}). Programmes should be planned so that groups of northern and southern objects are observed together.
The times until horizon, rotator and azimuth limits, if any, are displayed by the TCS.
The WHT can rotate by a total of 500° in azimuth and the azimuth displayed by the telescope computer is in the range −175° to +355° (approximately). Objects with azimuths in the range 180° to 355° can therefore be observed with the telescope in one of two positions. On source change, the telescope will always drive to the nearer of these azimuths consistent with the limits.
The field of view of an altazimuth telescope rotates as the telescope tracks. At the Cassegrain focus of the WHT, this rotation is compensated by a turntable, driven under computer control. The turntable has 500° of travel. The mode of operation of the turntable depends on the precise requirements of the observation. The options are:

1. A given position angle on the sky (e.g., if a particular slit PA is required, or if a guide star is only available at one PA).

2. Compensation for field rotation, but with no constraints on PA, so that the sky PA is allowed to alter on source change in order to minimise rotation, but is thereafter held constant.

3. Rotator tracking the sky, but with the position angle reset so that the slit is vertical whenever a new source is selected.

4. Rotator stopped, so that the field maintains a constant orientation with respect to the vertical.

The last option may be suitable for spectrophotometric observations in which the slit has to be kept close to the vertical to minimise the effects of atmospheric diferential refraction, but guiding is only possible by viewing the reflection of the object itself from the slit jaws (off-axis guide stars move). An easier alternative is to set the PA of the rotator equal to the parallactic angle (or parallactic angle – 180°, whichever is closer) at the beginning of an observation, and to allow it to track thereafter.
The turntable suffers from the same problem as the telescope close to the zenith: the parallactic angle changes rapidly with time (see Appendix B).
At Prime focus the range of rotator travel is only 358°, so some position angles cannot be acquired, and much more care needs to be taken at the start of an exposure that the turntable will not reach one of its limits before the end.
Summary of Altazimuth problems:

- Zenith blind spot (telescope will not track within 0.21° of the zenith).

- Avoid long slews in Azimuth by grouping objects north and south of Dec 28° 45' together.

- Azimuth limits: −175° to 355°.

- Rotator options: specific sky PA; floating sky PA; stopped.

2.1.6 Acquisition and guiding

2.1.6.1 Overview

Acquisition and Guiding (A&G) units are available at the Prime, Cassegrain and UES Nasmyth foci of the WHT. Autoguiding is also possible at the GHRIL focus (with derotation optics) using a pellicle beamsplitter to feed a television camera. Guide stars for the autoguiders can normally be found with the Guide Star Server (GSS) system, which uses the *HST's* Guide Star Catalogue; this is described in section 2.4

2.1.6.2 Cassegrain acquisition & guider Unit

The layout of the Cassegrain A&G Unit is shown in Figure 2.8. It is described in some detail in La Palma Technical Note 56. Briefly, the unit has a full field of 15 arcminute diameter at the nominal telecope focus, 15 cm below the A&G to instrument interface. The following functions are provided

- **Acquisition.** This is carried out via an extendable probe carrying a mirror feeding a Westinghouse ISEC TV camera. When used direct, this provides a 1.5 arcmin field at the telescope scale of 4.51 arcsec/mm. It is possible to interpose a focal reducing system, which provides a larger field of 4 arcmin at a scale of 12 arcsec/mm. The TV camera is provided with a filter wheel with six filter positions. The filters normally mounted are B (BG28), V (BG 38), R (RG 630), CLEAR (UBK7) and EMPTY. The B, V, R, and CLEAR filters all have the same thickness, and the TV can be focussed independently to compensate for different filter thicknesses.

- **Slit Viewing.** The ISIS slit, which is tilted by 7.5°, can be imaged via a one to one transfer lens and flat into the same TV camera used for acquisition, with field sizes identical to those provided by the acquisition system. Note however that the Autoguider (see below) can vignette the return beam from the slit under some circumstances.

- **Autoguider.** The autoguider consists of a CCD detector head fed by a right angled prism, and focal reducing optical system with a field diameter of 1.8 arcmin. The present CCD has 385x288 22 micron pixels covering a field of 1.5x1.1 arcmin at a scale of 0.23 arcsec/pixel. The centre of the autoguider field rotates about the centre of the main field at a radius of 110 to 150 mm (8.2 to 11.2 arcmin) and the entire probe assembly has a radial displacement of 40 mm. The extreme edge of the autoguider field is partially vignetted, but only by about 5%. The autoguider has an azimuthal scan of 180°, so the total area scanned at a field scale of 4.51 arcsec/mm equals 152 square arcmin or 0.04 square degrees. This gives a good chance of finding a star brighter than 11th magnitude at the galactic equator or 13th magnitude at the galactic pole *(C.W.Allen, Astrophysical Quantities, publ. Athlone Press, 1976)*. The first 35° of the range of travel of the autoguider probe causes vignetting of the slit-viewing optics and is not normally used.

  The autoguider is provided with a filter wheel with six filter positions. CLEAR (UBK7), B (BG28), V (BG38), I (RG630), OPAQUE and EMPTY. The B, V, I and CLEAR filters all have the same thickness. The autoguider can be focussed independently to compensate for different filter thicknesses.

- **Comparison lamps.** A calibration system is provided consisting of an integrating sphere into which light is fed directly from two hollow

Figure 2.8: Three views of the Cassegrain acquisition and guider unit for the WHT. (a) Plan, showing the autoguider, cable wrap and filter slides. (b) Elevation, showing TV, autoguider and comparison system. (c) Elevation, showing the large and small feed mirrors and the auxiliary port.

cathode lamps (Cu-Ar and Cu-Ne), and light from a further six lamps (a choice from Cs-Ne, Fe-Ar, Fe-Ne, Th-Ar, Al/Ca/Mg-Ne, Na/K-Ne, and Deuterium) imaged via fused silica lenses onto 3 mm diameter fused silica light guides. Any combination of lamps may be used simultaneously, but the throughput of the light guides is very low (about 10%). The exit pupil of the integrating sphere is fitted with an obscuring disk to simulate the telescope entrance aperture obscuration, i.e. the secondary mirror structure. The reverse side of the acquisition mirror is used to feed the calibration light to the instrument. This enables simultaneous object acquisition and spectral calibration.

The light guides incur losses of about a factor of ten, so the lamps which are fed directly are very much brighter. Lamps can be interchanged by technical staff upon request.

Two eight-position filter wheels are provided for the comparison system. ND and colour filters similar to the set used on the INT A&G comparison system are provided to give a range of ND from 0 to 5. Two filter positions in each wheel are available for colour filters, BG24, GG375 and GG495 filters are normally mounted.

- **Filters.** Two filter slides, situated below the autoguider assembly, provide colour and ND filtering. Each slide carries five filters in cells. The filter cell carrier may be removed and alternative cells fitted. The filters have a maximum diameter of 85 mm. Neutral filters ND0.3, ND0.9, ND1.2, ND1.8 and ND3.0; and colour filters UG1, BG38, GG495, RG630 and WG320 are normally mounted, but others are available mounted in spare cells, and can be fitted on request. The cells for the two filter slides are identical.

- **Polarisation calibration.** For polarisation module calibration, a special double cell containing two dichroic polymer filters (i.e. Polaroid) with their polarizing axes mutually at right angles, may be fitted to the carrier.

- **Auxiliary focus.** A large mirror may be inserted to feed to a focal plane at right angles to the main telescope beam, and outside the A&G box, to enable the use of fibre-optic aperture plates and fibres to feed a spectrograph or other instrument. The full 15 arcmin field is available. Guiding in this configuration is not possible with the internal autoguider due to obscuration by the feed mirror, so coherent fibre bundles will have to be used for guiding.

  An alternative mirror (small feed flat), may be extended from the opposite side of the case, coplanar with the fibre-optic feed mirror, to direct light to a CCD camera or other small instrument at the auxiliary focus. A six-position filter wheel for 50mm filters and a shutter are provided for use with a CCD. The field available is 4.5 arcmin and the autoguider may be used.

The recommended method for finding guide stars is to select them from the Space Telescope Guide Star Catalogue (GSC) using the GSS software described in section 2.4. The coordinate conversions between position and probe coordinates are given in *"The Guide Star Search Software: Preliminary User Guide*, by R.A. Laing.

2.1.6.3 Nasmyth acquisition and guider unit (UES side)

The Utrecht Echelle Spectrograph (UES), on the drive side Nasmyth platform of the WHT, has a dedicated A&G box. This has been upgraded to allow guiding on objects down to V=17 in good seeing. The features of the A&G system are:-

- 2 fibres bundles: for slit viewing and one for off-axis guiding. It is possible to view the fields from both fibres on the CCD simultaneously.
- Each fibre bundle has a field of view of $\sim 18 \times 18$ arcsecs.
- It is possible to guide using either fibre.
- The autoguider software allows read out and display of both windows, whilst guiding on either.
- It will be possible to adjust the focus for each fibre.
- Image scale on CCD will be in the range 0.15 to 0.20 arcsec/pixel.
- Wavelength coverage of the fibres is 4000–7000Å.
- The TCS software has been modified to allow for differential refraction correctly.
- Magnitude limit V=17 in either fibre bundle.

The layout of the A&G unit is shown in Figure 2.9. The derotation optics give a full field of 5 arcmin diameter. The following functions are provided:

- **Acquisition.** Two field viewing options are provided: autoguide fibre and TV slit viewing.
  - Typically the pointing of the WHT is better than 1.5 arcsec rms. Hence, with good target coordinates, *normal* practice is to acquire the target *directly* onto the slitviewing fibre, which has a field of 18 arsec.
  - Alternatively it is possible to initially acquire the target using the TV slitviewer option. Here the entire 5 arcmin field (at a scale of about 1 arcsec/pixel) can be viewed off the slit jaws onto a Westinghouse ISEC TV. This operation is relatively slow — the A&G mirror must be moved so that the TV pickoff mirror views the slit, the slitangle *must* be set to zero degrees, all main beam filter wheels must be set to clear postion, and the dekker

Figure 2.9: The acquisition and guider unit for the Utrecht Echelle Spectrograph at the Nasmyth focus of the WHT. (a) Side view (b) Plan view

must be removed. The field observed will even then be partially obstructed by the slit-viewing probe, in particular the central part of the TV field will be obstructed; once the object has been identified, a standard aperture offset will be needed to bring it onto the centre of the slit.

This slit viewing option cannot be used during the exposure.

- **Slit viewing during an observation.** The image on the slit jaws can be monitored during an exposure using the slit viewing probe. This fibre-optic light guide relays the image to the CCD autoguider camera (as used for acquisition). The field is 18 arcsec square. It is possible to autoguide on the slit image, and this is the recommended method if no off-axis guide star is available or if the derotation optics are not in use.

- **Off Axis Autoguiding** An alternative method of autoguiding is to use an offset guide star. This option is implemented using a pierced autoguider mirror and movable guide probe. The beam emerging from the telescope (via the derotation optics) is intercepted by the autoguider mirror. In the resulting reflected focal plane there is a fibre-optic guide probe, which is used to relay stellar images to a CCD autoguider. The autoguider mirror can be moved transversely in order to place different parts of the mirror in the beam, allowing for different modes of operation. Three of these modes use holes cut in the autoguider mirror to allow for unvignetted fields of view at the slit of approximately 15 arcsec (point source observations, no sky), 70 arcsec (shortslit — allows for good sky subtraction and is the normal option when observing in echelle mode) and 160 arcsec (longslit — monochromatic imaging observations).

  The field remaining for offset guide stars in these three cases is approximately 16, 13 and 8 sq. arcmin respectively, allowing 50 per cent vignetting of the autoguider beam.

  For very bright objects, it is possible to attenuate the light with one of the 11 autoguider filters, which include a range of neutral density (ND0.5, ND2.0, ND3.0, ND5.0) and colour filters (RG9, RG610, GG455, VG9, BG28, UG11, BK7).

- **Comparison lamps.** The A&G unit provides for up to 6 different calibration lamps. However as of 1994 the only lamps provided are the thorium-argon lamp for wavelength calibration, and quartz-halogen for flat-fielding. To achieve high brightness, the system uses a diffuser rather than an integrating sphere. Correct pupil imaging is provided. Each lamp has a shutter, allowing it to be left on to stabilise prior to a calibration exposure. The calibration lamp unit is detachable and can be used for laboratory tests of other WHT instruments when the UES is not in use.

The calibration unit has two filter wheels, one containing a selection of colour filters (FG15, FG13, RG6, UG3+GG475, RG780, KG5, LB120, FG3, F512), the other a range of neutral density filters (ND0.5–ND4.0). However, the use of the ND filters is not recommended because they introduce some fringing to the calibration spectra.

- **Main Beam Filters.** There are separate filter wheels for ND and colour filters. The wheels have 10 positions and take filters up to 80 mm in diameter (5 arcmin) and with a thickness of 10 mm (ND) or 25 mm (colour). The normally mounted set of colour filters is: UG11, UG1, BG28, BG38, GG385, GG420, GG495, OG590, RG715, RG830. Also, any of the TAURUS narrow band interference filters can be used with UES. (These would be needed to isolate individual orders when observing with UES in long slit mode.) *Note: Advance notice is needed to use TAURUS filters, as the correct mount may have to be manufactured.* Each wheel also has a clear position which is used when viewing the slit directly with the CCD camera.

  It has been found that the ND filters introduce an unacceptable degree of fringing, hence their use is discouraged. It should be noted that it is unlikely that ND filters would be needed when observing astronomical sources.

- **Polarisation calibration.** There is a filter wheel for polarisers or other auxiliaries. This has 10 positions and takes polarisers up to 80 mm in diameter and 15 mm in thickness. *To date (1994) no spectropolarimetry facility is planned for UES.*

The GSS software may be used to locate suitable guide stars for the UES It is quite likely that targets at high galactic latitude will not have suitable guide stars in the catalogue due to the small size of the unvignetted field. In this case guide stars can sometimes be found by searching.

2.1.6.4 The Prime Focus A&G Unit

Guiding facilities at the prime focus of the WHT are provided by the prime focus instrument platform (PFIP). This is designed for use with direct imaging CCD cameras, and provides no acquisition facilities, as it is assumed that acquisition will be carried out with the main detector. The layout of the PFIP is shown in Figure 2.10. The following functions are provided.

- **Shutter** - There is an iris shutter of 100mm diameter, which lies 55 mm below the nominal focal plane, giving an unvignetted field of 80 mm (23.5 arcmin) diameter.

- **Filters** - The filter wheel has seven positions and accepts filters of up to 125mm diameter. There is a set of “Harris” BVRI filters of this size, and adaptors can be made to accomodate smaller filters. A set of adaptors for 50mm square filters exists. Details of the filters available are given in Appendix D

- **Autoguider** - There is an offset autoguider which consists of a diagonal pickoff mirror, a magnifying lens, and a coherent bundle feed to a standard RGO CCD autoguider head. The field of view of the autoguider at any one time is limited by the size of the coherent bundle to 25 arcsec square. The autoguider probe has a travel of 110 mm in the x direction (tangential in the centre of its travel) and 20 mm in the y direction (radial in the centre of the x travel), so that the autoguider probe can cover a total field of view 188 sq arcmin. Most of this field is in the partially vignetted region of the field of the corrector, although the vignetting is always less than 45%. The lens assembly at the input end of the guide bundle can be moved through 8 mm in order to adjust the focus to compensate for telescope focus adjustments (for example to accomodate filters of different thicknesses). Guide stars can be identified and the required probe positions calculated using the Guide Star Search facility, described in section 2.4.

Although the PFIP has been designed to support CCD imaging cameras, other instruments can be mounted on it, subject to a maximum weight of 70 kg, and a moment of 70 kg m. The nominal focal plane is 40 mm behind the mounting plane.

2.2 The 2.5-m Isaac Newton Telescope (INT)

2.2.1 General description

The Isaac Newton Telescope (INT) has a 2.54-m diameter primary mirror with a focal ratio of f/2.94. It uses a polar-disc/fork type of equatorial mount, as illustrated in Figure 2.11. The corrected f/3.29 prime and f/15 Cassegrain foci have been commissioned. Both foci are equipped with instrument rotators and with autoguiders. In addition, the Cassegrain acquisition and guidance (A&G) box contains an integrating TV camera for field viewing. A second camera is attached to the wide-field finder telescope. This is used for locating guide stars for the autoguider as an alternative to the Guide-Star Server (GSS) and, to a limited extent, for field verification. The INT is normally operated by a night assistant. Fuller details are given in the INT User Manual (*ING La Palma Manual No XX*).

2.2.2 Summary of mechanical performance

- **Telescope limits:**

  Zenith distance $< 70°$
  -6 h $<$ hour angle $< +6$ h (above pole)
  Declination $> -30°09'30''$

  Operation below the pole is possible, but only gains a small extra area of sky; consider it in exceptional circumstances.

Figure 2.10: The Prime Focus Instrument Platform plan view (above), and side view (below)

Figure 2.11: Schematic views of the INT from the east and north.

Table 2.3: Summary of mirror characteristics for the INT

Element	Shape	Asphericity	Working Diameter(mm)	Focal length (mm)	Separation from primary (mm)	Material
Primary	Paraboloid	-1	2540	7475		Zerodur
Secondary	Hyperboloid	-2.214	531	-1813	6017	Fused silica
Finder:						
Primary	Paraboloid	-1	405	2104		Pyrex
Flat	Flat		135		1600	Low expn glass

Note that the lower windshield causes vignetting for zenith distances $> 57°$ and is raised for such observations.

Figure 2.12 shows the area of the sky normally accessible to the INT.

- **Speed limits:** Maximum speeds for hour angle and declination are $0.5° \ s^{-1}$ and $1.3° \ s^{-1}$ respectively.

- **Tracking and pointing:**

  Pointing accuracy: rms residual of a global fit = 5 arcsec
  Tracking accuracy:
  (unguided) < 1 arcsec in 3 minutes; < 2 arcsec in 10 minutes
  (guided) < 0.3 arcsec
  Offsetting accuracy: Less than 1 arcsecond using the AUTOFFSET command.

2.2.3 Optics

Tables 2.3 and 2.4 summarise the optical characteristics of the INT. Spot diagrams for the various foci are shown in Figures 2.13 and 2.14.

The three elements of the prime focus corrector are of UBK7 glass, coated to minimize reflections and thus improve efficiency and reduce ghosts. The first two elements are not interchangeable and have a broad-band, single layer MgF_2 coating. The rear element of the corrector, however, is available in several coating options, summarized in Table 2.5. Single layer coatings produce reflectivities smaller than 2% per surface over the appropriate wavelength range given above. Three-layer coatings give reflectivities of less than 0.5% per surface, but the performance deteriorates very rapidly (to higher reflectivities than uncoated glass) outside the useful wavelength range.

Figure 2.12: The area of sky accessible to the INT. Lines of equal zenith distance are drawn on a plot of declination against hour angle.

Figure 2.13: Spot diagrams for images at the f/15 Cassegrain focus of the INT, showing the dependence on field radius and the effects of defocussing.

Figure 2.14: Spot diagrams for the prime focus of the INT with the three-element corrector at different wavelengths and field radii. The scale is shown by a circle of radius 1.0 arcsec.

Table 2.4: Optical characteristics of INT foci

Focal station	Prime (uncorrected)	Prime (corrected)	Cassegrain	TV finder
Focal length (mm)	7475	8357	38130	2104
Focal ratio	f/2.94	f/3.29	f/15	f/16
Field diameter (arcmin)				
(no vignetting)		40	20	15
(50% vignetting)		52	22	
Scale (arcsec/mm)	27.6	24.7	5.41	98
Diameter of central obstruction (mm)	914	914	914	139
Focus/mirror shift(**1**)			27	

1) Movement of focus position for unit movement of secondary mirror

Most observations use the broad band/blue corrector. Note that changing from one rear element to another is a major operation and is a day-time job. Frequent changes are strongly discouraged.

Table 2.5: Coating options for rear element of INT prime focus corrector

Waveband	Coating	Useful Range (AA)
Broad Band/Blue	Single layer MgF_2 matching first two elements	3500-7400
UV	Single layer MgF_2	<5000
V and R	Three-layer MgF_2 + ZrO_2 + Al_2O_3	4300-8000
R and I	Three-layer MgF_2 + ZrO_2 + Al_2O_3	6000-11000

2.2.4 Telescope control

NOTE: The INT and JKT are controlled using very similar software and hardware. This section therefore applies equally to the two telescopes.
The INT is controlled by a Perkin-Elmer 3220 computer interfaced through CAMAC. This drives the main HA and Dec axes, the Cassegrain instrument rotator, the focus and the dome and provides an interface to the autoguider. Data entry is primarily by typed commands at the user interface terminal, but actions (such as a telescope slew) are initiated by pressing buttons on a control desk. Adjustments to the telescope tracking are made using a handset.

In order to plan a set of observations, the observer will have to consider positions, finding charts, catalogue formats and the need for blind offsetting (Section 2.2.5) and guide stars (Section 2.2.6).

2.2.5 Planning observations

NOTE: The INT and JKT are controlled using very similar software and hardware. This section therefore applies equally to the two telescopes.

2.2.5.1 Positions, finding charts and offsets

The pointing accuracy of the INT is sufficiently high that acquisition near the centre of the slit or prime-focus CCD (within 5 arcsec, say) is usually possible. Positions should therefore be measured to better than 2 arcsec. Blind offsets on the INT are reliable to less than 1 arcsec using the AUT-OFFSET command, which uses the Autoguider probe motions to determine the offset.
Two coordinate systems are supported : mean pre-IAU76 and geocentric apparent of the date and time of observation; post-IAU76 (eg J2000) coordinates are accepted and should be used. Neglect of the difference between pre- and post-IAU76 systems gives rise to a maximum error of < 1 arcsec in practical cases, which is small compared with the pointing error. Optional parameters are proper motions (epoch assumed to be the same as equinox) and differential tracking rates in RA and Dec.

2.2.5.2 Catalogues

User input catalogues are either typed into the TCS (Telescope Control System) computer on line, or loaded via the 1600bpi 9-track tape. A tape in the right format can be prepared and loaded by support staff, given a user catalogue on VMS or Unix. Observation catalogues may be be typed into the telescope computer directly through the user interface or using the OS32 editor. If you have an extensive catalogue this is best done in the afternoon before you start observing. Catalogues can of course be saved to disc, so they are available from night to night, but will normally be deleted at the end of an observing run.
It is possible to select guide stars in advance of an observing run (see Section 2.4. on the Guide Star System and Section 2.2.6 for allowed positions). Their positions should be entered in the catalogue in the normal way.
A catalogue for the telescope computer is a set of user interface commands, exactly as typed in at a keyboard. The relevant commands are given below. Minimum matching is used, and portions of commands which may be omitted are given in brackets (e.g. the command SOURCE may be shortened to SO). Spaces or semi-colons may be used as separators, the latter being essential if the command is abbreviated (see RA and DECLINATION, below). Anything following an asterisk is treated as a comment and is ignored. The following commands are available:

- **SO(URCE)** defines a new catalogue entry. The format is SO(URCE name. A source name may have up to 20 alphanumeric characters. Embedded spaces are forbidden.

- **R(A)** enters the Right Ascension. The format is hours, minutes, seconds. The last two are optional, but the command must be terminated by a semi-colon if they are omitted. Spaces are not required between the hours, minutes and seconds.

- **D(ECLINATION)** enters a declination. The format is degrees, minutes, seconds. Again, the minutes and seconds may be omitted if the command is terminated by a semi-colon. Spaces are not required between the degrees, minutes and seconds.

- **EQ(UINOX)**. For mean positions, a leading letter indicates the coordinate system:
  B implies mean pre-IAU76 or FK4 (default)
  J implies mean post-IAU76 or FK5 (not yet supported)

  A number indicates the epoch of the mean equator and equinox of that system (e.g. B1950.0, J1987.5).

  The remaining option is APPARENT (abbreviable to A), for which no number is required.

- **P(ROPER-MOTION)** sets the proper motions. The corresponding epoch is assumed to be the same as the equinox.

- **/R(A)** proper motion in RA in sec/yr

- **/D(ECLINATION)** proper motion in Declination in arcsec/yr.

A catalogue may be in free format. For legibility and neatness, however, it is worth adhering to a more rigid tabular format with one object per line of the file. The format should be as follows:

- The file should consist of 80-byte records. Consequently, no more than 80 characters per line are allowed.

- The filename must consist of up to 8 alphanumeric characters, starting with a letter, and must have the extension .CAT.

- There should be no non-alphanumeric characters (tabs, line feeds, etc.) anywhere in the file.

- A line specifying default parameters and the coordinate type should be given at the beginning of the file, for example:

  .DEFAULT EQUINOX B1950 P/R 0.0 P/D 0.0

  sets the default equinox to 1950 and the default proper motions to zero and specifies mean coordinates. If these parameters are not specified explicitly for objects in the file, then they will take these values.

- The format should be:

  SO OBJECT R hh mm ss.ss D +dd mm ss.s P/R +s.sss P/D +s.sss EQ B yyyy.y

  with the coordinate type, proper motions and equinox omitted if they do not change.

2.2.5.3 System Catalogues

The catalogues currently available at the INT and JKT are:

- **PTGRID**: a grid of astrometric stars for pointing calibration.
- **SPECPHOT**: a catalogue of spectrophotometric standards with accurately known positions and proper motions.
- **UBVRIxxx**: a set of catalogues of photometric standards for imaging, based on the Landolt equatorial standards.
- **BRIGHT**: The twenty brightest FK5 stars, useful for daytime pointing and tracking tests, or checking gross pointing difficulties.
- **LAND06**: Landolt (1992) photometric standards between 0 and 6 hours RA.
- **LAND612**: Landolt (1992) photometric standards between 6 and 12 hours RA.
- **LAND1218**: Landolt (1992) photometric standards between 12 and 18 hours RA.
- **LAND1824**: Landolt (1992) photometric standards between 18 and 24 hours RA.

2.2.6 Acquisition and guiding

2.2.6.1 Overview

A&G units are provided at both the Cassegrain and prime foci of the INT. Suitable guide stars can normally be found with the Guide Star System, described in section 2.4

2.2.6.2 Finder telescope

A finder telescope is available on the INT. A TV camera can be used to view a field 33 × 25 arcmin in size.

2.2.6.3 Cassegrain acquisition and guider Unit

At the rear of the INT primary mirror cell is the Cassegrain turntable which can be rotated by 365 degrees, and onto which an A&G unit is mounted. The Cassegrain A&G Unit of the INT has been designed primarily for use with the Cassegrain Intermediate Dispersion Spectrograph (IDS) and Faint Object Spectrograph (FOS-1). Nevertheless, the overall philosophy of the design has been to incorporate a range of facilities which would be required by most instruments operating at the Cassegrain focus. Figure 2.15 shows the layout of the A&G unit. The full field is 20 arcmin in diameter, but the comparison lamps and filters are only useful over a more restricted field of 4 arcmin, matching that of the IDS.
The following functions are provided:

- **Acquisition:** Figure 2.16 shows the details of the optical system for viewing the acquisition field. A Westinghouse extended S20 TV camera views a 1.8 $\times$ 1.8 arcmin element of the 20 arcmin diameter unvignetted Cassegrain field (on- or off- axis). The TV display includes labels giving orientation and scale.

  A filter wheel is available for the TV camera allowing up to four circular filters to be loaded. These filters are not immediately accessible, as it is envisaged that most users would not require them to be replaced. The filters currently available are BG28, BG38, RG630 and clear (UBK7).

Figure 2.15: Three views of the Cassegrain acquisition and guider unit of the INT, showing the autoguider, TV camera, comparison system and filters. (a) and (b) Elevation, (c) Plan

Figure 2.16: The optical system for viewing the acquisition field at the Cassegrain focus of the INT.

- **Slit viewing.** A simple movement of the flip mirror allows viewing of the light reflected from the slit jaws using the acquisition TV. This facility gives visual confirmation of the position of the target on the entrance aperture of the instrument, as well as an approximate estimate of the seeing profile.

- **Autoguider.** An autoguider is available which allows offset guiding using stars anywhere in a 90 square arcmin field. The area available for guide stars is shown in Figure 2.15. Guide stars should have magnitudes in the range $7 < m_V < 13$.

  Ideally guide stars should be selected in advance of the observing run using GSS (section 2.4). Alternatively, an overlay showing the IDS slit and the area within which guide stars may be selected can be superimposed on the TV image of the finder field. A guide star can then be selected visually, and the A&G Unit TV and/or autoguider probes can be directed to that position. Care must be taken to avoid selecting a guide star so positioned in the field that the autoguider probe obstructs the on-axis star-beam.

A filter wheel is available for the autoguider beam allowing up to four circular filters to be loaded. These filters are not immediately accessible, as it is envisaged that most users would not require them to be replaced. The filters currently available are BG28, BG38, RG630 and clear (UBK7).

- **Comparison lamps.** The A&G Unit includes reference sources for calibrating the wavelength scale and the photometric response of the attached instrument. The lamps are housed in an integrating sphere which can contain up to two hollow-cathode lamps and one tungsten lamp; more than one source at the time can illuminate the slit. Illumination of the slit by the comparison lamps is achieved by movement of a dedicated mirror.

  The standard set-up consists of a tungsten lamp as continuum source, and copper-argon and copper-neon discharge lamps for wavelength calibration. A further selection of the following discharge lamps is offered: Th-Ar, deuterium Fe-Ne, Fe-Ar, Al/Ca/Mg-Ne, Na/K-Ne, Cu-He, and helium. Arc maps are available for the Cu-Ar (La Palma Technical Note 52), Cu-Ne (La Palma Technical Note 35) and Th-Ar lamps (La Palma Technical Note 91).

  The comparison lamps have two dedicated ND filter wheels, providing a wide range of ND filtering (La Palma Technical Note 22).

- **Filters.**

  Two main trays are available for ND and colour filters common to the star and lamp beams. The trays can be loaded with up to 5 filters each (plus a clear position). The filters are 45 mm $\times$ 60 mm $\times$ 3 mm in size. The two main filter trays are easily accessible, allowing rapid replacement of the trays' contents. Care must be exercised when removing the filter trays, since the two trays (colour and ND) are *not* interchangeable.

  The colour filters normally available are UG1, BG28, BG38, GG385, GG395, GG495, RG630, RG695 and RG830. The wavelength dependence of transmission of these filters is given in Appendix D. The following ND filters are available; ND = 0, 0.3, 0.6, 0.9, 1.0, 1.2, 1.5, 1.8, 2.0 and 3.0.

2.2.6.4 Prime focus acquisition and guider unit

This is mainly used with the prime focus CCD camera. The A&G unit is mounted on a rotator, which allows the detector to be rotated to any position angle, although it is normally operated at one of the cardinal points. The default orientation is 180°. The following facilities are provided:

- **Acquisition.** No direct viewing of the field is available for the prime focus. The telescope points sufficiently accurately that any object with

Figure 2.17: The area within which guide stars may be chosen for use with the autoguider at the Cassegrain focus of the INT. Stars may be selected in the shaded area. If the autoguider probe is moved closer to the centre of the field, then the slit is obscured. Partial obscuration occurs in the area shaded with dashed lines. The field outside the circle is heavily vignetted, but bright stars may be usable. The orientation of the diagram on the sky is given for the instrument rotator in PA = 0°. At other PA's, the diagram must be rotated anticlockwise by the PA.

Figure 2.18: The area within which guide stars may be selected for use with the autoguider at the prime focus of the INT. (a) Scale drawing of the locations of chip, rotator axis and guide-star acquisition field, showing probe-coordinate limits. (b) A sketch showing the general relation between guide probe and sky coordinates for any PA.

a reasonably accurate position can be acquired close to the centre of the CCD detector. This can be verified using a short CCD exposure.

- **Autoguider.** The prime focus autoguider is identical to that in the Cassegrain acquisition and guider unit.

  The detector is an FW-130 image dissector with an S-20 photocathode. As there is insufficient space to accommodate a filter wheel or slide, a single fixed filter is used with the autoguider. The choice of this filter is a compromise between a match to the FW-130 response and to the spectral response of the instruments used at prime focus. At present a broad-band green filter is used.

  Ideally guide stars should be selected in advance of the observing run, using GSS or Figure 2.18 which shows the area of sky within which guide stars may be selected. Alternatively, they may be selected from the finder telescope, and then acquired by scanning a 2.5×2.5 arcmin area around the selected position. Stars with magnitudes in the range $7 < m_V < 13$ will probably be suitable.

- **Comparison lamps.** No comparison lamps are provided.

- **Filters.** The filter wheels, one of which can be mounted at a time, are similar to those used for the JKT Cassegrain system. Each filter wheel carries up to 6 filters, each of which is 50 mm square. The filters available include broadband UBVRIZ, as well as a range of emission line filters. The narrow band filters are shared between the INT, JKT and WHT auxiliary port. The filters available are listed in Appendix D.

2.3 The 1.0-m Jacobus Kapteyn Telescope (JKT)

2.3.1 General description

The Jacobus Kapteyn Telescope (JKT) has a parabolic primary mirror of diameter 1.0 m with two interchangeable secondaries. It is equatorially mounted, on a cross-axis mount, which allows operation east or west of the pier. Normally it is East of the pier, if operation West of the pier is required the user should contact the telescope manager in advance to ensure that the appropriate pointing model is in place. There is a choice of two secondary mirrors. The f/8.06 Harmer-Wynne system uses a spherical secondary and a doublet corrector to give a field of 90 arcmin diameter for photographic astrometry over a wide field. The other secondary is a hyperboloid, which gives a conventional f/15 Cassegrain focus. The telescope is shown in Figure 2.19.
The JKT is normally operated by the observer. Further details of the telescope and its control system are given in the "Jacobus Kapteyn Telescope User Guide".

Figure 2.19: Schematic views of the JKT. (a) From the north (b) From the west

2.3.2 Summary of mechanical performance

- **Telescope limits:**

  Zenith distance $< 84°$
  -6 h $<$ hour angle $< +18$ h (telescope East of pier)
  -18 h $<$ hour angle $< +6$ h (telescope West of pier)

  There are no explicit declination limits.

  The fully-lowered windshield which sits on the dome lintel sets a further limit. Because of the asymmetry of the telescope, the limits are different east and west of the pier (see La Palma Technical Note 28).

  Figure 2.20 shows the area of sky accessible to the JKT.

- **Speed limits:** Hour angle and declination: $1.0° \ s^{-1}$; Dome rotation: $1.5° \ s^{-1}$.

- **Tracking and pointing:**

  Pointing accuracy: rms residual of a global fit $<$ 15 arcsec
  Tracking accuracy:
  (unguided) $<$ 1 arcsec in 3 minutes; $<$ 3 arcsec in 10 minutes
  (guided) $<$ 0.3 arcsec
  Rotator positioning: $<$ 0.2 arcsec over the whole field
  Offsetting accuracy: $<$ 0.3 arcsec over 10 arcmin

2.3.3 Optics

Details of the individual optical elements are collected in Table 2.6. Table 2.7 gives the most important parameters of the two optical configurations available, illustrated in Figure 2.21. The two optical systems share the same parabolic primary, with a clear diameter of 1.000 m and a focal length of 4.596 m. Two secondary mirrors are available on interchangeable top ends, as follows:
(a) a spherical secondary which, together with the primary mirror and an afocal doublet, constitutes the f/8.06 Harmer-Wynne system described in *Monthly Notices of the Royal Astronomical Society, vol 177, p25p 1977*. This configuration gives a highly corrected flat focal plane, 90 arcmin in diameter, located 515mm behind the primary mirror. The angular scale is 25.6 arcsec/mm. As can be seen from the spot diagrams reproduced in Figure 2.22, this system gives images smaller than 0.5 arcsec in diameter over the unvignetted field for incident light wavelengths in the range 3650 Å to 8521 Å. It is not envisaged that the f/8.06 focus would normally be used without the corrector; astronomers interested in using this system for non-standard applications (as for example with their own instruments) should discuss their requirements with RGO staff.
(b) a hyperbolic secondary constituting, with the primary, a conventional f/15 Cassegrain system. The curved focal surface is located 760 mm behind the pole of the primary mirror, giving a 34.4 arcmin diameter field with a

Figure 2.20: The area of sky accessible to the JKT. Lines of constant zenith distance are drawn on a plot of declination against hour angle. The horizon and hour-angle limits are shown for the two possible cases: (a) Telescope west of the pier (b) Telescope east of the pier

Table 2.6: Summary of mirror characteristics for the JKT

Element	Shape	Asphericity	Working Diameter (mm)	Focal length (mm)	Separation from primary (mm)	Material
Primary	Paraboloid	-1	1000	4596		Cervit
f/8 Secondary	Sphere	0	477	4381	2738	Zerodur
f/15 Secondary	Hyperboloid	-3.545	307	1811	3342	Zerodur
Afocal doublet	Sph. surfaces		326	Afocal	914	UBK7
Finder (doublet)	Sph. surfaces		200	3250		

Table 2.7: Optical characteristics of JKT foci

Focal station	Harmer-Wynne	Cassegrain	Finder
Focal length (mm)	8060	15000	3250
Focal ratio	f/8.06	f/15	f/16.25
Field diameter (arcmin)			
(no vignetting)	90	34	10,30,90(**2**)
(50% vignetting)	93	50	
Scale (arcsec/mm)	25.6	13.8	63.5
Diameter of central obstruction (mm)	618	406	
Focus/mirror shift(**1**)	4	11.7	

1) Movement of focal position for unit movement of secondary mirror
2) Depends on eyepiece used

scale of 13.8 arcsec/mm. As shown in Figure 2.22, the total aberrations on a flat focal surface passing through the nominal focal position on axis are calculated to be up to about 2 arcsec in diameter over the unvignetted field. Clearly, the off-axis images can be slightly improved by focussing the telescope at a compromise position for the field of view of interest.

The maximum movement of the secondary mirrors is ±20 mm about the nominal focus position. For the f/15 system this produces a shift of 241 mm about the optimum focal position; the on-axis image size is calculated to grow approximately linearly with focus shift up to a maximum diameter of 0.3 arcsec. Use of the Harmer-Wynne f/8.06 system at other than the nominal focal position is not recommended without prior ray-tracing.

Figure 2.21: Optical layout of the JKT, showing the f/8.06 Harmer-Wynne and f/15 Cassegrain configurations.

Figure 2.22: (a) Spot diagrams for images at the f/8.06 focus of the JKT for various wavelengths and field radii. The diameter of the circle is 1.0 arcsec. (b) Spot diagrams for a flat surface at the f/15 Cassegrain focus of the JKT.

2.3.4 Telescope control

See section 2.2.4.

2.3.5 Planning observations

See section 2.2.5

2.3.6 Acquisition and guiding

2.3.6.1 Overview

Three acquisition and guider units are available, one dedicated to the Wide Field Photographic Camera (WFC) at the f/8.06 focus, one dedicated to CCD imaging at the f/15 Cassegrain focus, and one for use with other instruments at the f/15 focus. In fact, only the first two incorporate an autoguider. Guide stars can normally be found using the Guide Star System, described in section 2.4.

2.3.6.2 Finder telescope

The JKT has a 20 cm refracting visual finder telescope with a focal ratio of f/16.25. Depending on the eyepiece used, fields of 10, 30 and 90 arcmin may be viewed visually from the observing floor. The finder is only used to diagnose gross pointing problems and for fun.

2.3.6.3 Acquisition and guider unit for the f/15 Cassegrain focus (CCD)

A dedicated A&G unit is available for observations at f/15 with the CCD camera. This is described in more detail in the "JKT CCD Users Guide" (La Palma User manual no. XVIII). Figure 2.23 is a diagram of the A&G unit.
The facilities provided are:

- **Acquisition.** A Westinghouse intensified TV camera with an S-20 photocathode is used, with integration on target and recursive filtering in software. The TV field is 9.5 × 7.5 arcmin in size, divided into 512 × 512 pixels with a pixel size of 1.11 × 0.88 arcsec. The limiting magnitude when used direct is $m_v = 15$. With full integration (256 frames + recursive filtering) the limiting magnitude is $m_v = 20$. Both of these limiting magnitudes are for a dark sky. No filters are provided. The TV views the field by reflection off a movable flat. It cannot view the field when the CCD is in use.

- **Autoguider.** It is possible to use offset guide stars in an annular region around the target position. The outer boundary is a circle of radius 17 arcmin and the inner boundary is an ellipse with semi-minor and -major axes of 10 and 13 arcmin. The PA of the major axis is usually east-west, but the whole camera can be rotated by support

Figure 2.23: The acquisition and guider unit used with the CCD camera at the f/15 Cassegrain focus of the JKT, showing grisms, filters, shutter assembly, TV camera, autoguider, drift- scan table and CCD cryostat.

staff if necessary. The guide stars must have magnitudes $m_v < 12$ (13 under very good conditions).

Guide stars can be found most efficiently using the Guide-Star Server (GSS), see section 2.4. Alternatively, they can be acquired by offsetting the telescope so that the field is viewed (in sections) by the acquisition TV camera. There is an automatic procedure to perform the search.

The autoguider has two sets of filters: ND and colour. For the highest accuracy at large zenith distances, the colour filter should be similar to that of the CCD camera. This minimises the effects of atmospheric differential refraction.

It is important to note that the autoguider cannot be focussed independently, so the total physical thickness of the filters in front of the autoguider must match that of the CCD filter in use. This presents no difficulty for the standard La Palma filters, but observers bringing their own filters should check the "JKT CCD Users Guide" (La Palma User Manual XVIII), where a list of the available autoguider filters is given, together with their thicknesses.

- **Comparison lamps.** There are no comparison lamps.

- **Filters.** The filter wheels, one of which can be mounted at a time, are similar to those used for the INT prime focus unit. Each filter wheel carries up to 6 filters, each of which is 50 mm square. The filters available include broadband UBVRIZ, as well as a range of emission line filters. The narrow band filters are shared between the INT and JKT. The filters available are listed in Appendix D.

2.3.6.4 Acquisition unit for the f/15 Cassegrain focus (non CCD)

This acquisition unit is used for all instruments at the f/15 focus except the CCD camera, which has a dedicated A&G box, and the Multi-Purpose Fotometer, which mounts directly on to the telescope. The instruments concerned are the Peoples' Photometer, the Richardson-Brealey Spectrograph, and 'own' instruments. Figure 2.24 is a schematic diagram of this acquisition unit.
The following facilities are provided:

- **Acquisition and slit viewing.** A Westinghouse intensified TV camera with an S-20 photocathode is used, with integration on target and recursive filtering in software. The TV field is 4.1 × 4.1 arcmin, divided into 512 × 512 pixels with a pixel size of 0.48 arcsec. The limiting magnitude when used direct is $m_v = 15$. With full integration (256 frames + recursive filtering) the limiting magnitude is $m_v = 20$. Both of these limiting magnitudes are for a dark sky. A set of Wratten neutral density filters are available (ND = 0, 2, 3, 4).

Figure 2.24: The acquisition unit used with the photometers and spectrographs at the f/15 Cassegrain focus of the JKT, showing the acquisition mirror, TV camera and comparison system.

This unit has remotely operated flat mirrors which can either direct the image from the field direct to the TV, direct the light off the slit jaws of a spectrograph, or be removed entirely

- **Guiding.** There is no autoguiding capability. For the spectrograph, the observer is expected to guide manually using the slit-viewing option described above; for the photometer, to rely on telescope tracking.
- **Comparison lamps.** Comparison lamps are available in an integrating sphere. The lamp light is directed to the instrument by a mirror on the rear of the field-viewing flat.

2.3.6.5 Acquisition and guider unit for the f/8.06 focus

The A&G unit is part of the Wide-Field Photographic Camera (WFC), and can only be used with that instrument. See the "1-m camera users manual" (La Palma Users' Manual V) for more details.
The following facilities are provided:

- **Acquisition.** There is no acquisition TV camera for viewing the field direct. Instead, a guiding probe views a quadrant of the field about 0.6 square degrees in size (the area of the sky recorded on the plate is approximately 1.77 square degrees). The quadrant sampled is determined by the orientation of the instrument turntable. The probe is mounted on (x,y) slides which have a maximum travel of 120 mm. Each axis is encoded in units corresponding to a linear motion of 0.1 mm (2.6 arcsec). For visual acquisition and guidance an eyepiece with double crosswires and red illumination is available to view the field through the guiding probe. The eyepiece can be rotated with a gooseneck to different positions for ease of viewing. It is also possible to view the full 90 arcmin field through a field eyepiece which can be mounted in place of the plate-holder.
- **Autoguider.** Once a suitable guide star has been acquired, its image can be directed onto the autoguider by means of a movable prism. The autoguider is equipped with two filter wheels, each having three positions plus clear, for colour (U, J, F) and neutral density (ND = 0.5, 1.0, 2.0) filters respectively. The detector is an FW-130 image dissector with an S-20 photocathode.

  It is possible to find guide stars at the telescope using an eyepiece as described above. However, this is a very inefficient use of observing time, and probe positions should therefore always be computed in advance, preferably with GSS.
- **Comparison lamps.** A 25 step spot-sensitometer is used for calibration purposes. During an exposure light is projected continuously through the calibration wedge and the filter onto one corner of the plate. A series of apertures is available to optimize the intensity of the calibration source according to the exposure time and plate/filter

combination in use. Each plate is identified by projecting onto an unexposed corner the information carried in the top left-hand corner of the corresponding observing card, consisting of: (i) telescope identification; (ii) plate number; (iii) plate–centre coordinates.

- **Filters.** The following broad-band filters are available: UG1, GG 385, GG 395, GG 455, GG 495, RG 630 and RG 715. The filters are 250 × 200 × 4 mm and are coated with single-layer broad-band anti-reflection coating. Relevant transmission curves, supplied by the manufacturers for uncoated filters, are collected in Appendix D. Additionally, sub-frame assemblies are provided to hold 100 mm × 100 mm interference filters. Two filters centred at 5007 Å and 6563 Å are currently available.

2.4 The Guide Star Server System at the ING Telescopes

Guide stars for the WHT, INT or JKT autoguiders may be found from the HST's *Guide Star Catalog*, which is kept on disc and CD ROM at the Observatory. The basic catalogue contains about 19 million objects in the magnitude range 6–16, of which 15 million are stellar. It is based on two single-epoch, single passband Schmidt surveys with plate epochs between 1975 and 1983. Objects are classed as stellar or non-stellar. The limiting V magnitude is about 15.6 in uncrowded regions (brighter in crowded areas). Astrometry is based on the AGK3, SAOC and CPC catalogues. The density of stars in the GSC is sufficiently large that suitable guide stars can be found almost everywhere, except in cases where the autoguider viewing area is especially small (*e.g.,* WHT UES).

Absolute positional errors vary from 0.5 arcsec at the original plate centres to 1.1–1.6 arcsec at the N or S plate edges. Relative errors at 30 arcmin separations vary from 0.3–0.8 arcsec depending on hemisphere and magnitude. Hence the positions are *not quite accurate enough* to be used for reference stars for blind offsetting into narrow (≤ 1.0 arcsec) slits. These positions should only be used for blind offsetting into slits if a wide slit is being used or if some uncertainty in the final slit position can be tolerated (*e.g.,* offsetting onto an extended source).

The *Guide Star Server* (GSS) is a package which finds guide stars for the offset autoguiders at the different focal stations of the JKT, INT and WHT. It takes the target's position in any of the co-ordinate systems supported by the individual telescope's control system, together with the rotator (*i.e.,* spectrograph or camera) position angle, and outputs a list of suitable guide stars with positions and predicted coordinates of the autoguider probes.

Magnitude limits for selecting stars can be altered, and there is an option to produce a simple listing and plot of all the nearest Catalog stars (useful for making finding charts and for offsetting).

The GSS can be run from any account on the VAX cluster on La Palma, or on the Software Development Vax (GXSEG0) at Cambridge. The server can be run from the account **GSS** on GXSEG0; the password is available from software development group staff.

The guide star catalogue may also be accessed directly from the WHT Instrument Control Computer using the TAG I-task.

A User Guide is available from La Palma or Cambridge support staff, and it is kept in each telescope's control area.

2.5 Carlsberg Automatic Meridian Circle

The Carlsberg Automatic Meridian Circle (CAMC) is operated jointly by the Copenhagen University Observatory, the Royal Greenwich Observatory and the Real Instituto y Observatorio de la Armada en San Fernando, Spain. Although not one of the Isaac Newton Group of telescopes, it is nevertheless part of the Observatorio del Roque de los Muchachos: a brief description is given in this section.

The CAMC measures the positions and magnitudes of stars, planets and minor planets brighter than $m_v \sim 14.5$. The measurements are made with a photoelectric scanning-slit micrometer as the objects cross the north-south meridian of the telescope. The positions and magnitudes of about 600 objects are measured each night to an accuracy of about 0.12 arcsec and 0.04 magnitude. Repeated observations on 4-6 nights produce a mean accuracy of 0.08 arcsec and 0.03 magnitudes.

The telescope is a refractor with an objective of 17.8 cm diameter and focal length of 266 cm. The observing procedure is entirely automatic, with acquisition and on-line data reduction controlled by two HP mini-computers.

The CAMC is not a common-user facility. Requests for observations of particular star lists or solar system objects should be made to one of the three partner institutions. Stars are given a priority between 1 (high) and 6 (low) by an international management committee. A list of several hundred stars given priority 1 will normally be completed within a year. Lists of several thousand stars of lower priority will probably take two or three years to complete.

The results of observations are published annually in catalogues; however, results will be released to users in advance of publication where this is desired. As well as the position and magnitudes, the catalogues contain the improved proper motions of stars derived by combining the CAMC position with previous epoch observations retrieved from a data bank which includes the large photographic catalogues, AC, PPM, Yale, AGK2 and AGK3. The accuracy of the proper motions so derived is about 0.003 arcsec/year.

From its observations of about 50 photometric standards, the CAMC provides nightly values of atmospheric extinction in V for La Palma. A file of these is held in LPINFO and can be consulted via any Starlink node.

Examples of programmes which have been undertaken by the CAMC are as follows:

- 2000 G-type dwarf stars within 30 pc: derive proper motions for a kinematically unbiased photometric catalogue to investigate the "G-dwarf problem".

- 6000 reference stars (m_v = 10-12) in fields of QSOs : derive accurate positions for reduction of photographic plates, and so derive optical positions of QSOs to link with radio (VLBI) positions.

- A few RS CVn stars : monitor magnitude variation for light-curve determination.

- 63 minor planets : positions for dynamical studies and magnitudes for physical studies.

- Uranus, Neptune : positions to up-date numerical integrations required in connection with VOYAGER II encounters.

Chapter 3

Overview of instruments

3.1 The instrument package

The INT and JKT have a restricted set of "core" instruments, which should cover the requirements of a large fraction of users. The number of instrument changes on these telescopes is kept to a minimum to reduce costs and increase reliability. However, the design of the WHT allows much greater flexibility, since it is straightforward to switch between Cassegrain and the two Nasmyth focal stations. A much greater variety of instruments may therefore be left on the telescope. A broad functional division between the WHT, INT and JKT as regards common-user instruments is given in Table 3.1.

Table 3.1: Functional division of telescopes

WHT:	Spectroscopy over a wide range of resolving powers Multi-Object Spectroscopy CCD imaging (faint objects, high resolution) Fabry-Perot imaging spectroscopy High-resolution and other projects in a laboratory environment Infra-Red imaging (from late 1995)
INT:	Intermediate and low-dispersion spectroscopy CCD imaging
JKT:	CCD imaging Photoelectric photometry Spectroscopy of bright stars (Wide-field astrometry)(**1**)

(1) The JKT wide field camera is not currently (1995) offered as a common user instrument.

Table 3.2 summarises the instruments and detectors **offered as common user instruments** as of mid-1994.

Table 3.2: Instruments available

Focus	Instrument	Detector
WHT:		
Cassegrain	ISIS double spectrograph	Tektronix and EEV CCDs; IPCS
	Faint-object spectrograph (FOS-2)	Coated GEC CCD
	TAURUS-2 (Imaging Fabry-Perot)	Tektronix and EEV CCDs; IPCS
	Low Dispersion Survey Spectrograph	Tektronix and EEV CCDs
	CCD Imaging(**1**)	Tektronix and EEV CCDs
Nasmyth	GHRIL	Tektronix and EEV CCDs
	Utrecht Echelle Spectrograph	Tektronix and EEV CCDs; IPCS
Prime	CCD Imaging (F/2.8)	Tektronix and EEV CCDs
	Autofib Fibre positioner(**2**)	Tektronix CCD (WYFFOS)
INT:		
Cassegrain	Intermediate dispersion spectrograph	Tektronix and EEV CCDs
	Faint-object spectrograph (FOS-1)	Coated GEC CCD
Prime	CCD imaging	Tektronix and EEV CCDs
JKT:		
f/15	People's Photometer	
	Richardson-Brealey Spectrograph	Tektronix and EEV CCDs
	CCD imaging	Tektronix and EEV CCDs

(1) F/11 imaging at the auxiliary port of the Cassegrain A&G box.
(2) The Autofib multi-fibre positioner will be commissioned in early 1995. It will be used in conjunction with the WYFFOS fibre spectrograph, which will physically be on the GHRIL side Nasmyth platform, although it will be fed with fibres from the prime focus.

The rest of this manual describes these instruments in more detail. Instruments which perform a similar function are grouped together, to help potential observers decide which is the optimum instrument for their application. Chapter 4 describes the imaging instruments, whilst Chapter 5 describes the instruments available for spectroscopic observations. The various detectors available are described in Chapter 6. Chapter 7 describes the instruments for photometry and polarimetry. Details of the support for users' own instruments are given in Chapter 8.

3.2 Instrument control

3.2.1 Overview

The instruments and detectors on all three telescopes are designed to be controlled from minicomputers running under the ADAM environment, which has also been adopted as a standard by Starlink, UKIRT, JCMT and the AAT. Note however that the implementations of this system on La Palma differ considerably between telescopes. The INT and JKT and their instruments are controlled by Perkin-Elmer 32-bit computers, whilst the WHT uses DEC Vax machines.

3.2.2 INT and JKT

The control of instruments and telescopes is usually separated, although the two computers can communicate and for some applications the telescope is controlled from the instrumentation computer. The user interacts with the instrument-control software via the ADAM command language, which provides for data entry and checking, prompting, defaults and some procedural capability. A set of device-dependent tasks communicate, through CAMAC, with the individual instrument microprocessors. The configuration of each instrument in use is shown on a graphical Mimic display and spectra or images can be displayed on a Lexidata image display or a Printronix printer. Some data-assessment routines are available at the telescope. All data from electronic detectors are written to tape in FITS format.

3.2.3 WHT

The WHT instruments and detectors, and optionally the telescope, are controlled from a single Vax (the system computer) using the ICL user interface to the ADAM environment. The architecture of the WHT system is more sophisticated than that of the INT and JKT equivalents. The new features are: MicroVax computers replacing Perkin-Elmer machines; more powerful microprocessors linked to the system computer by Ethernet; full integration of the telescope, instruments and detectors; a powerful detector-memory system with data-assessment capability; and a networked Sparcstation with rapid access to the data in the detector memory system for online data reduction using the *iraf* system or the Starlink software collection.

Chapter 4

Imaging instruments

4.1 Introduction

Many different options are available for two dimensional imaging. In recent years the emphasis has been put on developing CCD systems and it is now possible to obtain CCD images at the following focal stations.

- JKT Cassegrain focus (f/15)
- INT prime focus (f/3.29)
- WHT Cassegrain Auxiliary port (f/11)
- WHT Prime focus (f/2.8)

In addition the TAURUS imaging Fabry-Perot, and the LDSS multi-object spectrograph, which are described in detail in chapter 5 can be used without their Etalon and Grism respectively to obtain broad-band or narrow-band images of the sky. These should only be used in exceptional circumstances, in the case of TAURUS these circumstances include the use of narrow band ($\leq$ 30 Å bandpass) filters, where the passband is broadened and shifted significantly by the fast converging beam of the prime focus options.
Section 4.2.1 describes the various CCD imaging systems, whilst Section 4.3 discusses how to decide which option is appropriate for a given application. The facilities provided by the Ground-based High Resolution Imaging Laboratory (GHRIL) on the WHT are described in section 4.4.1.

4.2 CCD imaging

4.2.1 Overview

The CCDs currently available on the ING telescopes are described in Chapter 6, although the availability of CCDs changes rapidly, and users should contact the RGO for the latest information. Information on CCD availability is published regularly in *Spectrum*. The CCDs in most common use at the time of writing are EEV P88300 1242 x 1152 pixel chips (thick), and Tektronix 1024 pixel square thinned chips. A small format thinned GEC chip is available at the INT. Field sizes quoted in Table 4.1 are for some of these chips.

Table 4.1: Summary of options for CCD imaging

Telescope	Focal station	Focal ratio	Geometric aperture (sq. m)	Scale (arcsec/mm)	Chip	Pixel size (arcsec)	Fieldsize (sq. arcmin)
JKT	Cassegrain	f/15	0.66	13.8	Tek	0.33	5.6 square
					EEV	0.31	6.4×5.9
INT	Prime	f/3.29	4.41	24.7	Tek	0.59	10.1 square
					EEV	0.55	11.5×10.6
WHT	Cassegrain(**1**)	f/2.11	12.47	23.25	EEV	0.52	9.0 diameter(**2**)
					Tek	0.56	9.0 diameter(**2**)
		f/3.96	12.47	12.40	EEV	0.27	5.6×5.29(**3**)
					Tek	0.30	5.1 square(**3**)
	Cassegrain(**4**)	f/10.94	12.47	4.51	EEV	0.10	2.1×1.9(**5**)
					Tek	0.11	1.8 square(**5**)
	Cassegrain(**6**)	f/2.0	12.47	24.60	EEV	0.55	11.4×10.6
					Tek	0.59	10.1 square
	Prime	f/2.81	12.47	17.55	EEV	0.39	8.2×7.5
					Tek	0.42	7.2 square

1) These figures are for observations at Cassegrain focus with TAURUS-2 as a focal reducer. The field sizes are for the large broad-band filters, if standard 50mm filters are used in the focal plane filter wheel the field is reduced.
2) Limited by the optics of the instrument.
3) The unvignetted field of Taurus-2 with the f/3.96 camera is 6.1 arcmin in diameter, so the field of the chip is partly vignetted.
4) These figures are for observations at Cassegrain or Nasmyth foci direct.
5) The field at the Auxiliary port is limited by the shutter to 2.0 arcmin diameter.
6) These figures are for observations at the Cassegrain focus with LDSS-2.

4.2.2 The JKT CCD Camera

The JKT CCD camera and its dedicated A&G box form one unit, described in more detail in Section 2.3.6.3. In addition to facilities for acquisition and guiding, the following are provided:

- **Grisms.** These are for slitless spectroscopy and are described in Section 5.4.

- **Filter wheels.** The filter wheels carry up to six 50 mm square filters. There are ample spare wheels to mount any particular set of filters that the observer requires, but only one wheel can be mounted at a time. Changing the filter wheel is a manual operation and may take up to 20 minutes. If possible, avoid a change during the night.

  A large set of 50mm filters is available, and is shared between INT, JKT and WHT Auxiliary port. Details are given in Appendix D.

- **Drift-scan table.** The drift scan table allows the chip to be moved across the focal plane by a stepping motor driving a lead screw. As the chip moves it is read out a row at a time, the progress being displayed by the instrumentation computer. Until the chip has moved one column's length the rows will not have received their full exposure. This is known as the "ramp-up". It is an unavoidable overhead with this technique which is consequently not economic unless used over several times the length of one column. Drift scanned exposures are implicitly flat fielded in the column direction and only need to be flat fielded in the row direction.

- **CCD detector.** The available detectors are summarised in Table 4.1.

4.2.3 INT prime focus unit

When imaging at the prime focus of the INT is required, the top ring assembly which otherwise carries the secondary mirror support is replaced by a top ring carrying the INT Prime Focus Unit. In addition to the facilities for acquisition and guiding described in Section 2.2.6, the following are provided:

- **Filters.** The filter wheels carry up to six 50 mm square filters. There are ample spare wheels to mount any particular set of filters that the observer requires, but only one wheel can be mounted at a time.

  A large set of 50mm filters is available, and is shared between INT, JKT and WHT Auxiliary port. Details are given in Appendix D.

- **CCD detector.** The available detectors are summarised in Table 4.1.

4.2.4 CCD imaging at the WHT

4.2.4.1 Imaging with TAURUS-2

TAURUS-2 is described in more detail in Section 5.9. There is a choice of either an f/2.11 or an f/3.96 camera in TAURUS-2, giving a scale and field-size summarised in Table 4.1. Please note that TAURUS-2 was not designed to do high speed photometry, and so a fast shutter is not available for timing exposures. In general exposure times of <10 sec should be avoided. This can be especially important to bear in mind when selecting standard stars. In addition to the facilities provided by the Cassegrain A&G unit described in Section 2.1.6.2, the following are provided:

- **Filters.** There are two filter wheels in TAURUS-2, at the telescope focus and in the collimated beam.

  The wheel in the focal plane of the telescope takes up to 8 filters, each of which can be up to 125 mm in diameter. Note that small filters placed in the telescope focal plane may restrict the field of view, and in particular the 50 mm square filters, which are standard on the INT and JKT, will restrict the field available with TAURUS-2 to less than 3.76 arcmin.

  The focal plane filter wheel is tiltable, allowing the central wavelength of the filter to be varied (see Section 5.9.

  The filter wheel in the collimated beam takes up to 8 filters, each of which can be up to 76 mm in diameter. Note that the diameter of the collimated beam is about 68 mm (see Section 5.9), so that filters smaller than this will cause vignetting when placed in the collimated beam. In particular, this will be the case for the 50 mm square filters used on the INT and JKT.

  Appendix D summarises the larger filters available specifically for TAURUS-2 observations.

- **CCD detector.** The available detectors are summarised in Table 4.1.

4.2.4.2 Imaging at the Cassegrain Auxiliary port

The Cassegrain Auxiliary port is on the side of the A&G box, and is fed by the small feed flat. A small filter box is bolted to the Auxiliary port; this contains a standard filter wheel which has 6 positions for 50mm square filters. Because the cryostat and filter box must be removed in order to access the wheel, the maximum number of filters which can be used in any one night at this focus is 6. The filter wheel and shutter are driven remotely by the A&G box 4ms computer and the CCD controller respectively.
Because the optics before the filter wheel consist of three reflecting surfaces the Auxiliary port has the highest (efficiency $\times$ collecting area) in the ultraviolet of all ING imaging systems, and is particularly recommended for

deep U band imaging. As inserting the small feed flat takes only a few seconds it is also very useful when imaging observations form a small part of a mainly spectroscopic programme. It also gives the best spatial sampling of the available imaging options, and is recommended when resolution is of the highest priority.

- **Filters.** A glass "Harris" BVRI filter set, and a $CuSO_4$ + UG1 U band filter, each 50mm square, are provided for the WHT. All filters in the INT and JKT sets (Appendix D in particular the emission line and redshifted Hα filters, must be shared with the other telescopes.

- **CCD detector.** The available detectors are summarised in Table 4.1.

4.2.4.3 Imaging with LDSS-2

LDSS-2 is described in more detail in Section 5.7. Although primarily a spectroscopic instrument it can be used for deep broad-band imaging, and its imaging mode is often used to select targets for deep spectroscopic observations. A broad-band BVR filter set is provided, and because of the large number of air-glass surfaces in LDSS, and the fact that the anti-reflection coatings are optimised over the range 370-750 nm, LDSS is not recommended for imaging observations outside this range.

- **Filters.** A set of BVR "Harris" filters is provided to fit in the LDSS filter wheel, which is in the collimated beam. No other filters are large enough to accomodate the entire collimated beam.

- **CCD detector.** The available detectors are summarised in Table 4.1.

4.2.4.4 Imaging at the WHT Prime Focus

The Focal ratio at WHT Prime is f/2.8, which gives an image scale of 17.5 arcsec/mm. The corrector is specified to give images better than 0.3 arcsec total encircled energy (FWHM will be considerable better than this) longward of about 3800 Angstroms, and out to 20 arcmin radius. Because of the sheer thickness of glass in the corrector the transmission in the U band is 60%, although in B it is 80%. Thus its primary purpose will be imaging in broad and intermediated passbands longward of 3600 Angstroms.
The Atmospheric Dispersion Corrector (ADC) provides compensation for atmospheric dispersion at wavelengths from 3200$\mathring{A}$ to 1μm, and at zenith distances from 0 to 73 degrees.
The unvignetted field of the corrector is 40 arcmin in diameter although some of this is required for the off axis CCD autoguider, which moves within a rectangular field near one edge of the unvignetted field. The field of view of the autoguider at any one time is 0.2 sq arcmin; the total field accessible to the autoguider is 210 sq arcmin, although this is partially vignetted.

The Prime Focus Instrument Platform is described in more detail in section 2.1.6.4.
The filter wheel will accomodate filters up to 125mm in diameter, and there is a dedicated set of "Harris" broad-band filters of this diameter. The field size at the focal plane is limited by a shutter, 100mm in diameter, which lies about 20mm below the focal plane. The unvignetted focal plane is in excess of 90mm in diameter. This corresponds to 26 arcmin.

- **Filters.** A set of BVR "Harris" filters is provided to fit in the prime focus filter wheel. Adaptors are provided for standard 50mm filters (Appendix D, and can be provided for other sizes.
- **CCD detector.** The available detectors are summarised in Table 4.1.

4.3 Which system ?

4.3.1 Choice of Focal Station

Firstly select which telescope/detector combination gives the required field of view combined with adequate sampling. Table 4.1 gives the scale and field size for each combination of focal station and CCD.
The pixel size required to give adequate sampling is rather difficult to determine, and depends upon the application. For faint stellar photometry it is important to sample the images well; packages such as DAOPHOT work best if the pixel size is a quarter of the point source FWHM or less. For surface photometry of extended objects the sampling can be coarser; in this case the resolution will not be degraded significantly as long as the pixel size is a half of the stellar FWHM or less.

4.3.1.1 Optical performance

The Taurus and LDSS focal reducers, and to a lesser extent the two prime focus correctors, contain a large number of glass elements which limit the efficiency outside the wavelength range for which the optics, and particularly the anti-reflection coatings are optimised. For this reason imaging in U and I with Taurus and especially LDSS is not recommended. The Cassegrain auxiliary port of the WHT, and the JKT direct CCD camera, provide the most efficient options for U band imaging.

4.3.1.2 Optical Distortion

Optical systems, particularly those involving refractive elements, do not have a constant plate scale over the field, but there is a radial distortion pattern which takes the form:-

$$r_{true} = k_1 r_{fp} + k_2 r_{fp}^3 + k_3 r_{fp}^5$$

where r_{true} is the distance of an object from the optical axis, as measured on the sky (in arcseconds), and r_{fp} is its distance from the optical axis in mm. k_3 is rarely significant. Table 4.2 lists the significant terms for imaging focal stations.

Table 4.2: The Optical Distortion terms for ING Imaging stations

Telescope	Imaging System	k_1 arcsec/mm	k_2 arcsec/mm^3	k_3 arcsec/mm^5
JKT	F/15	13.75	0	
JKT	F/8	25.59	-5.25 x 10^{-6}	
INT	Prime	24.7	-9.202 x 10−5	
WHT	Prime	17.57	-4.1185 x 10^{-5}	
WHT	Cass/Aux	4.51	0	
WHT	Taurus F/2	23.24	9.713 x 10^{-4}	-1.536 x 10^{-6}
WHT	Taurus F/4	12.406	1.0794 x 10^{-3}	7.74 x 10^{-7}
WHT	LDSS	24.60	-1.595 x 10^{-3}	

A popular technique for obtaining deep imaging data is "dithering", or subdividing the long exposure into a number of shorter exposures, and moving the telescope pointing position by a small amount (typically in the range 5 to 30 arcsec) between exposures. Image frames are then transformed to a common reference frames by appropriate resampling software, and then combined. In the presence of optical distortion about a field centre *which changes on the sky between exposures* a simple shift will not necessarily register the images correctly, and a proper correction for the optical distortion may be necessary. This is discussed in more detail by D. Carter in *Gemini, number 39, page 14*, where techniques for recombining images are also discussed. If dithering is to be employed, then it is important to chose a focal station where the distortions are small, and if a complete correction for the distortion is necessary to ensure that the image sampling is good enough for this.

4.3.1.3 Optical performance

The Taurus and LDSS focal reducers, and to a lesser extent the two prime focus correctors, contain a large number of glass elements which limit the efficiency outside the wavelength range for which the optics, and particularly the anti-reflection coatings are optimised. For this reason imaging in U and I with Taurus and especially LDSS is not recommended. The Cassegrain auxiliary port of the WHT, and the JKT direct CCD camera, provide the most efficient options for U band imaging.

Taurus is only recommended for applications involving narrow-band interference filters, which it is desirable to place in the collimated beam. The passband of narrow-band interference filters is broadened and shifted by the fast converging beam of INT and WHT prime focus.

4.3.1.4 WHT and INT Prime Focus

The WHT prime focus has the following advantages over INT prime:-

- The collecting area is a factor of 2.8 greater.
- With a CCD with 24 micron pixels the sampling of the image on the WHT will be appropriate for seeing of about 0.8 arcsec, which is the median seeing in summer, wheras on the INT in the good seeing the images will be undersampled.

4.3.2 Signal to noise

A major factor in deciding which focal station and CCD to use is how to get the required signal-to-noise ratio in the minimum observing time.
As is discussed in some detail in Section 6.4, the noise level in any CCD image consists of three components, the Poisson noise in the signal, the Poisson noise in the sky background, and the read-out noise. By adding these components in quadrature, the signal to noise ratio (SNR) for stellar objects can be derived:

$$SNR = \frac{S_{obj}}{\sqrt{S_{obj} + R \times (S_{sky} + \sigma^2)}} \tag{4.1}$$

$$S_{obj} = E \times k \times 10^{-0.4 m_{obj}} \times \delta\lambda \times A_e \times t \tag{4.2}$$

$$S_{sky} = E \times k \times (a^2 \times 10^{-0.4 m_{sky}}) \times \delta\lambda \times A_e \times t \tag{4.3}$$

S_{obj}	=	Total signal from object being observed
S_{sky}	=	Signal per pixel from sky background
R	=	Number of pixels in seeing disk
σ	=	RMS readout noise in electrons per pixel
E	=	Responsive quantum efficiency of the CCD
k	=	number of photons s^{-1} A^{-1} cm^{-2} at the bottom of the atmosphere from a star of magnitude $m_v = 0$. At 548 nm $k \simeq 1000$ photons s^{-1} A^{-1} cm^{-2}
m_{obj}	=	apparent magnitude of the object being observed
m_{sky}	=	sky brightness in magnitudes per arcsec^2 (see section 1.3.2)
a^2	=	pixel area in arcsec^2
$\delta\lambda$	=	effective filter bandwidth in Å
A_e	=	effective aperture of telescope, or geometrical collecting area × efficiency
t	=	exposure time in seconds

These equations can be adapted straightforwardly to spatially extended objects, by putting R equal to the number of pixels in a spatial resolution element, and m_{obj} equal to the apparent brightness of the object in magnitudes per spatial resolution element.

The number of counts obtained in each pixel of a CCD image is actually expressed in ADU (Analogue to Digital converter Units). However, the calculation of the signal-to-noise ratio must be done in terms of detected electrons. The conversion factor between these two numbers (electrons/count) is known as the "gain" and is different for each CCD.

The signal-to-noise ratio which can be obtained with a CCD depends only on the following four chip parameters: quantum efficiency at the required wavelength, readout noise, pixel size and saturation level. One further factor may limit exposure time – cosmic ray detection rate. For broad-band imaging the readout noise is really only important for the currently little used RCA CCD, so for most of the dynamic range of the CCD the signal-to-noise ratio depends upon the square root of the exposure time. Deep exposures should be split into a number of shorter exposures, the length of the short exposures should be sufficient that readout noise is unimportant; should be short enough that objects of interest are not saturated, and ideally should be short enough that there are a number of separate exposures which can be used to filter out the cosmic ray events.

4.3.3 Quantum Efficiency of the CCDs

The thinned chips offer a substantial advantage in quantum efficiency over the thick chips, and this advantage is greater at bluer wavelengths. Chapter 6 describes the CCDs currently available at the ING telescopes, and updates will be published regularly in *Spectrum*. Technical notes 92 and 93 give details of the next generation and the current generation of CCD cameras respectively, and charatcteristics of operational cameras are available on the World-Wide Web servers at Cambridge and La Palma.

Table 4.3: Colour terms for the TEK2 chip at WHT Prime Focus. The Colour terms are given in the sense of (Observed − Landolt *Astronomical Journal* **104**, *340*, 1992).

Passband	Fitted Colour	Colour Term	R.M.S.
U	(U−B)	−0.128	0.051
B	(B−V)	−0.064	0.033
V	(B−V)	−0.007	0.032
R	(V−R)	−0.029	0.027
I	(R−I)	−0.123	0.023

4.3.4 Cosmetic effects and fringing

The thinned RCA chip, and to a lesser extent the thinned Tektronix chips, suffer from fringing at red wavelengths. It is possible to remove the fringing by subtracting a "fringe map", which is a deep exposure of a blank area of sky. Currently the RCA chip is not recommended under any circumstances.

Table 4.4: Colour terms for the TEK3 chip at INT Prime Focus. The Colour terms are given in the sense of (Observed − Landolt).

Passband	Fitted Colour	Colour Term	R.M.S.
U	(U−B)	−0.111	0.032
B	(B−V)	−0.083	0.016
V	(B−V)	−0.031	0.012
R	(R−I)	−0.013	0.015
I	(R−I)	−0.055	0.016

Table 4.5: Colour terms for the TEK4 chip on the JKT. The Colour terms are given in the sense of (Observed − Landolt).

Passband	Fitted Colour	Colour Term	R.M.S.
U	(B−V)	−0.179	
B	(B−V)	−0.060	
V	(B−V)	+0.004	
R	(B−V)	−0.011	
I	(B−V)	−0.055	

4.4 High-Resolution Imaging

4.4.1 Ground Based High Resolution Imaging Laboratory (GHRIL)

The GHRIL is a permanent facility on one of the Nasmyth platforms of the WHT. It is a large optical table on which users can set up their own instruments. It is aimed primarily at high resolution imaging, but other programmes may profit as well.
The GHRIL enclosure has a large "optics room" for the optical table and other equipment, and a smaller "control room" in which there can be a little light. They are connected by means of a revolving dark-room door. The optical table is 250 cm × 135 cm and has a 2.5 cm rectangular grid of tapped (M6) holes. The WHT optical axis runs parallel to the long side of the table, about 30 cm from the edge and at a height of 15 cm. The position of the f/11 focus is on the table, about 25 cm from the front edge with the optical derotator or no derotator in place, and about 15cm from the edge with the infra-red derotator in place. Inserting or removing the derotation optics is a daytime operation.

4.4.1.1 Optics

The following optical components are available. These are mainly used for interfacing purposes, and users should supply as far as possible their own components for their experiments:

- Microscope objectives to magnify the image
- ND filters

- Standard RGO, Harris and KPNO broad-band filters (Appendix D).
- Optical rails and various component holders (Newport)
- Flat mirrors, beamsplitters, achromats and single lenses.

Communication with the telescope control MicroVax is possible via an RS232 link, enabling the User Interface and the Information display of the TCS to be run in the GHRIL control room.
Full technical details of the GHRIL optics, detectors and PCs are given in "ING La Palma Technical Note 81: GHRIL User Notes" by M.N. Devaney, and potential GHRIL users should consult this document.

4.5 Imaging Polarimetery

ISIS (Section 5.6) can be used as an orthodox focal reducer, with a convenient plate scale of 0.3 arcsec per 22 micron pixel. The optical quality of the instrument is excellent on-axis, although towards the edges of the field there is some chromatic aberration (this does not matter in a spectrometer). The mirror which replaces the grating in this mode is silver-coated, and so the throughput of the red channel is good (5 reflections at 98% each).
The important use of the instrument in this mode is as a specialised imaging polarimeter, as both the existing modulator and analyzer, as used for spectropolarimetry, can be employed. As in the case of spectropolarimetry, a dekker mask is necessary whose duty fraction is fixed by the angular throw of the below-slit analyser, and by cross-talk (scattered light) between the separated images in each plane of polarisation. The instrument has been successfully used with a dekker consisting of a series of slots. This accomodates wavebands as long as R – the throw of the analyser decreases with increasing wavelength. The current arrangement gives seven slots on the sky of 6 x 100 arcsec unvignetted, separated by 11 arcsec.
The principal limitation in practice is that filters have to be changed manually, as the small below-slit filter slides in ISIS have to be used. Likewise swapping from red to blue channels involves manual operations.

4.6 Infrared Imaging

Pat Roche (Oxford) is currently building an infrared camera for the WHT, based on the design of UKIRT's IRCAM-3, and using the dewar from UKIRT's IRCAM-1. Although primarily intended as the detector for a Martini-like Adaptive Optics system (currently being built at Durham), it will also be offered as a common-user instrument for JHK' imaging. (Unfortunately none of the WHT spectrographs would be suited to IR spectroscopy with this camera.) Initially WHIRCAM will be mounted at GHRIL, as it's closed-cycle cooling pump exchanges heat with high pressure helium delivered via a flexible hose from a compressor. This means that to mount the IR camera at cassegrain will require a special hose-feeder, as the cassegrain cable wrap is too small for the minimum curvature limits of the He hose.

WHIRCAM: The dewar/cryostat is that of UKIRT's old IRCAM-1, but with a doublet lens mounted in an extended cold 'snout'. The doublet (40 mm diam) collimates an expanding f/11 input beam, producing a 16 mm diameter cold stop at the secondary image (lyot stop), located between the filter wheels [*I J H K L' K*-short plus *K*-narrow band at S(1), H_2 and Br(γ) lines] and a triplet lens. The triplet converts the collimated beam to f/5.5, giving an image scale on the detector of 0.27 arcsec/pix, and a FOV of 68x68 arcsec. [With Martini-3, a pair of mirrors prior to the telescope's focal plane will f-convert from f/11 to f/55, resulting in a 3.3 mm diameter cold stop, achieved with a small aperture in the second filter wheel, and an image scale of 0.05 arcsec/pix — the *WHT* diffraction limit is 0.13 arcsec at *K* and 0.08 arcsec at *J*.] The cold snout is about 130 mm long and attaches to the front of the dewar. The front of the snout is 137 mm beyond telescope focus, and the detector is 316 mm beyond the front of the cold snout. The dewar itself is 380x380x240 mm (XYZ), with the optical axis 100 mm above the bottom of the dewar. Preamps are mounted in a 100 mm cubed box attached to the rear of the dewar. The closed-cycle coolant pump is about 400x400x480 mm, and attaches to the top of the dewar. The dewar plus c-c-c pump weigh 67 kg. Heat from the c-c-c pump is extracted by compressed He attached to the pump via two flexible hoses attached to a compressor (a cube about 400 mm per side, which consumes about 1.5 kW).
Detector: 256x256 InSb array, 30μm pixels, cooled to 35K by a closed cycle high pressure He cooling system. Typically, qe $\sim$ 80%, dark current = 1 e^-/s, readout noise = 30 e^-, and wavelength range = 0.8 - 5.5 μm (if the thermal background of *WHT* is too high for this to be possible, imaging will be restricted to a wavelength range = 0.8 - 2.3 μm = J to K).
Electronics: The readout/detector control is a virtual copy of the ALICE rack built for UKIRT's IRCAM-3 (and CGS-4), which is controlled by a DEC VAXstation 4000 via Ethernet. The chip can also be continuously displayed via 3 coax cables to an RGB monitor. Control software is a copy of UKIRT's IRCAM-3, except for the stepping motor controllers (two filter wheels and one focus) and the telescope interface (for writing coords, etc to the headers).
Timescale: WHIRCAM is expected to be completed by December 1994, and ready for commissioning on the *WHT* in February and June 1995.
Magnitude Limits: Based on the performance of IRCAM3 on UKIRT (courtesy of Colin Aspin, JAC), and assuming the same sky brightness and extinction as at Mauna Kea,[1] estimates of saturation and limiting magnitudes are (but note that these are rough estimates only):

- **Saturation Magnitudes**

  For a minimum exposure time of 0.12s, observing point source with 0.5 arcsec seeing, and assuming a bias-subtracted linear-well capacity of 60K e^-)

[1] The average mag/airmass determined from observations at the Carlos Sánchez Telescope at Teide Observatory by M, Kidger – see Spectrum No.1, March 1994, p14 – were A_J = 0.14, A_H = 0.06, A_K = 0.14, compared to A_J = 0.11, A_H = 0.07, A_K = 0.09 at Mauna Kea

Pix scale = Seeing =	0.27 arcsec/pix 0.5 arcsec
J	~8.6
H	~8.4
K	~7.8

- **Background-Limited Exposure Times.**

  Minimum exposure times needed for noise due to sky to dominate the readout noise (40 e^-), assuming gain of 6 e^-/DN.

Pix scale =	0.27 arcsec/pix	
Sky Noise/RN =	1.0	3.0
J	~3s	~9s
H	~1s	~3s
K	~0.5s	~1.5s

- **Limiting Magnitudes**

  For point source with 0.8 arcsec seeing and a 2 arcsec aperture to 5σ (20%) photometry.

Pix scale = Seeing =	0.27 arcsec/pix 0.8 arcsec					
Exp (sec) =	10	100	900	1800	3600	14400
J	18.6	19.9	21.1	21.4	21.8	22.6
H	17.8	19.1	20.3	20.6	21.0	21.8
K	17.0	18.3	19.5	19.8	20.2	21.0

Chapter 5

Spectroscopic instruments

5.1 Overview

A wide range of different instruments is available for spectroscopic observations:

- For low dispersion spectroscopy of faint objects, two versions of the RGO-Durham Faint Object Spectrograph are available, on the INT and WHT.
- For low to intermediate dispersion spectroscopy of bright objects, the Richardson-Brealey spectrograph is available on the JKT.
- Low dispersion slitless spectroscopy can be carried out using grisms in the JKT CCD camera.
- For intermediate dispersion spectroscopy, the Intermediate Dispersion Spectrograph on the INT, and ISIS on the WHT, are available. These both offer a wide choice of gratings and dispersions.
- The principal high dispersion instrument is the Utrecht Echelle Spectrograph on the WHT. High dispersion spectroscopy is also possible using Manchester Echelle Spectrograph on the INT or WHT, although this is not currently offered as a common user instrument, and its status must be checked with its owner before an application is made.
- For multiple object spectrosopy, LDSS-II on the WHT gives high throughput at low dispersions over a 12 arcmin square field of view with a multi-slit system, while the WHT prime focus facility (WYFFOS+Autofib2), due to be commissioned in mid-1995 will provide intermediate resolutions (about half ISIS resolution for the same grating), over a 40 arcmin to 1 degree diameter field with fibre feeds for up to 150 objects.
- Fabry-Perot imaging spectroscopy can be carried out using TAURUS-2 on the WHT.

The rest of this chapter gives detailed descriptions of each of these instruments.

5.2 Faint Object Spectrograph

Two versions of the Faint Object Spectrograph (FOS) exist on La Palma, one on the WHT and one on the INT, both built as a result of a collaboration between the RGO and the Department of Physics of Durham University. The FOS is a highly efficient fixed format CCD based spectrograph, designed for low resolution (15-20Å) spectrophotometry, over a wide spectral range. The optical design, described by Charles Wynne (*Optica Acta, 1982, 29, 1557*) is based on a Schmidt camera working without a collimator in the diverging beam from the Cassegrain focus. The major components are shown in figure 5.1. The dispersion is provided by a transmission grating and a cross dispersing prism (grism), which together give a multi-order format covering the wavelength range 3500Å to 10500Å for FOS-1 on the INT, and 3500Å to 9700Å for FOS-2 on the WHT. As a result of locating the CCD within the camera, there are a small number of optical surfaces and minimum vignetting, which produces a system which is more efficient than most conventional spectrographs. In addition, the fixed spectral format of the device makes it relatively straightforward to carry out on-line data reduction and analysis operations. These include wavelength and flux calibration, as well as redshift determination.

FOS-1 is mounted below the IDS, and FOS-2 is located below ISIS, sharing the same slit and calibration facilities. This location offers the advantage that it is straightforward to change between FOS and IDS/ISIS during the night. For FOS-1 this involves removing a single folding prism, a manual operation normally carried out by support staff which takes about half an hour. For FOS-2, the folding mirror can be removed remotely under computer control. Alternatively, it is possible to use a dichroic to observe simultaneously with the blue arm of ISIS and the FOS (see Section 5.6). Some important parameters of the two version of FOS are summarised in Table 5.1.

5.2.1 FOS-1

The INT Faint Object Spectrograph Reference manual

Slit and dekker unit. FOS-1 uses the same slit and dekker unit as the IDS (see Section 5.5). A special dekker is available for use with FOS-1.

The folding flat is placed approximately halfway along the light path from the slit to the grism. It has a plane glass surface, with an extended blue response silver coating.

The grism has a 150 lines/mm plane transmission grating on the front surface. A ray from the slit centre to the centre of the grating surface makes an angle of 6.892 degrees with the normal to the surface and with the normal to the grating rulings. The central ray at a wavelength of 8000Å is diffracted normal to the grating. The grism as a whole

Table 5.1: Summary of FOS parameters

	FOS-1	FOS-2
Telescope	INT	WHT
Focal ratio	f/15	f/10.94
Image scale (arcsec/mm):		
at slit	5.41	4.51
at detector	58	35
Detector type	coated GEC(EEV) P8603 CCD 578×385 pixels active area pixel size = 22 micron	
Pixel size (arcsec)	1.24	0.80
Wavelength range (Å):		
first order	5000-10500	4600-9700
second order	3500-5500	3500-4900
Dispersion (Å/pixel):		
first order	10.7	8.7
second order	5.4	4.3
Resolution (pixels)	1.5	1.6

is a cemented assembly of the transmission grating, cross dispersing prisms of Schott SK5 and LF5 glass, and an aspheric corrector plate of Schott K10 glass.

The camera mirror is coated with an extended blue response silver coating and is expected to keep its high reflectivity, as the system is not let up to atmospheric pressure, except for maintenance.

Camera. This has a focal ratio of f/1.4 giving a slit to detector reduction factor of 10.7. The dispersion at the detector is 486 Å mm^{-1} in first order and 245 Å mm^{-1} in second order. The camera consists of an aspheric corrector plate cemented to the underside of the grism/prism assembly and the silver-coated spherical mirror. A field flattening lens produces a flat focal plane at which the detector surface is located. The detector package is small enough to fit within the shadow of the telescope's secondary mirror to minimize obscuration losses. The optical system has a resolution of 33 μm FWHM (minimum slit width) at the camera focus corresponding in the spectral direction to 16 Å in first order and 8 Å in second order, and in the spatial direction to 1.9 arcsec.

Detector. The detector for FOS-1 is a GEC(EEV) P8603 CCD coated by ESO to enhance the blue response. This chip is described in more detail in Chapter 6. The CCD is mounted inside the camera body, and is cooled via a copper cold finger leading to a cryostat bolted to the side of the instrument. There are plans to upgrade this to a thinned but otherwise similar chip.

The cryostat contains sufficient liquid nitrogen to keep the CCD cool for more than 12 hours, and is bolted to the side of the FOS frame, connecting via a copper cold finger through the side of the camera body to the CCD. It could be cooled to 120K, but is normally operated at 150K, stability being achieved using a small heater.

5.2.2 FOS-2

The design of the original FOS was adapted to the WHT by Sue Worswick. The main components are as follows:

Slit unit and dekker slide. FOS-2 uses the same slit unit and dekker slide as ISIS (see Section 5.6).

The grism has a 150 lines/mm plane transmission grating on the front surface. A ray from the slit centre to the centre of the grating surface makes an angle of 6.892 degrees with the normal to the surface and with the normal to the grating rulings. The central ray at a wavelength of 8000Å is diffracted normal to the grating. The grism as a whole is a cemented assembly of the transmission grating, cross dispersing prisms of Schott SK5 and LF5 glass, and an aspheric corrector plate of Schott K10 glass.

The camera mirror is coated with an extended blue response silver coating and is expected to keep its high reflectivity, as the system is not let up to atmospheric pressure, except for maintenance.

Camera. This has a focal ratio of f/1.4 giving a slit to detector reduction factor of 7.8. The dispersion at the detector is 400 Å mm^{-1} in first order and 200 Å mm^{-1} in second order. The camera consists of an aspheric corrector plate cemented to the underside of the grism/prism assembly and the silver-coated spherical mirror. A field flattening lens produces a flat focal plane at which the detector surface is located. The detector package is small enough to fit within the shadow of the telescope's secondary mirror to minimize obscuration losses. The optical system has a resolution of 33 μm FWHM (minimum slit width) at the camera focus corresponding in the spectral direction to 13.2 Å in first order and 6.6 Å in second order, and in the spatial direction to 1.2 arcsec.

Detector. The detector for FOS-2 is a GEC(EEV) P8603 CCD coated by ESO to enhance the blue response. This chip is described in more detail in Chapter 6. The CCD is mounted inside the camera body, and is cooled via a copper cold finger leading to a cryostat bolted to the side of the instrument. There are plans to upgrade this to a thinned but otherwise similar chip.

The cryostat contains sufficient liquid nitrogen to keep the CCD cool for more than 12 hours, and is bolted to the side of the FOS frame, connecting via a copper cold finger through the side of the camera body to the CCD. It could be cooled to 120K, but is normally operated at 150K, stability being achieved using a small heater.

5.2.3 Performance

The main factors governing the suitability of FOS for astronomical observations are the spectral resolution and the efficiency. As far as resolution goes, FOS works at a lower resolution than most conventional spectrographs. Under normal working conditions with a 1-2 arcsec slit, the resolution is 15-20Å in first order (8-10Å in second order). Thus FOS is suitable for studying emission line objects (AGN, HII regions, planetary nebulae), or continuum studies. It is questionable whether FOS is suited to studies of narrow absorption line objects (solar type stars etc.) where absorption features would fill only 1-2 pixels. One advantage of FOS is that it is considerably faster than a conventional spectrograph, and so is likely to be useful for those objects which are too faint for their spectra to be obtained at a high enough signal to noise in reasonable integration times with other instruments.

5.2.3.1 Efficiency

The efficiency curves for FOS-I and FOS-II are plotted as a function of wavelength in Figures 5.2 and 5.3 respectively. The peak efficiency of FOS-1 in first order is 76 per cent, and for FOS-2 is about 70 per cent.
The efficiency of the *total* system (atmosphere, telescope and FOS with the extended blue response CCD) derived from observations of flux standards under photometric conditions is 12.5% for FOS-1, and 17% for FOS-2, at 7000Å, measured at the zenith.
The AB magnitude for 1 photon/s/Å/ at the zenith is given in Tables C.1.1 and C.1.1 in Appendix C.

5.2.3.2 Stability

For FOS-1 the image of a spectral line moves by about 0.03 pixels per hour in the dispersion direction as the telescope tracks through zenith, and the worst flexure in a test tracking $\pm$ 5 hours RA is 0.15 pixels per hour. For FOS-2 the image of a spectral line moves by about 0.02 pixels per hour in the dispersion direction as the telescope tracks through zenith. Since the design philosophy of FOS calls for integrations to be broken up into periods of no more than 2000 seconds this corresponds to a shift of less than 0.01 pixels in a typical integration.

5.2.3.3 Wavelength resolution and range

See Table 5.1.

Figure 5.1: FOS

Figure 5.2: The efficiency of FOS-1

Figure 5.3: The efficiency of FOS-2

5.2.3.4 Calibration facilities

The versions of FOS on the INT and WHT use the calibration facilities provided by the A&G boxes described in Sections 2.2.6.3 and 2.1.6.2 respectively.

5.2.4 Operation

With a cross-dispersed spectrograph, there is a tradeoff between full spatial coverage along the slit and the requirement that the two spectral orders should not overlap, to ensure for example that the first order image of the sky does not contaminate the second order image of the object. Various dekkers are provided to allow you to make your choice. Alternatively, a colour filter can be used to suppress the second order light.

5.2.4.1 FOS-1

For FOS-1, observations can use several methods of sky subtraction, summarised in Table 5.2. The most common way of operating FOS-1 is to use mode D – that is, a central 25 arcsecond aperture, giving both orders, without any field lens. For most applications, there is sufficient sky as well as the target spectrum in the 25 arcsecond aperture for sky subtraction, especially for point like sources. The format of a FOS-1 mode D spectrum is shown in Figure 5.4.
Mode A uses the spectrograph on-axis and allows a 12 arcsec separation between the star and sky aperture; no field-lens is required. By completely separating the star and sky order pairs, Mode B allows a limited 2-dimensional capability of 25 arcsec slit length. Since the star-sky separation is 85 arcsec, a higher throughput is obtained by using a clear field-lens behind the slit. For slit lengths greater than 25 arcsec (Mode C), it is sensible to observe first order only, and the second spectral order is filtered out using a GG495 field-lens behind the slit. A long slit can of course be used with the two spectral orders, but sky subtraction is then very difficult.

Table 5.2: Operating modes for FOS-1

Mode	Max Slit Length (arcsec)	Star-Sky Separation (arcsec)	Field Lens
A	5.0	12	No
A	2.0	12	No
A	1.2	12	No
B	25.0	85	Yes (Clear)
C	200.0		Yes (GG495)
D	25.0		No

Figure 5.4: Format of a FOS-1 mode D spectrum

5.2.4.2 FOS-2

FOS-2 has equivalent modes of operation to FOS-1 modes B,C and D, although the dimensions of the apertures and separations do differ slightly. These are shown in Table 5.3. Again, the most common way of operating FOS-2 is to use Mode D – that is, a central 20 arcsecond aperture, giving both orders, without any field lens. For most applications, there is sufficient sky as well as the target spectrum in the 20 arcsecond aperture for sky subtraction, especially for point like sources.

Table 5.3: Operating modes for FOS-2

Mode	Max Slit Length (arcsec)	Star-Sky Separation (arcsec)	Field Lens
B	20.0	100.0	No
C	180.0		Yes (GG495)
D	20.0		No

As with ISIS, it is possible to use FOS-2 with any of the following observing modes – that is slitless, multi-slit, fibre-fed and polarimetry modes. See section 5.6 for details.

5.2.5 Data Reduction

Although there are some private data reduction software packages for immediate reduction of FOS data, we recommend the STARLINK packages SCP and SAM, written by J.R. Lewis (described in *Starlink User Notes Nos* 148 & 149). Alternatively, FIGARO software can be used (the FIGARO commands CDIST and SDIST can be used to track the curved orders). The procedure (*apall* in iraf can also be used for this.

5.2.6 FOS versus ISIS

In terms of *signal alone* (counts/s/Å), FOS-2 is more efficient than ISIS in the red. This is partially offset by the greater sensitivity of the Tektronix CCDs used on ISIS. Detailed differences can be seen by comparing the Oke 'AB' magnitudes which give 1 count/s/Å for each, from Tables C.1.1 and C.1.1 in Appendix C. However, the *signal–to–noise* ratio obtained in an astronomical spectrum often depends also on the spectral resolution achieved. For example, even with the lowest–dispersion ISIS grating in the red (R158R), the spectral resolution obtained is about a factor 4 better than that of FOS, and sky–subtraction longwards of 7000Å can often be much more accurate with the better resolution. As FOS is optimised for red light, ISIS probably has as good a throughput at blue and violet wavelengths. If this is then coupled with the higher quantum efficiency of the Tektronix CCD then it is likely that the most efficient way to proceed is to use FOS-2 for first order in the red, a dichroic with a crossover wavelength of around 5000 Å, and a low dispersion grating on the ISIS blue arm with the Tektronix CCD. Alternatively Tektronix CCDs can be used on both arms of ISIS, although these suffer from fringing at red wavelengths.

5.3 The Richardson–Brealey Spectrograph (RBS)

5.3.1 Overview

The Richardson-Brealey Spectrograph (RBS) available at the f/15 Cassegrain focus of the 1.0-m JKT was built at the University Observatory, St Andrews from the original design by Richardson and Brealey (*Journal of the Royal Astronomical Society of Canada, vol 67, p165, 1973).* It is an efficient, light-weight, robust and stable, off-axis spectrograph, intended primarily for low- to medium-resolution stellar spectroscopy. Having no computer-controlled components it is completely reliable, but grating angles etc must be set manually. The detector can be any of the standard JKT CCDs; users will notice some features provided for its original photographic use.

5.3.2 Design

In the following description the telescope is assumed to be parked pointing to the zenith, with the spectrograph mounted. Figure 5.5 shows schematically the main optical components of the spectrograph. These are:

- **Filter slide.** A filter slide common to both star and calibration beams is available above the slit. The slide is operated manually and is located within a simple spacer between the spectrograph and the A&G Unit.

  The following Schott glass colour filters are available: BG28, BG38, UG1, GG385, GG395, GG495, RG630, RG695, RG830. Filters are 25 mm in diameter and 2.5 mm thick.

  Two ND filters, 25 mm in diameter and 2 mm thick, are available: ND=1.42, 3.0.

- **Dekker and slit assemblies.** At the entrance to the spectrograph are a dekker mask, the slit assembly and a shutter located in front of the slit. The shutter is controlled via the CCD software. The dekker has a star slot 1.7 mm (23.5 arcsec) long, projecting to 0.475 mm at the detector, an 'arc' position and normal long slit (out).

  The slit assembly is interchangeable so as to allow the use of a number of slits of fixed width. Two slits are available, of widths 73 μm and 110 μm (1.0 and 1.5 arcsec respectively). For a typical slit-to-detector reduction factor of about 4.1 (weakly dependent on the angle of incidence on the grating) these slit widths project to approximately 18

μm and 27 μm at the detector. Access to the slit assembly and optical components is by removing the side-panel. The slit position angle can only be set manually by rotating the instrument turntable with the telescope at zenith park.

- **Collimator.** The collimator, an off-axis paraboloid, is located at the base of the pipe projecting from the bottom of the spectrograph. The focal length is 750 mm, giving a beam of diameter 50 mm. The collimator is interchangeable and is offered with two coating options which maximize reflectivity in the blue and red spectral regions respectively.

- **Gratings.** There is a choice of four first-order gratings, all working blaze-to-collimator. The most important characteristics are summarized in Table 5.3.2 below. Gratings are 57 mm × 57 mm × 10 mm in size. The gratings are mounted with three M3 bolts onto a turntable, and a tangent screw on each grating assembly ensures precise location of the grating relative to the turntable. Grating angle is selected by manual rotation of the turntable using a calibrated knob and a scale with vernier. The *"Richardson-Brealey Spectrograph Manual" (La Palma User Manula XI)* gives details of the dependence of central wavelength, dispersion and slit-to-detector reduction factor on grating angle (Note - the new tables should be used as given in the supplement).

Table 5.4: Characteristics of gratings for the Richardson Brealey Spectrograph

Ruling (lines/mm)	Central wavelength (Å)	Dispersion (Å/mm)	Dispersion Å/(24 micron)pixel	Wavelength Range (Å)
300	7500	160	3.84	3000-10000
600	4400	80	1.92	3000-10000
1200	4400	40	0.96	3000-10000
2400	4400	19	0.46	3000- 6800

- **Camera.** The camera is an f/4 off-axis Maksutov system, comprising a two-element corrector, and spherical mirror and a field flattener with adjacent prism to direct light to the focus on the front face of the spectrograph (refer to Figure 5.5). The focal length is 208 mm. Like the collimator, the camera mirror and two correcting elements are interchangeable and two sets are available with coatings which maximise efficiency in the blue and red spectral regions respectively. The red set of optics makes better use of the red sensitivity of the CCD and can be used to the blue cut-off with some loss of efficiency. Focussing of the spectrograph is achieved by movement of the camera mirror, controlled by a micrometer screw on the camera mirror assembly. A

Hartmann mask, located on the slide in front of the collimator, allows the best focal position to be set with an accuracy of ± 50 μm.

- **Detector.** The spectrograph has been designed to work in conjunction with a CCD camera. Any chip available generally for the JKT may be used.

5.3.3 Performance

5.3.3.1 Resolution

Observations with a 1.5 arcsec slit produce arc lines with a FWHM of about 40 μm, well matched to the 24 μm pixel size of the Tektronix CCD. Table 5.3.2 summarises the dispersion in Å/pixel obtained when each grating is used with the Tektronix CCD.

5.3.3.2 Signal

A rule of thumb is that with the 2400 grating at 500nm an exposure of $5 \times 10^{(0.4\mathrm{V})}$ seconds gives 30,000 counts/Å.

5.3.3.3 Stability

The spectrograph possesses a high degree of stability. Flexure has been found to produce typically 1 μm of image shift along the dispersion direction for one hour of integration and telescope motion. The shift is regular and not discontinuous.

5.3.4 Calibration facilities

The spectrograph is interfaced to the telescope through the JKT 'Ellis' Cassegrain acquisition unit, where the calibration sources are housed (see Section 2.3.6.4). Cu-Ar and Cu-Ne hollow-cathode lamps are available for wavelength comparison, and a tungsten filament lamp as a source of white light.

5.4 Grisms on the JKT CCD camera

The JKT grisms are little used, and potential users should check their availability with support staff before applying to use them. The JKT CCD camera and its dedicated A&G unit are described in detail in Sections 2.3.6.3 and 4.2.2. In addition to using this as an imaging instrument, it is possible to carry out low resolution slitless spectroscopy with one of two grisms. The grisms are identical except for their blaze; one is blue and the other red. The efficiency of both of these grisms as a function of wavelength is plotted in Figure 5.6.
When used in first order, the dispersion is 11.2 Åpixel on the Tektronix chip (pixel = 24 microns), so that with 1 arcsec seeing the spectral resolution is

Figure 5.5: The JKT Richardson-Brealey Spectrograph

Figure 5.6: Efficiency curves for the JKT CCD camera grisms

about 32 Å (FWHM). Note that when observing in the red, it is necessary to use a colour filter to remove second order blue light.

5.5 Intermediate Dispersion Spectrograph (IDS)

The INT Intermediate Dispersion Spectrograph Reference manual

5.5.1 Overview

The Intermediate Dispersion Spectrograph (IDS) is the principal common-user instrument at the Cassegrain focus of the INT. The IDS design is a folded-input, flat-bed instrument. It is mounted – along with the Faint Object Spectrograph (FOS-1, see section 5.2.1) – below the Cassegrain A&G box (see section 2.2.6.3). Figure 5.7 shows the overall optical layout. Either IDS or FOS-1 operation is selected by installing or removing the folding prism, so that both spectrographs, and indeed both cameras of the IDS, albeit with different detectors, can be used consecutively during the same night. The acquisition TV camera, and autoguider, as well as the calibration and comparison lamps, above-slit neutral-density and colour filters are all located in the separate A&G unit to which the spectrograph is attached. Dekker masks, the slit assembly and below-slit filters are located within the main body of the spectrograph itself.

5.5.2 Design

The layout of the IDS is shown in Figure 5.7. The main components are:

- **Slit and dekker unit.** The same slit and dekker unit is shared by the IDS and FOS-1. The maximum slit length is 44.3 mm (4 arcmin); the slit width is variable from 40 μm (0.216 arcsec) to 2 mm (10.82 arcsec) in steps of 5 μm (0.027 arcsec). The entire slit assembly can be removed, although operations staff must be made aware of this requirement well in advance, as it is necessary to remove the IDS from the telescope to do this. Dekker masks are interchangeable in sets; individual sets of 8 apertures and a clear position, can be made up according to observing needs. Several standard dekkers, incorporating single slots, pairs of slots, a “comb”, and a coronographic set-up, are always available. Detailed information can be found in a folder at the Console Room of the INT.

- **Filter slides.** In addition to the above-slit filter slides in the A&G unit (see Section 2.2.6.3), there are 2 below-slit filter slides, each of which has 3 colour or ND filter positions. One of these positions is always clear. Five colour filters are currently available: UG11, BG18, BG24 and BG38, measuring 19 mm $\times$ 60 mm $\times$ 2 mm and made from Schott glass, plus a 25 mm x 25 mm solid copper-sulphate crystal filter. The wavelength dependence of the transmission of these filters is shown in Appendix D. The copper sulphate filter cuts out the red

Figure 5.7: The INT Intermediate Dispersion Spectrograph

part of the spectrum from 600 – 650 nm upwards. Its is usually used to cut out the first order FOS-1 spectrum, or the red leak of the UG11 filter. The neutral density filters below the slit provide a choice of ND = 0.5, 1.0 and 1.5. Note that the use of filters below the slit may make it necessary to refocus the spectrograph.

- **Collimator.** The focal length of the collimator is 1275 mm which gives a collimated beam with a diameter of 85 mm. There is a choice of three different collimators, with different coatings for maximum reflectivity in the wavelength range of interest. The collimators can be exchanged during the night by the support staff. The collimator is mounted on a remotely-driven sliding carriage, making it possible to focus the spectrograph under computer control.

- **Cross-disperser.** A transmission grism, R60B with 60 lines mm^{-1} and blazed at 4800 Å, can be inserted into the collimated beam in the 235 mm camera to provide a cross-dispersion option. This is normally used in conjunction with an R150 echelle grating, which is blazed at roughly 3 μm. The FOS-1 dekker mask is used to limit the slitlength to 25 arcsec in order to avoid order confusion. The wavelength range and dispersion provided by this grating in each order, for a grating angle of 62°, are summarised in Table 5.5.2.

Table 5.5: Characteristics of the IDS echelle grating

Order	Central wavelength (Å)	Wavelength range (Å)	Dispersion (Å/mm)
3	8800	down to 7500	94
4	6600	5800 - 8000	70
5	5250	4800 - 6200	56
6	4400	4100 - 5000	47
7	3750	3600 - 4200	40
8	3300	3200 - 3650	35
9	2950	up to 3250	31

- **Gratings.** The gratings have a ruled area of 102 mm × 128 mm. A wide selection is available, and some of the important characteristics of each grating are summarised in Tables 5.6 and 5.7. Grating changes can be made during the night by support staff.

- **Cameras.** Two cameras are available with the Intermediate Dispersion Spectrograph. Both are of the folded short-Schmidt type, described in detail by Wynne *(Monthly Notices of the Royal Astronomical Society, vol 180, p485, 1977)*. The focal lengths of the two cameras are 235 mm and 500 mm.

Table 5.6: Characteristics of the IDS gratings with the 235 mm camera

Name(**1**)	Origin(**2**)	Ruling (lines/mm)	Blaze (Å)	Efficiency(**3**) (%)	Central wavelength (Å)	Dispersion(**4**) (Å/mm)	Entrance slit for 45 μm at detector (arcsec)
R150V	B+L	150	5250	66	5500	271.3	1.55
R300V	NPL	300	5460	72	5500	138.5	1.58
R400B	B+L	400	3900	50	4000	104.5	1.59
R400V	B+L	400	5100	72	5500	104.5	1.62
R400R	B+L	400	7250	59	8000	104.4	1.67
R600R	B+L	600	6700	65	7000	69.8	1.74
R600IR	B+L	600	10000	70	8500	70.2	1.79
R632V	NPL	632	5460	72	5500	66.5	1.67
R831R	B+L	831	7500	65	8000	50.7	1.91
R900V	B+L	900	5100	69	5000	46.4	1.76
R1200U	J-Y	1200	3500	68	3500	35.3	1.73
R1200B	J-Y	1200	4000	76	3500	35.3	1.73
R1200Y	B+L	1200	6000	68	6500	35.2	2.00
R1200R	B+L	1200	8000	66	7000(**5**)	34.8	2.06
H1800V	PTR/NPL	1800	5300	64	5000(**5,6**)	23.2	2.10
H2400B	J-Y	2400	4000	60	3500(**5,7**)	17.5	2.06

1) Prefix R for ruled grating; prefix H for holographic grating.
2) Key: NPL = National Physical Laboratory; B+L = Bausch and Lomb; J-Y = Jobin-Yvon; PTR/NPL = PTR replica from NPL master.
3) Absolute efficiency values measured at RGO.
4) At low and intermediate dispersions the dispersion changes little with central wavelength.
5) Near maximum useful angle of incidence
6) Optimized for 5000-7000 Å.
7) Optimized for 3500-5500 Å.

Table 5.7: Characteristics of the IDS gratings with the 500 mm camera

Name(**1**)	Origin(**2**)	Ruling (lines/mm)	Blaze (Å)	Efficiency(**3**) (%)	Central wavelength (Å)	Dispersion(**4**) (Å/mm)	Entrance slit for 45μm at detector (arcsec)
R150V	B+L	150	5250	66	5500	132.2	0.77
R300V	NPL	300	5460	72	5500	66.1	0.78
R400B	B+L	400	3900	50	4000	49.6	0.78
R400V	B+L	400	5100	72	5500	49.7	0.78
R400R	B+L	400	7250	59	8000	49.9	0.81
R600R	B+L	600	6700	65	7000	33.3	0.84
R600IR	B+L	600	10000	70	8500	33.4	0.87
R632V	NPL	632	5460	72	5000	31.6	0.81
R831R	B+L	831	7500	65	8000	23.9	0.89
R900V	B+L	900	5100	69	5000	22.1	0.84
R1200U	J-Y	1200	3500	68	3500	16.7	0.83
R1200B	J-Y	1200	4000	76	3500	16.7	0.83
R1200Y	B+L	1200	6000	68	6500	16.4	0.92
R1200R	B+L	1200	8000	66	8000	15.5	0.95
H1800V	PTR/NPL	1800	5300	64	5500(**6**)	10.5	0.98
					7000	9.8	1.10
H2400B	J-Y	2400	4000	60	3500(**5,7**)	8.1	0.93
					6000	6.8	1.23

1) Prefix R for ruled grating; prefix H for holographic grating.
2) Key: NPL = National Physical Laboratory; B+L = Bausch and Lomb; J-Y = Jobin-Yvon; PTR/NPL = PTR replica from NPL master.
3) Absolute efficiency values measured at RGO.
4) At low and intermediate dispersions the dispersion changes little with central wavelength.
5) Near maximum useful angle of incidence
6) Optimized for 5000-7000 Å.
7) Optimized for 3500-5500 Å.

Along the direction of the slit (i.e. perpendicular to the dispersion direction), the focal lengths of 235 and 500 mm imply slit to detector reduction factors of 5.43 and 2.55 respectively, and hence scales at the detector of 29.4 and 13.8 arcsec/mm.

Along the dispersion direction, the slit to detector reduction factor is more complicated, since it depends on the grating angle. Tables 5.6 and 5.7 give the slit width in arcsec which projects to 45 microns at the detector, when each grating is used at its central wavelength.

The same tables also list the dispersion provided by each grating and camera combination. It can be seen that a wide range of dispersions is available, from 7 to 270 Å/mm.

- **Detectors.** The IDS can be used with any of three CCD detectors: a coated EEV, image frame size 1242×1152 pixels, pixel size 22.5×22.5μm, a thinned Tektronix, image frame size 1024×1024, pixel size 24×24μm or a thinned GEC, image frame size 385×578, pixel size 22×22μm. Spectral response curves and other details of the available chips have been published in Gemini, June 1992, **36**, p. 23. Changing the detector on a particular camera can only be carried out during the day. It is possible however, to have one CCD set up on one camera and another CCD on the other, and operate the two systems consecutively during the same night. Switching from one camera to the other only requires the grating to be rotated (or exchanged), an operation normally carried out by support staff, and the control software to be reinitialized.

5.5.3 Performance

5.5.3.1 Wavelength range and resolution.

Tables 5.8 and 5.9 gives for each CCD/camera/grating configuration the wavelength range, the dispersion in Å/pixel, and the slit width projecting to one pixel at the detector. With the exception of the 1800 and 2400 lines/mm gratings, the wavelength coverage does not significantly vary with the central wavelength. For proper sampling, the wavelength resolution cannot be less than about 2 pixels. In general a slit width should be used which projects to about 2 pixels at the detector. If a wider slit is used to increase the total throughput of the instrument, the wavelength resolution will be degraded.

It is normal for gratings to be installed with the blaze directed towards the collimator. It is worth noting is that if a grating were to be mounted with the wrong orientation, with the blaze directed towards the camera, there would be a dramatic decrease of throughput. In the case of the holographic 2400B grating, however, the dispersion will be affected too, and, in fact, a resolution improvement of about 20% can be obtained at high anamorphic magnification, but only at the cost of a drastic loss of efficiency.

Table 5.8: IDS Wavelength range and resolution (235 mm camera)

		EEV CCD 1242 22.5μm pixels			GEC CCD 578 22μm pixels			TEK CCD 1024 24μm pixels		
Grating (a)	λ_c	(1)	(2)	(3)	(1)	(2)	(3)	(1)	(2)	(3)
R150V	5500	7570	6.10	0.77	3430	5.96	0.76	6665	6.51	0.82
R300V	5500	3860	3.11	0.79	1760	3.05	0.77	3400	3.32	0.84
R400B	4000	2910	2.35	0.80	1325	2.30	0.78	2565	2.51	0.85
R400V	5500	2910	2.35	0.81	1325	2.30	0.79	2565	2.51	0.86
R400R	8000	2910	2.35	0.83	1325	2.30	0.81	2565	2.51	0.89
R600R	7000	1950	1.57	0.87	885	1.54	0.85	1715	1.68	0.92
R600IR	8500	1960	1.58	0.89	890	1.54	0.87	1725	1.69	0.95
R632V	5500	1860	1.50	0.83	845	1.46	0.81	1630	1.60	0.89
R831R	8000	1415	1.14	0.95	645	1.12	0.93	1245	1.22	1.02
R900V	5000	1290	1.04	0.88	590	1.02	0.86	1140	1.11	0.94
R1200U	3500	980	0.79	0.86	445	0.78	0.84	865	0.85	0.92
R1200B	4000	980	0.79	0.86	445	0.78	0.84	865	0.85	0.92
R1200Y	6500	975	0.79	1.00	445	0.77	0.98	865	0.85	1.06
R1200R	7000	965	0.78	1.03	440	0.77	1.00	855	0.84	1.10
H1800V	5500	640	0.52	1.05	295	0.51	1.03	570	0.56	1.12
H2400B	3500	480	0.39	1.03	220	0.38	1.00	430	0.42	1.10

1) Wavelength range (Å)
2) Dispersion (Å/pixel)
3) Slit width projecting to 1 detector pixel (arcsec)

Table 5.9: IDS Wavelength range and resolution (500mm camera)

		EEV CCD 1242 22.5 μm pixels			GEC CCD 578 22 μm pixels			TEK CCD 1024 24 μm pixels		
Grating	λ_c	(1)	(2)	(3)	(1)	(2)	(3)	(1)	(2)	(3)
R150V	5500	3688	2.97	0.38	1680	2.91	0.37	3250	3.17	0.41
R300V	5500	1850	1.49	0.39	840	1.45	0.38	1620	1.59	0.42
R400B	4000	1385	1.12	0.39	630	1.09	0.37	1215	1.19	0.42
R400V	5500	1385	1.12	0.39	630	1.09	0.38	1220	1.19	0.42
R400R	8000	1390	1.12	0.41	630	1.10	0.40	1225	1.20	0.43
R600R	7000	925	0.75	0.42	420	0.73	0.41	815	0.80	0.45
R600IR	8500	930	0.75	0.44	420	0.73	0.43	820	0.80	0.46
R632V	5500	880	0.71	0.41	400	0.70	0.40	775	0.76	0.43
R831R	8000	670	0.54	0.44	300	0.53	0.43	585	0.57	0.47
R900V	5000	620	0.50	0.42	280	0.49	0.41	540	0.53	0.45
R1200U	3500	470	0.38	0.41	210	0.37	0.40	410	0.40	0.44
R1200B	4000	470	0.38	0.41	210	0.37	0.40	410	0.40	0.44
R1200Y	6500	460	0.37	0.46	205	0.36	0.45	400	0.39	0.49
R1200R	7000	430	0.35	0.47	195	0.34	0.46	380	0.37	0.50
H1800V	5500	290	0.24	0.49	130	0.23	0.48	255	0.25	0.52
	7000	270	0.22	0.55	120	0.22	0.54	240	0.24	0.58
H2400B	3500	220	0.18	0.47	100	0.18	0.45	195	0.19	0.50
	6000	185	0.15	0.62	85	0.15	0.60	165	0.16	0.66

1) Wavelength range (Å)
2) Dispersion (Å/pixel)
3) Slit width projecting to 1 detector pixel (arcsec)

5.5.3.2 Stability

Worst case flexure on the IDS 500mm camera is 0.15 pixels/hour, and on the 235mm camera 0.40 pixels/hour.

5.5.3.3 Throughput

The efficiency of the IDS is best considered as the product of three components; collimator, grating and camera. The efficiency curves of the IDS collimators and gratings are given in Figures 5.8 and 5.9 respectively.

The efficiency of the cameras can be split into two components, one due to the geometry of the cameras (e.g. size of the central obstruction) and one due to losses at each coated surface. For small grating angles, the geometric efficiencies of the 235 mm and 500 mm cameras are about 67 per cent and 73 per cent respectively. At large grating angles (greater than about 44° and 60° for the 235 and 500 mm cameras respectively), the geometric efficiency drops off rapidly due to overfilling of the grating. This will occur for example when the 2400B grating is used in the red.

Each camera contains two aluminium mirrors, with a reflectivity of perhaps 85 per cent, and four air/glass surfaces with single layer anti-reflection magnesium fluoride coating, each of which has a reflectivity of about 2 per cent at 5500 Å. We therefore expect the 235 mm and 500 mm cameras to have total effective efficiencies of 45 per cent and 49 per cent respectively.

5.5.3.4 Performance of cross-dispersion option

The wavelength coverage provided by the cross dispersion option depends on the physical size of the detector. The current generation of large format CCD detectors (the EEV CCD has dimensions of 25.9 by 27.9 mm) are capable of covering the wavelength range in one exposure.

5.5.4 Calibration facilities

Comparison lamps for the IDS are mounted in the INT Cassegrain A&G box, which is described in more detail in Section 2.2.6.3. Three lamps can be fitted, one of which is always the tungsten lamp, used as a white light source. The standard set-up is a tungsten lamp, copper-argon and copper-neon discharge lamps for wavelength calibration. The following discharge lamps are also offered: Deuterium, Th-Ar, Fe-Ne, Fe-Ar, Al/Ca/Mg-Ne, Na/K-Ne, Cu-He, and He. Arc maps are available for the Cu-Ar, Cu-Ne, Th-Ar, He and Al/Ca/Mg-Neon (La Palma Technical Note 70).

5.6 ISIS

The ISIS Reference manual

Figure 5.8: Efficiency curves for the IDS collimators

Figure 5.9: Efficiency curves for the IDS gratings

5.6.1 Overall layout

ISIS and FOS-2 comprise three spectrographs sharing a common slit unit, dekker slide, optics for spectropolarimetry, and some filter slides. FOS-2 lies directly below the optical path, and is designed to provide the highest throughput at a dispersion of 400 Å/mm in first order, and 200 Å/mm in second order. Each of the two arms of ISIS is a conventional spectrograph, with interchangeable reflection gratings, and a horizontal optical layout. The optical components of the two arms, and the anti-reflection coatings on those components, are optimised for specific wavelength ranges. The upper arm is optimised for the range 3000 - 6000 Å, and is called the BLUE arm, whilst the lower arm is optimised for the range 5000 - 10000 Å, and is called the RED arm. Light is fed into the two arms of ISIS by 45° folding mirrors or prisms on the optical axis of the telescope and at the levels of the respective collimators. The folding mirror for the blue arm can be replaced by one of a range of dichroic filters, which reflects blue light and transmits red light, allowing simultaneous use of the blue arm of ISIS with either the red arm or FOS-2.

5.6.2 Polarisation optics

There are four optical components immediately above the dekker slide and immediately below the slit assembly which are used exclusively for polarimetric observations. The principles behind spectropolarimetric observing, and the ISIS/FOS-2 system, are described in detail in *The ISIS Spectropolarimetry Users' manual*, by J. Tinbergen and R.G.M. Rutten. Briefly the polarisation optics consist of:-

- A quarterwave plate, at present borrowed from the People's Photometer, effective over the wavelength range 3000-11000 Å, which can be inserted into the beam, set to any position angle, or rotated continuously at a speed of several Hz. The quarterwave plate converts circular into linear polarisation, so that the Savart plate (linear beamsplitting polariser) can detect its presence. Rotating the quarterwave plate rotates the linear polarisation striking the Savart plate. The quarterwave plate should only be used for point sources.

- A halfwave plate, 40mm diameter to facilitate long-slit observations, which can similarly be set to any angle or rotated continuously. Rotating the halfwave plate through n degrees results is a rotation of $2n$ degrees of the polarisation vector of the light. The halfwave plate is usually mounted below the quarterwave plate, which gives the largest field of view and best slit viewing for linear polarisation studies. It is possible to interchange these plates, although this requires that ISIS be taken off the telescope.

- A calcite block or Savart plate, located in a tray immediately below the slit. This is effective over the wavelength range 3300-11000 Å, and

Figure 5.10: Exploded view of the optical components of ISIS and FOS-2, showing the light paths through the components.

gives two beams separated by an amount which depends upon wavelength, but is in the range 2.1 - 2.6 mm over the effective wavelength range. The two beams are 100% polarised, orthogonally, and their relative intensity depends upon the polarisation vector of the incoming beam. Use of the Savart plate requires the spectrograph to be refocussed by 9600μm in the Blue arm, and 9300μm in the red in the sense that both collimator positions must be increased. Full details of the Savart plate are given in *"The ISIS spectropolarimetry users' manual" (La Palma Users Manual XXI)*.

- A polaroid filter, located in the same tray. This is used when full spatial coverage is required, and it is therefore impossible to use the dekkers which are used with the Savart plate. However for accurate spectropolarimetry the Savart plate is preferred.

5.6.3 The slit area

The slit is common to the two arms of ISIS, as well as FOS. The slit length is 53 mm (4 arcmin), and the width is continuously variable between 30 μm (0.14 arcsec) and 5 mm (22.6 arcsec). The slit is polished and aluminised and inclined to the optical axis of the telescope at an angle of 7.5 degrees to allow viewing of the reflected image in the A&G box TV camera. The width is driven by a linear motor, and encoded. The slit unit is a two position carriage, one position contains the conventional long slit, and the other position is a two position cross slide, containing a wide aperture which is used for mounting multi-slit masks, and the slit end of the ISIS fibre system. This cross slide is itself remotely driven from the ISIS 4ms microprocessor. Dekkers are mounted in 8 position slides, which are inserted in a driven mechanism immediately above the slit. The slides are interchangeable. At present there are two dekker masks, one for general use and one for spectropolarimetry (Table 5.10).
The long slit unit has gaps at each end, and it is important to use a long slit dekker (position 6 or 7) when observing, and not to observe with the dekker out (position 0). Ghosting is reduced considerably by use of the long slit dekkers.

5.6.4 Folds and Dichroics

There is a remotely driven three position slide mechanism which contains options for the blue fold. One of these positions is clear; the others contain any of: a folding prism; a 45 degree mirror; or any of a number of dichroic filters, which are listed in Table 5.11. There are five interchangeable slides for this slide mechanism. If the folding prism is used then the blue arm of ISIS will require a substantial refocus, in the sense that the blue collimator position must be increased by about 26000 microns compared with the value for a mirror or dichroic.

If a dichroic filter is in the beam the optical thickness of the material introduces a focus offset for the red arm or FOS. The focus offset for the red

Figure 5.11: The Polarimetry optics, slit area components, folds, and below slit filters of ISIS and FOS-2.

Table 5.10: ISIS/FOS Dekker Slides

Slide position	General dekker
1	1.2 arcsec hole
2	20 arcsec slot
3	Two 20 arcsec slots 100 arcsec apart
4	1.2 arcsec occulting bar in 20 arcsec slot
5	Clear
6	Clear
7	Clear
8	Clear

Table 5.11: ISIS Dichroic Filters

Dichroic Name	Half Power point of crossover (Å)	Width of crossover (Å)	Half power point of blue rolloff (Å)	Focus Offset for Red Arm (microns)
4500	4550	500	$<$3100	$\sim$250
5400	5300	450	3350	$\sim$400
5700	5700	350	3450	$\sim$750
6100	6100	400	3800	$\sim$750
7500	7200	800		$\sim$250

arm, in microns, is tabulated in Table 5.11. The value of the red collimator position is always higher if a dichroic is in the beam than if the red fold position is clear.

The 7500 Å dichroic gives only a 2 arcminute unvignetted field along the slit, and is generally used for stellar observations.

The red fold consists of a remotely driven two position slide; one position is clear while the other contains a silver mirror with a reflective stack overcoat to send light into the red arm.

5.6.5 Below Slit filters

There are four 2-position remotely driven filter slides: two in the blue arm beam just after the blue fold; and two below the blue fold but above the red fold; the latter two are for use with both the red arm of ISIS and FOS-2. There is a range of neutral density and colour filters for use in these slides. The blue arm filter slides are normally used to hold neutral density filters for when the IPCS is in use; the red arm filter slides are used to hold long pass filters to cut out second order blue light. The red arm filters slides can also hold a coloured field lens for use with FOS-2 in multi-slit mode. Care must be taken when mounting the slides since, although the red arm slides do fit in the blue arm slots and vice-versa, this will cause vignetting.

5.6.6 Collimators

Both collimators are off-axis parabaloids with a focal length of 1650mm, and provide a collimated beam of 150mm diameter. The coating material on the collimators is optimised for the wavelength range of the particular camera, and is silver with a reflective stack overcoat for the red collimator and aluminium for the blue camera.

As with most astronomical grating spectrographs, an image of the pupil is formed on the grating in order to minimise the grating size required.

The collimators are remotely driven by stepper motors and their position is encoded. The spectrograph arms are normally focussed by driving the collimators; and the collimator position is repeatable to better than 10 μm. With no extra refractive components (dichroics, prisms, Savart plate, filters) between the slit and the collimators the *nominal* focus positions for the ISIS collimators are 6000μm for the blue arm, and 9000μm for the red arm. The spectrograph should be focussed with the collimators within 3000μm of these nominal values, otherwise the spectrograph will be astigmatic, and the best focus on a spectral line will result in a degradation of the spatial resolution along the slit.

5.6.7 The ISIS gratings

Nine gratings are provided for ISIS, four for the red arm and five for the blue arm. The first letter of the grating name denotes the method of manufacture, eight of the nine gratings are copies of ruled masters manufactured by Milton Roy, whilst H2400B is a holographic grating manufactured by Jobin Yvon.

Figure 5.12: The ISIS Collimator Assembly

Table 5.12: ISIS grating properties

Grating name	Blaze (Å)	Dispersion (Å/mm)	Wavelength Pixel (Å) EEV	Tek	IPCS	Spectral range (Å) EEV	Tek	IPCS	Slit Width (arcsec) for 50μm (detector)
R158B	3600	120	2.70	2.88	1.26	3350	2949	3225	0.77
R300B	4000	64	1.44	1.54	0.67	1788	1576	1720	0.78
R600B	3900	33	0.74	0.79	0.35	919	809	887	0.82
R1200B	4000	17	0.38	0.41	0.18	472	420	457	1.00
R2400B	Holo	8	0.18	0.19	0.08	224	195	215	1.15
R158R	6500	121	2.72	2.90		3378	2970		0.78
R316R	6500	62	1.40	1.49		1733	1525		0.82
R600R	7000	33	0.74	0.79		919	809		0.90
R1200R	7200	17	0.38	0.41		472	420		1.15

The number denotes the number of lines per millimeter. The last letter of the name indicates which arm of ISIS it is intended for; those ending in B are intended for the blue arm, and those ending in R for the red arm. However the grating cells are identical, and all gratings will mount in either arm. All gratings have a ruled area of 154 x 206 mm. Grating R1200B was ruled in two halves; this can be seen quite easily if the grating is held up to the light.

Gratings can be used either blaze to collimator or blaze to camera. Use blaze to camera gives somewhat higher dispersion, but as the anamorphic reduction factor is reversed this is at the expense of a greatly reduced slit to plate reduction factor, *especially* at high dispersions. The ISIS gratings are almost invariably used blaze to collimator, and the slit widths given in table 5.12 are for this configuration.

Table 5.12 gives the parameters of the gratings, and the pixel size and spectral range obtained with EEV and Tektronix CCDs (22.5 and 24 micron pixels respectively) and for the blue gratings with the CCD-IPCS (10.5 micron pixels). The final column in the table below gives the slit width in arcseconds which will project to 50 μm on the detector.

There is also a single silver coated plane mirror in a grating cell, originally intended for alignment purposes, but which can be used in place of the gratings for direct imaging at a plate scale of 14.9 arcsec/mm. To use the mirrors for imaging they should be mounted in the grating cells, which should then be set to the autocollimation angles. The autocollimation angles are 35500 millidegrees for the red arm and 30800 millidegrees for the blue arm.

The grating cell angles are driven by a stepper motor from the ISIS 4ms microprocessor, and their positions are encoded by Ferranti 35HA optical absolute encoders. The units for these mechanisms are millidegrees, and the encoders are accurate to 3 millidegrees, and repeatable to 2 millidegrees. The grating angle offsets are grating independent.

Figure 5.13: The ISIS Grating Cells

5.6.8 Cameras

The ISIS blue and red cameras are of a folded Schmidt design, with a focal length of 500 mm giving a scale of 14.9 arcsec/mm along the slit. The air-glass surfaces of the refracting elements of the two cameras are coated with anti-reflection coatings optimised for the respective wavelength ranges, and the reflecting elements are coated with silver plus a reflective stack for the red arm, and aluminium for the blue arm.

5.6.9 Cross-Dispersers

Each arm has a slide for an optional cross-dispersing grism, although at present only the blue cross-disperser has been purchased. The cross-disperser is a special ruling 100 lines/mm fused silica grism blazed at 4400 Å. This will be used in conjunction with a prime disperser which is a Bausch and Lomb 75 lines/mm grating blazed at 3μm, to provide complete spectral coverage from 3000 - 5600 Å on an EEV P88300 or Tek 1024 CCD or the IPCS on the blue camera. The cross-dispersed mode will use orders 5 to 10, and the maximum slit length to avoid order overlap will be 30 arcsec. The spectral resolving power of the cross-dispersed mode is about 2200. Figure 5.14 shows the format of the cross-dispersed spectrum superimposed on the outlines of the IPCS and a TEK 1024 CCD.

5.6.10 Throughput

Nearly all of the light losses within ISIS are due to reflective and air-glass surfaces. There is a small loss of light (<10%) in each camera due to optical vignetting; and for the highest dispersions there is some loss due to overfilling of the grating. The throughput of ISIS has been measured by C.R. Jenkins and P. Terry, and their results are discussed in detail in *ING La Palma Technical Note no. 88*. Briefly the throughput of the red channel without the grating is measured to be 51%, and that of the blue channel without the grating to be 42%. These measurements were made with a HeNe laser at 6300 Å, and thus for the blue arm are slightly beyond the wavelength range over which it is optimised. The values for the red arm are also slightly low as the red fold mirror in use at the time was below its specification.
The efficiencies of the ISIS gratings have been measured in the laboratory and are presented in Figure 5.15. The holographic grating has a lower efficiency than the ruled gratings, and is also used at a grating angle such that the beam overfills the grating, resulting in some light loss.

5.6.11 Overall performance of the system

Table C.1.1 in Appendix C gives sensitivity values for ISIS and FOS-2 measured from wide slit observations of spectrophotometric standards, in the case of ISIS with the low dispersion (158 line/mm) gratings. These measurements give the overall performance for the entire system, including atmosphere, telescope, spectrograph and detectors. The performance is expressed as a magnitude (AB magnitude in Oke's system; see for instance

Figure 5.14: Format of the output of the blue cross-disperser, with IPCS (solid lines) and EEV P88300 CCD (dashed lines) outlines superimposed. The solid lines represent the outline of the IPCS field in a typical format, and the dashed lines a TEK 1024 chip. The crosses mark the points at which the grating efficiency drops to half of its peak value in that order. The central wavelength of each order is marked.

Figure 5.15: Efficiency curves for the ISIS gratings

Oke, Astrophys. J. suppl. **27**, 21, 1974) which gives a measured count rate of 1 photon/second/Å at the detector.

5.6.12 Stability and radial velocities

The original specification for ISIS was to have flexure no more that 5μm/hour along and perpendicular to the slit during telescope tracking. However measurements of the flexure caused by movements in elevation, and movements of the instrument rotator, suggest that flexure during tracking could be up to 15μm/hour. The cause of the extra flexure is not yet known, and until it is corrected it is recommended that observers requiring accurate radial velocities should take a calibration lamp exposure every 15 minutes.

Measurements of radial velocity standard stars taken during commissioning show that if care is taken with the calibration exposures it is possible to measure radial velocities to an r.m.s. accuracy in the range 1-2 km/s with the highest dispersion gratings (H2400B and R1200R) with either arm of ISIS. The *systematic* offset between ISIS radial velocities and the IAU velocity system is measured to be:-

$$(V_{IAU} - V_{ISIS}) = 8.9 \pm 4.9 km/s.$$

from blue arm observations of radial velocity standard stars and nebulae.

The stability of FOS-2 has been measured to be better than 1μm/hour when tracking an object through the zenith.

5.6.13 Scattered Light

Scattered light in ISIS is minimised by the use of optimised anti-reflection coatings, and if scattered light would be a serious problem for a particular observation it is important to exclude light of wavelengths other than those required, particularly wavelengths outside the range for which the coatings are optimised, from the optics by use of appropriate colour filters.

Diffuse scattered light has been shown to be below 2% by observations during commissioning of Quasar absorption lines known to be completely black.

Ghost images are caused by stray reflections within the spectrograph, and can either be in-focus images or images of the pupil. Pupil images take the form of the telescope pupil with the central obstruction, even if the illumination is from the comparison lamp system, because the illumination from the integrating sphere is designed to mimic exactly that of the telescope. This is not true of the comparison lamps for the fibre optic system.

There are a number of known ghosts in the ISIS system, these are listed below:–

- A ghost spectrum parallel to the primary spectrum which is seen in blue arm observations when a dichroic filter is used. It is caused by light reflected off the back surface instead of the front surface of the dichroic. It is strongest at wavelengths in the crossover region. The offset on the detector from the primary spectrum is 0.2 mm for the older (thin) dichroics; and 0.6 mm for the new (thick) dichroics.

- A Narcissus ghost pupil image which is caused by reflection between the surface of the CCD or its surrounds and the cryostat window. This appears strongest when caused by strong spectral features just off of the CCD, for example when looking at a Copper-Argon source at blue wavelengths at low dispersion, when the ghost is caused by reflection of the strong red lines from the surrounds of the CCD. If it is due to a continuum source the pupil image will be smeared in wavelength, and may be difficult to recognise as such. The intensity of this ghost is at the level of 10^{-4} of the primary source.

- A grating ghost caused by reflection between the grating and the aspheric plate of the camera when using grating R158R in the red camera. The ghosts images of all wavelengths add, so this ghost can appear quite strong.

- An in-focus ghost caused by a reflection from the folding prism, in either the red arm of ISIS or in FOS.

- Rowland ghosts, which are caused by periodic errors in the ruling of the gratings. These appear around strong emission or comparison lines, as satellite lines at the level of $>10^{-5}$ of the primary.

5.6.14 Wood's Anomalies in the ISIS gratings

Wood's anomalies are discussed in detail by P.G. Murdin in *ING La Palma Technical Note No. 76* in the context of INT IDS gratings, and a summary of the physical explanation for Wood's anomaly is repeated here.

Consider a reflection grating which produces a range of diffracted light in successive orders diffracted away from the normal. In some order, at some critical wavelength, the diffracted light lies in the plane of the grating. It is not possible for light beyond this point to be diffracted behind the glass of the grating. The power which would be sent into the forbidden region is redistributed back into the allowed orders. The power appears as an addition to the spectral response, with a sharp cut on at the critical wavelength and a steep decline to the red. This additional efficiency is almost entirely polarised perpendicular to the grating rulings.

Wood's anomalies occur at wavelengths:-

$$\lambda = d(\sin(\alpha) \pm 1)/n$$

where d is the grating groove separation; α is the grating angle (the angle between the grating normal and the collimator axis); and n is a positive or negative integer.

There are known to be Wood's anomalies in ISIS at 7200 Å (1200 grating, $n = 2$), 6400 Å (600 grating, $n = 4$) and 4400 Å (600 grating, $n = -2$).

Table 5.13: Summary of LDSS-2

Image scale at f/11 telescope focus	4.51 arcsec/mm
Image scale at f/2 camera focus	24.6 arcsec/mm
Collimator field of view	11.5 arcmin diam
Image size (90% encircled energy)	$< 30\mu$m imaging
	$< 40\mu$m spectroscopic
Design wavelength range	370–750 nm
Peak efficiency of main optics	84% at 600nm
Aperture wheel	8 positions (7 masks + 1 clear)
Filter wheel	8 positions (BVR + 1 clear)
Grism wheel	3 grism positions + 1 clear + 2 Harts

5.7 Low Dispersion Survey Spectrograph - LDSS2

The Low Dispersion Survey Spectrograph Reference manual

5.7.1 Overview

The Low Dispersion Survey Spectrograph LDSS-2 is a common-user wide-field multiaperture spectrograph mounted at the Cassegrain focus of the 4.2m William Herschel Telescope. LDSS-2 is similar to LDSS-1 (a non-common-user instrument at the AAT) but has a different optical design to cope with the WHT's f/11 Cassegrain focal ratio and to provide better images to exploit the superior seeing on La Palma.
LDSS-2 obtains spectra of many objects simultaneously using custom-made multiaperture masks held in the focal plane. Its high throughput and excellent sky subtraction provide good signal-to-noise spectra of faint objects while its large field of view and multiobject capability provide a large multiplex advantage for statistical projects.

5.7.2 Design

Fig. 5.16 shows a schematic diagram of LDSS-2 and Table 5.13 summarizes the main properties of the instrument.
The principle components are:

- **Aperture Wheel.** The telescope is focussed onto a multiaperture mask so that light passes through the apertures cut in the mask and enters the collimator. The masks are held in an 8-position wheel, allowing simple and quick changes between different masks. The multiaperture masks consist of a number of holes and slits (typically 330μm wide = 1.5 arcsec) cut in a brass disk. The masks can be made at the telescope close to the time of observation, using a specialized manufacturing facility which provides masks of very high quality.

Figure 5.16: Schematic of LDSS-2

- **Collimator.** The collimator converts the input f/11 beam into parallel light, before passing it through a filter and grism. The field of view has a diameter of 11.5 arcmin.

- **Grism Wheel.** Four grisms are provided of which 3 can be mounted in the grism wheel at any one time. These cover a range of spectral resolution $200 < R < 1000$, where $R \equiv \lambda/\Delta\lambda$ (see table 5.14).

- **Filter Wheel.** Up to 7 filters can be mounted in the filter wheel. Three broad-band filters (the BVR Harris set as used by NOAO) are provided together with 3 other filters designed for use in spectroscopic mode to suppress unwanted orders.

- **Camera.** The light is then focussed by the camera onto an external detector with a final focal ratio of f/2, giving an image scale of 24.6 arcsec/mm over a field of view with 11.5 arcmin diam. By using clear positions in the aperture and grism wheels, LDSS-2 can be used to give direct images in the chosen filter passband. The image size for 90% encircled energy is < 30 μm in direct imaging mode, and $\sim 40\mu$m in spectroscopic mode.

- **Detector.** LDSS-2 is normally used with the Tektronix 1024 CCD. In direct imaging mode this covers a 10.1 arcmin square field with an image scale of 0.59 arcsec/pixel.

- **Software.** An integral part of LDSS-2 is the LEXT software package which allows the observer to design the aperture masks, acquire the target fields and reduce the data. LEXT is a Starlink-compatible program which runs on a workstation at the telescope but can also be used at Starlink nodes.

5.7.3 Performance.

5.7.3.1 Efficiency

The throughput of the main optics and grisms as a function of wavelength are shown in Fig. 5.17.
The measured AB magnitude for 1 photon/s/Å is given in Table C.1.1 in Appendix C.

5.7.3.2 Wavelength Resolution and Range

The wavelength ranges and resolutions are summarized in Table 5.14

5.7.3.3 Multi-object capability

The maximum number of objects observable is limited by the number of spectra that will fit on the chip without overlapping. This is highly dependent on the distribution of target objects, but it is unusual to fit many more than ~ 30 objects on a single mask.

Figure 5.17: Laboratory measurements of the efficiency of, (a) the main optics (camera and collimator), (b) the grisms

Table 5.14: Grisms

Grism name	ruling density (/mm)	blaze wavelength (nm)	central wavelength (nm)	peak efficiency	dispersion (Å/pixel) with TekCCD	nominal resolution (Å)
Low	150	550	550	0.82	11.3	28.3
Med/Blue	300	500	550	0.76	5.3	13.3
Med/Red	300	600	550	0.74	5.3	13.3
High	600	500	420	0.64	2.4	6.0

5.7.4 Calibration Facilities

LDSS-2 uses the calibration facilities provided by the Cass A&G box as described in Section 2.1.6.2.

5.8 Utrecht Echelle Spectrograph (UES)

The Utrecht Echelle Spectrograph Reference manual

5.8.1 Overview

The Utrecht Echelle Spectrograph (UES) is the principal high-resolution spectrograph for the William Herschel Telescope. It offers the means to obtain spectra of objects as faint as ~ 17 magnitude with a resolving power R between $\sim 40\,000$ and $\sim 80\,000$. The spectrograph has been designed to operate from 3000 to 10 000 Å; the wavelength interval covered in a single exposure depends on the detector in use, and is typically in excess of 1000 Å. UES is permanently located in a thermally stable enclosure on one of the Nasmyth platforms at the f/11 focus of the WHT and can normally be deployed quickly from one of the other focal stations. The optical design of the spectrograph is very similar that of the University College London Echelle Spectrograph in use at the coudé focus of the Anglo-Australian Telescope, described by Walker & Diego 1985 (MNRAS, 217, 355). A detailed description of UES and its operation is given in the UES manual by S. Unger, M. Pettini and N. Walton (User Manual No. XXIII).

5.8.2 Design

The layout of the spectrograph is shown schematically in Figure 5.18. The slit S is at the focal plane of the telescope. The light from the slit image (beam a) is collimated (beam b) by an off-axis parabolic mirror C, and traverses the three cross-dispersing quartz prisms P1, P2 and P3 before beam c is incident on the echelle grating E. The axes of beams a, b and c are horizontal. The light is dispersed in the vertical plane (beam d) by the echelle grating (beam d) and is finally re-imaged by the camera.
The main components are as follows:

- **Slit unit.** The scale at the slit is 4.44 arcsec mm^{-1} (1 arcsec = 225 μm)[1]. The slit has a maximum length of 5 arcmin; a dekker of continuously variable width is used to define the slit length. The slit width can be set to between 0.09 and 90 arcsec. The entire slit assembly can be rotated from -12 to $+11$ degrees relative to the nominal position; this is required to ensure that the slit image is perpendicular to the direction of dispersion (along the spectral orders). A shutter is mounted at the rear of the slit. The slit jaws are polished so that they can be viewed with the acquisition TV or by the autoguider.

[1] With the Nasmyth image derotator in the beam, which is the normal mode of operation of UES

Figure 5.18: Schematic of the Utrecht Echelle Spectrograph (UES).

- **Collimator.** There is a choice of two collimators which can be selected remotely. One collimator has been coated for best performance at wavelengths below 4000 Å, while the other is silver coated for high reflectivity longwards of 4000 Å. The collimators are off-axis paraboloids with focal length of 2359 mm; the diameter of the collimated beam is 215 mm. A Hartmann unit is available in front of the collimator assembly for focusing the spectrograph.

- **Cross-dispersing prisms.** Unlike most other echelle spectrographs in use on 4-m class telescopes, UES uses prismatic cross-dispersion to separate the echelle orders. The reasons which led to this choice are discussed in the article by Walker & Diego referenced above. Compared with grating cross-dispersers, prisms offer the advantages of higher efficiency and more uniform inter-order spacing. In order to maintain high efficiency down to 3000 Å, the UES prisms are made of extremely homogeneous fused silica. However, the prism size demanded by the optical design is beyond the limits of current manufacturing technology. In order to provide sufficient cross-dispersion, three smaller prisms are used in series; each prism is in turn composed of three smaller units optically contacted together by means of a UV transmitting fluid.

- **Echelle grating.** Two are available (and remotely selectable). Both were manufactured by Milton Roy, have ruled area of 204 $\times$ 408 mm and nominal blaze angle of 63.4 degrees. One echelle grating has a ruling of 31.6 grooves/mm, while the other has 79 grooves/mm. The spectral formats produced by the two echelle gratings are detailed in Tables 5.8.2 and 5.8.2.

  Both echelles provide the same linear dispersion at the detector, and therefore the same resolving power for a given slit width. However, the free spectral range of the former is 2.5 times shorter than that of the latter; consequently, the spectral orders are 2.5 times closer together with 31.6 than with the 79 grooves/mm echelle grating. Thus, the 31.6 ruling is the preferred choice when continuous wavelength coverage of the echelle orders is the overriding consideration, while the 79 is the grating most often used for observations requiring accurate registration and subtraction of the sky signal along the slit (the maximum slit length which can be accommodated with the 79 grooves/mm echelle is 2.5 times greater than with the 31.6).

- **Camera.** This is of folded Schmidt design with a field flattener lens, and is described by Wynne 1977 (MNRAS, 180, 485). The focal length is 700 mm. The nominal, unvignetted field of view is 38.5 $\times$ 18.8 mm, the longer dimension being along the echelle orders.

- **Detectors.** Any of the detectors available on the WHT (see Chapter 6) can be mounted on UES. The most commonly used detector is one of the thinned Tektronix chips, which has a high efficiency over a broad range of wavelengths. For observations of faint objects the IPCS is the detector of choice, because of its extremely low dark count and lack of read-out noise. Note that of the detectors currently available, only the IPCS, with its 10 micron pixels, can sample the full resolving power of UES.

Table 5.15: Spectral Format of the 31.6 grooves/mm Echelle Grating — Sample Orders

Order	Start λ (Å)	Central λ (Å)	End λ (Å)	FSR (Å)	FSR (mm)	LD (Å/mm)	CD λ_{min} (mm)	CD λ_{max} (mm)	Order Sep (mm)
189	3005.97	3013.94	3021.92	15.9	12.9	1.240	0.01	1.15	1.15
163	3485.51	3496.23	3506.96	21.4	14.9	1.439	27.07	28.00	0.93
142	3999.48	4013.61	4027.75	28.3	17.1	1.652	45.08	45.86	0.78
126	4505.17	4523.12	4541.07	35.9	19.3	1.861	56.84	57.53	0.68
114	4977.00	4998.93	5020.85	43.9	21.3	2.057	64.69	65.31	0.62
103	5505.52	5532.38	5559.23	53.7	23.6	2.277	71.24	71.80	0.57
95	5966.32	5997.89	6029.46	63.1	25.6	2.468	75.66	76.20	0.54
81	6990.28	7033.69	7077.11	86.8	30.0	2.895	82.87	83.37	0.50
71	7967.06	8023.56	8080.07	113.0	34.2	3.302	87.80	88.30	0.49
63	8969.86	9041.62	9113.38	143.5	38.6	3.721	91.81	92.32	0.52
57	9904.94	9992.60	10080.25	175.3	42.6	4.112	95.00	95.56	0.56
52	10847.29	10952.60	11057.91	210.6	46.7	4.507	97.93	98.56	0.63

FSR: - Free Spectral Range
LD: - Linear Dispersion
CD: - Cross Dispersion

5.8.3 Performance

5.8.3.1 Scale at the detector

The demagnification of the UES camera gives a scale of 15.0 arcsec/mm (1 arcsec = 67 microns) in the spatial direction (along the slit) and 23.3 arcsec/mm (1 arcsec = 43 microns) in the spectral direction (across the slit and along the echelle orders).

5.8.3.2 Wavelength resolution

In its normal mode of operation, UES is used with a 1 arcsec wide entrance slit, producing a resolution element of 43 microns at the detector. This corresponds to a resolving power $R = \lambda/\Delta\lambda = 54\,000 = 5.5 km/s$ at

Table 5.16: Spectral Format of the 79 grooves/mm Echelle Grating — Sample Orders

Order	Start λ (Å)	Central λ (Å)	End λ (Å)	FSR (Å)	FSR (mm)	LD (Å/mm)	CD λ_{min} (mm)	CD λ_{max} (mm)	Order Sep (mm)
75	2992.98	3013.06	3033.15	40.2	31.2	1.286	0.00	2.89	2.89
65	3451.37	3478.12	3504.88	53.5	36.1	1.484	26.50	28.86	2.36
56	4001.42	4037.47	4073.52	72.1	41.8	1.723	46.08	48.04	1.96
50	4476.59	4521.81	4567.03	90.4	46.9	1.929	57.23	58.96	1.73
45	4968.08	5023.90	5079.72	111.6	52.1	2.144	65.51	67.07	1.56
41	5446.42	5513.66	5580.90	134.5	57.2	2.353	71.54	72.98	1.44
38	5870.33	5948.60	6026.87	156.5	61.7	2.538	75.76	77.12	1.36
32	6952.66	7063.02	7173.38	220.7	73.2	3.014	83.60	84.86	1.25
28	7927.09	8071.22	8215.35	288.3	83.7	3.444	88.58	89.82	1.25
25	8858.22	9039.00	9219.78	361.6	93.7	3.857	92.35	93.65	1.30
22	10037.15	10270.57	10503.99	466.8	106.5	4.382	96.37	97.83	1.46

FSR: - Free Spectral Range
LD: - Linear Dispersion
CD: - Cross Dispersion

all wavelengths. With currently available CCDs this resolution element is just sampled adequately with two detector pixels; the IPCS allows better sampling of the instrumental profile with four detector pixels. The optical quality of the spectrograph can deliver $R \simeq 100\,000$ with a sufficiently narrow slit (0.5 arcsec). While the WHT seeing is often well matched to such narrow slits, only the IPCS with its 10 micron pixels can at present take advantage of the resulting resolving power.

5.8.3.3 Wavelength coverage

While the spectrograph is designed to be efficient from 3000 to 10000 Å, only a fraction of the full range is passed by the camera field of 38.5 × 18.8 mm. The wavelength interval encompassed by these dimensions is a function of wavelength; representative values are $\simeq$ 700 Å at 4000 Å and 2700 Å at 6500 Å. Even these intervals will be covered fully (i.e. with no gaps between successive echelle orders) only for some combinations of echelle grating and detector. For example, with the 1024 × 1024 micron pixel Tektronix CCD and the 31.6 grooves/mm echelle, continuous spectral coverage is possible only for wavelengths less than approximately 5750 Å; further into the red two CCD exposures are required to cover the free spectral range of this grating. With the IPCS and the 79 echelle, two exposures are needed to encompass the full FSR at all wavelengths where the IPCS may be used in preference to a CCD (i.e. shortward of $\sim$ 5500 Å).

5.8.3.4 Order separation

The separation of successive spectral orders on the detector is a function of both wavelength and echelle grating in use. The function has a minimum near 7500 Å, where adjacent orders are separated by 1.24 and 0.49 mm with the 79 and 31.6 echelle gratings respectively. The corresponding separations on the sky, which in turn determine the maximum slit lengths usable before orders overlap, are 18.6 and 7.5 arcsec respectively; in practice somewhat smaller values (~ 17 and ~ 6 arcsec) would be used to ease data extraction from the 2-D frames. Maximum order separation is in the ultraviolet; for example at 3500 Å successive orders are separated by 35 and 14 arcsec with the 79 and 31.6 echelle gratings respectively. For this reason, the 31.6 echelle is normally used for observations of objects which are much brighter than the sky, while the 79 grating is more appropriate for fainter objects, requiring accurate sky subtraction with minimum deterioration of the S/N.

By using an order sorting filter to separate a single echelle order (at Hα, for example), it is possible to use UES to obtain spatially resolved observations of extended objects up to the full 5 arcmin length of the slit (with some minor vignetting at the edges). Any of the TAURUS narrow band filters listed in Appendix D can be used for this purpose.

5.8.3.5 Throughput

A useful figure of merit for UES is that at 4000 Å an object with $AB_{4000} = 17.0$ (defined as usual above the atmosphere), observed through a wide slit (no light losses at the slit), will produce 1 electron/s/Å when observed with the Tektronix CCD. This figure can be converted to a more useful count rate by adopting: *i)* 67% transmission for the atmosphere at ZD = 30 degrees; *ii)* 65% transmission through a 1 arcsec wide slit in 1 arcsec FWHM seeing; *iii)* a pixel size of 0.043 Å in the spectral direction. With these parameters, an object with $AB_{4000} = 17.0$ will give a count rate of ≈ 19 electrons per wavelength bin per 1000 s integration, adding all the counts along the slit. From these guidelines, approximate exposure times for objects of interest can be estimated. Obviously, the final S/N will include contributions from sky subtraction and systematic sources of noise such as read-out, dark current and cosmic rays.

The count rates obtained with the IPCS at 4000 Å are approximately 6 times lower than the above values.

Table C.1.1 in Appendix C lists values of AB magnitude giving 1 electron/s/Å for the combination WHT+UES+Tektronix CCD over the full optical range, from 3500 to 8500 Å (the estimated errors are ± 0.1 mag).

5.8.3.6 Stability

UES is located in an enclosure which uses active thermal control to stabilize the temperature of the spectrograph. Normally, image shifts at the detector are 1 micron per hour or less.

5.8.4 Acquisition and guiding

The UES is normally used with the Nasmyth image derotator, so that the orientation of the slit on the sky remains constant while the telescope is tracking the source. If preferred, the derotator can be set to track the vertical direction on the sky, so as to align the wavelength spread produced by differential atmospheric refraction along the length of the slit. This procedure is recommended to avoid light losses at the slit when recording a wide wavelength range, since UES has no atmospheric dispersion compensator.
UES has a dedicated acquisition and guiding unit (Section 2.1.6.3, which uses a CCD autoguider. This allows *(a)* direct viewing of the field and of the slit, for target acquisition; *(b)* guiding off light reflected from the slit jaws (when bright objects are being observed); and *(c)* offset guiding from nearby stars.
There are drawbacks, however. First of all, the field of view passed by the image derotator, and therefore accessible to the autoguider, is limited to a diameter of 5 arcmin; secondly, only small portions of this field can be viewed by the autoguider at any one time, by means of optical fibres which can be moved in x and y.
Since October 1994, the limiting magnitude of the UES autoguider is around V=17 in good seeing in bright time. For most UES targets guiding from the slit image should be possible, if the programme object is fainter than this then an offset guide star must be used.

5.8.5 Calibration facilities

The UES A&G unit provides a range of comparison lamps (both emission line and continuum), and neutral density, polarizing and colour filters. The UES Manual gives a full listing. The present set of neutral density filters is known to introduce a ripple in the signal at a level of a few percent peak-to-peak; possible replacements are currently being considered. Wavelength calibration normally uses a Th-Ar hollow-cathode reference lamp.

5.8.6 Operation, data acquisition and reduction

The operation of the system is described in detail in the UES Manual, which gives a full list of commands. Normally, only minimal setting-up by the user is required. The interface to the instrument is similar to that developed for UCLES at the AAT and, once the user has specified the desired echelle grating and central wavelength, the spectrograph is automatically configured to the optimum setting. Wavelength setting is normally accurate to within

1 CCD pixel. Standard procedures for checking the spectrograph focus are available at the telescope.

The software package ECHWIND, available at the WHT and at most STARLINK nodes, allows the optimum echelle format(s) to be selected prior to an observing run, depending on the detector to be used, spectral features of interest, etc.

Various software packages are available for the reduction of echelle spectra. Of these, the echelle-related commands within FIGARO, and the standalone package ECHOMOP by D. Mills of UCL, have been developed with the characteristics of UES (and UCLES) data in mind. A full atlas of the UES spectrum of the Th-Ar lamp from 3 000 to 10 000 Å, as produced by the 31.6 grooves/mm echelle grating is available from RGO (La Palma Technical Note No. 91).

Data can be transferred directly to the data reduction Sparcstation, where FIGARO and IRAF are available.

5.9 TAURUS-2

The Taurus-II Reference manual

5.9.1 Overview

TAURUS is a wide-field imaging Fabry-Perot interferometer designed to obtain spectra over a field of up to 9 arcmin with a resolving power anywhere between 2,000 and 100,000. Its main use is in measuring velocity fields of extended emission line objects — HII regions, planetary nebulae, supernova remnants and galaxies.

The principles behind the operation of TAURUS are described in detail by Taylor & Atherton *(Monthly Notices of the Royal Astronomical Society, vol 191, p675, 1980)*, Atherton et al. *(Monthly Notices of the Royal Astronomical Society, vol 201, p661, 1982)* and Taylor et al. *(Indirect imaging, ed. J Roberts, publ. CUP, p379, 1984)*. These papers also give a description of the original version of TAURUS, which is no longer available. TAURUS-2, the instrument currently in use on the WHT, is described in Unger et al. *(Monthly Notices of the Royal Astronomical Society, vol 242, p33p, 1990)*.

The way TAURUS operates is that the beam from the telescope is first collimated and then passed through a Fabry-Perot etalon. The field modulated by the Fabry-Perot interference rings is re-imaged by a camera onto a two-dimensional detector. The observing wavelength, and hence the order of interference at which the interferometer works, is determined by an order sorting filter, which can be placed either in the focal plane of the telescope, or in the collimated beam.

A TAURUS spectral scan normally consists of a large number (typically 60) of separate 2-dimensional images taken sequentially at different gap settings of the Fabry-Perot etalon, each giving a two-dimensional image in a different wavelength bin. By stacking these together it is possible to build up a 3-dimensional spectral line datacube.

5.9.2 Design

TAURUS-2 is the second generation instrument inspired by the success of the original TAURUS-1 wide-field imaging Fabry-Perot interferometer. The instrument was re-designed as a common-user facility and built under contract for both the WHT and the AAT by the Kapteyn Sterrenwacht, Roden. A major design goal of TAURUS-2 was that, unlike TAURUS-1, it should be a straightforward and flexible instrument to use. In order that the instrument can be reconfigured easily, it is possible to change remotely between a wide range of filters, etalons and apertures.
The major optical components of TAURUS-2 are shown schematically in Figure 5.19. The components are as follows:

- **Focal plane filter wheel.** This has 8 positions, each of which can hold a circular filter up to 125 mm in diameter. The filters available for use with TAURUS-2 are listed in Appendix D. The filters can be tilted remotely by up to 10° in order to shift the central wavelength to the blue (see 5.10.5).

- **Focal plane aperture wheel.** This has 8 positions, each of which can hold an aperture mask. Table 5.9.2 lists the aperture masks currently available.

Table 5.17: TAURUS-2 aperture masks

Position	Aperture
1	Clear, diameter 120 mm (9 arcmin)
2	Diffuser
3	Central pinhole, diameter 300 μm (1.35 arcsec)
4	Central hole, diameter 2 mm (9 arcsec)
5	Clear, diameter 120 mm (9 arcmin)
6	Clear, diameter 120 mm (9 arcmin)
7	Clear, diameter 120 mm (9 arcmin)
8	Pinhole matrix, grid spacing 10 mm (45 arcsec), pinhole diameter 200 μm (0.9 arcsec)

- **Variable iris.** The field diameter is defined by a variable iris placed at the f/11 Cassegrain focal plane.

- **Collimator.** The collimator has a focal length of 660.3 mm. The diameter of the collimated beam is 60.3 mm. The position of the collimated beam does however change as a function of field angle and wavelength, giving an effective total diameter for broadband wide-field observations of about 68 mm.

Figure 5.19: TAURUS-2

- **Pupil plane filter wheel.** This has 8 positions, each of which can hold a circular filter up to 76 mm in diameter. Filters with a smaller diameter than the collimated beam (about 68 mm) will cause vignetting. The filters available for use with TAURUS are listed in Appendix D.

- **Fabry-Perot etalon.** The Fabry-Perot etalons used in TAURUS-2 were constructed by IC optical systems. They are piezo-scanned and are stabilized in parallelism and gap by means of a Queensgate Instruments CS100 capacitance-micrometer servo-stabilization system. The optically contacted construction of the etalons renders them highly insensitive to vibrations and misalignment which could result, for example, from changes in orientation at the Cassegrain focus. The response time to a $\lambda/2$ (one order) step input is about 300 microseconds. Typical performance of the system is such that a 'mechanical' finesse N $>$ 50 can be maintained almost indefinitely. The Fabry-Perot etalons available are listed in Table 5.9.2. Note that the set of etalons previously advertised as being available for observations with TAURUS-1 *cannot* be used in TAURUS-2.

Table 5.18: TAURUS-2 etalons

Gap (μm)	Wavelength Range (Å)	Wavelength (Å)	Free Spectral Range (Å)	(km/s)	Resolution (Å)	(km/s)
125	4500-7000	5000	10	600	0.5	30
		6500	17	785	0.85	39
500	4500-7000	5000	2.5	150	0.125	7.5
		6500	4.2	195	0.21	9.75
86	3700-4500	3750	8.2	654	0.41	33

- **Camera.** There is a choice of either an f/2.11 camera or an f/3.96 camera, with focal lengths of 128.1 mm and 240.1 mm respectively. These cameras provide scales at the detector of 23.25 arcsec/mm and 12.40 arcsec/mm respectively.

- **Detectors.**

  TAURUS–2 can be used with either the CCD-IPCS photon counting detector or a CCD. The question of which detector should be used for a given programme is discussed below.

5.9.3 Performance

5.9.3.1 Field of view

There are a number of factors which limit the field of view of TAURUS-2: An absolute limit to the field size obtainable with TAURUS-2 is the field cutoff of the collimator, which is 9 arcmin.

When order sorting filters (see 5.9.4.2) are placed in the focal plane, they may further limit the field of view. The scale at the input focal plane is 4.51 arcsec/mm for TAURUS-2. The diameters of all the order sorting filters available for TAURUS-2 are listed in Appendix D. This constraint can be avoided by using filters in the pupil plane. However, using filters in the collimated beam leads to an increased risk of ghost images, and in the case of the smaller filters may cause vignetting.
The field of view of TAURUS-2 is not limited in the conventional way by the Jacquinot criterion *(Journal of the Optical Society of America, vol 44, p761, 1954)*. At high resolutions, the field will however be limited by the width of the interference fringes. The wavelength change across a detector pixel increase with both the distance from the field centre and with the resolution, so there exists an off-axis angle beyond which the wavelength change across a single pixel is greater than the spectral resolution. For a pixel size of p micron and a resolving power R, the off-axis angle in arcmin at which this results in a a degradation of resolution by a factor of $\sqrt{2}$ is given by:

$$\theta = k \times \frac{10^4}{R} \times \frac{50}{p} \tag{5.1}$$

$k = 12.5$ for TAURUS-2 with the f/2.1 camera
$k = 23.5$ for TAURUS-2 with the f/4 camera

The field size will also be limited by the amount of memory available to store the TAURUS datacube during the data acquisition process. is organised means that the field size must be an integer power of 2. The amount of memory available is currently 32 Mbyte, which taken together with the need to sample the spectral dimension properly, means that the largest datacube possible has dimensions of 256×256×60.

5.9.3.2 Spatial resolution

When TAURUS-2 is operated with the CCD-IPCS, there is a choice of 4 different pixel sizes; Table 5.9.3.2 lists the pixel sizes in arcsec for each camera. Note however, that although it is possible to obtain an IPCS pixel size as small as 10.5 μm, the detector limited resolution may be rather greater than this. The best resolution that has been obtained in practice is about 20 μm; a more typical value would be 30 μm.
TAURUS-2 can also be used with either the EEV or Tektronix CCD, and Table 5.9.3.2 gives the pixel scales provided by these detectors.

5.9.3.3 Spectral resolution

The spectral resolution obtained using TAURUS is equal to the free spectral range of the etalon divided by its finesse. The free spectral range is a function of the etalon gap and the wavelength, and is summarised for the etalons currently available in Table 5.9.2.
The etalon finesse depends on a number of factors, including the surface quality and reflectivity of the etalon plates, and the accuracy with which

Table 5.19: Pixel sizes in arcsec for TAURUS-2

Detector	IPCS resolution factor	Detector pixel size (μm)	Pixel size on sky (arcsec) f/2.1 camera	f/4 camera
CCD-IPCS	×1	84	1.95	1.04
CCD-IPCS	×2	42	0.98	0.52
CCD-IPCS	×4	21	0.49	0.26
CCD-IPCS	×8	10.5	0.24	0.13
EEV CCD		22.5	0.52	0.28
Tek CCD		24.0	0.56	0.30

they can be maintained in alignment. Values of the finesse measured on the telescope are typically about 20, and the spectral resolution obtained with this finesse for each of the TAURUS is etalons is given in Table 5.9.2.

5.9.3.4 Throughput

The efficiency of the TAURUS-2 focal reducer (i.e. camera and collimator) is shown as a function of wavelength in Figure 5.20. The peak efficiency is 65 per cent. The throughput of the Fabry-Perot etalons used in TAURUS is difficult to quantify, but should be in the range 70 to 90 per cent. The triple period interference filters used as blocking filters have a typical peak transmission of about 60 per cent. The peak efficiency of the complete system is therefore likely to be about 30 per cent.

5.9.4 Specifying the configuration of TAURUS

5.9.4.1 Choice of etalon

The correct etalon to use for a given project is one which gives the required spectral resolution, whilst at the same time providing a free spectral range which is larger than the velocity range of the emission-line region to be observed. Since the spectral resolution is directly dependent on the free spectral range, and there is in any case only a limited choice of etalons, it may not always be possible to satisfy both of these criteria.

It should be emphasised that if the free spectral range of the etalon being used is smaller than the velocity range of the emission-line region being observed, then emission from more than one interference order will be detected simultaneously, making interpretation of the date close to impossible. It is *not* possible to increase the observable velocity range by combining multiple observations obtained at slightly different wavelengths.

It is worth noting that the 86 μm etalon gives a similar wavelength range and resolution at [OII]λ3727 as the 125 μm etalon at [OIII]λ5007 and Hβ. One reason for using the former etalon is that by observing the [OII] doublet it should be possible to map the density distribution of the emission line

Figure 5.20: The efficiency of the TAURUS-2 focal reducer (i.e. camera plus collimator)

region as well as the velocity field; however, at the time of writing, this has not yet been tried in practice.

5.9.4.2 The need for order-sorting filters

An important point when planning observations with TAURUS is that since the interferometer operates at a high order of interference (typically a few hundred), it is necessary to isolate the wavelength region of interest using an order sorting filter. For observations of objects at high redshift, or of unusual emission lines, it is important to check that a filter with a suitable central wavelength is available. Also, the bandwidth of the filter should match the free spectral range of the etalon being used. If the bandwidth of the filter is less than the free spectral range of the etalon, this will restrict the wavelength range covered, whereas if the bandwidth of the filter is much larger than the free spectral range of the etalon, there is a risk of order confusion.

The filters can either be placed in the focal plane or the pupil plane, and there are a number of points to be considered before deciding which is most sensible. An advantage of using filters in the focal plane is that it is possible to shift the central wavelength to the blue (*not* to the red) by tilting the filter (Lissberger & Wilcock *Journal of the Optical Society of America, vol 49, p126, 1959*). At a tilt angle θ radians, the effective wavelength L_{eff} depends on the nominal wavelength L_{nom} as:

$$L_{eff} = L_{nom} \times (1 - \frac{\theta^2}{8.82}) \tag{5.2}$$

A disadvantage of using filters in the focal plane is that they may limit the available field size. This problem can be avoided by using filters in the pupil plane. As long as the diameter of the filter is larger than that of the collimated beam (about 68 mm) this will not cause vignetting. However, the risk of creating ghost images is greater.

It is important to note that the 50 mm square filters normally used for CCD imaging on the INT and JKT are *not* well suited for observations with TAURUS-2. When used in the focal plane filter wheel, they will restrict the field size to less than 3.76 arcmin. When used in the pupil plane filter wheel, they will cause vignetting. The larger filters which have been purchased specially for use with TAURUS-2 are listed in Appendix D.

5.9.4.3 Choice of detectors

TAURUS-2 is available for use with either the CCD-IPCS photon counting detector or with a CCD. In deciding which detector to use, the normal tradeoff has to be made between the higher quantum efficiency of the CCD, particularly in the red, and the lower detector noise of the IPCS. Which detector gives the optimum signal to noise depends on a number of factors, discussed in more detail in Chapter 6

However, in the case of TAURUS there is an additional factor to consider. A TAURUS spectral scan normally consists of a large number (typically 60) of separate 2D images taken sequentially at different gap settings of the Fabry-Perot etalon, each giving a two-dimensional image in a different wavelength bin. In order to minimize the effects of changes in atmospheric conditions during a scan, the integration time at each step should be kept to a minimum so as to complete a scan through the wavelength range as quickly as possible. When using the CCD-IPCS as a detector, the fact that there is no overhead associated with reading out each frame means that it is possible to scan through an entire datacube very quickly (typically 5-10 seconds), whilst the low noise level means that it is possible to add together the results of a large number of successive scans in order to obtain the required signal-to-noise ratio. In contrast, when using TAURUS with a CCD detector, it is likely to take 1-2 hours to complete a single scan of a datacube. This means that observations taken with the CCD-IPCS are much less likely to be affected by changes in atmospheric transparency than observations taken with a CCD.

5.10 WHT Prime Focus Spectroscopy Facility

A wide-field multi-object spectroscopy facility is currently under development for the WHT prime focus. Used with the prime-focus corrector and atmospheric dispersion compensator, it consists of a robotic fibre positioner with a choice of two fibre feeds, and an intermediate-dispersion spectrograph mounted on one of the Nasmyth platforms.

5.10.1 Description

Engineering details of most of the system can be found in the literature. The robotic fibre positioner, Autofib-2, was built at the University of Durham, and an account of the instrument is given by Parry et al. (in *Instrumentation in Astronomy VIII*, Proc. SPIE **2198** (1994), 125). Its control systems are described by Lewis, Jones & Parry (*ibid.*, 947). Much of the work on the first fibre feed has been carried out at the Royal Greenwich Observatory (RGO) and is described by Worswick et al. (*ibid.*, 44). The second fibre feed is still at the planning stage, but this will also be fabricated at RGO. The spectrograph itself is known as WYFFOS (WYde-Field Fibre-Optics Spectrograph); it, too, is being built at RGO, and a description is given by Bingham et al. (*ibid.*, 56).
Some of the main parameters of the facility are summarised in Table 5.10.1, and descriptions of the various components are given in the following paragraphs.

5.10.1.1 Autofib-2

Autofib-2 (AF2) is a ‘classical’ focal-plane pick-place fibre positioner, the third and most refined such instrument to be built by Parry’s group at Durham. The *(x,y)* carriage supports the gripper head; it also carries a machine-vision system that allows the exact position of any fibre to be measured by centroiding on the back-illuminated input-face. Fibre placement

Table 5.20: WHT Prime Focus System: Main Parameters

Field diameter	1 degree
Unvignetted field	40 arcmin
Plate scale	17.6 arcsec/mm (= 57.0 microns/arcsec)
Focal ratio	f/2.81
Fibre positioner	Autofib-2; capacity 160 fibres
Fiducial fibres	10 × 7-fibre guide bundles, res. 1 arcsec
Autoguider imageguides	1 fixed, 1 moveable
Science fibres (module 1)	126 × 153 micron (=2.7 arcsec)
Science fibres (module 2)	150 × 75 micron (=1.3 arcsec)
Cycle time	∼10 sec per fibre
Positioning accuracy	∼15 micron (absolute)
Science fibres length	26 metres
Slit optics (module 1)	Sapphire microlenses
Spectrograph	WYFFOS: Baranne white-pupil type
Collimator	f/8.2; (focal length=820mm)
Camera	f/1.2; (focal length = 132mm effective)
Dispersions (plane gratings)	11.5–0.8 Å/pixel
Dispersion (grism)	∼6 Å/pixel
Resolving power (echelle)	∼8000
Detector	Thinned Tektronix TK1024
Pixel size	24 micron square

can thus be made an iterative procedure, and there is a trade-off between placement accuracy and number of iterations (*i.e.* cycle time).
Two imageguides feeding the autoguider CCD camera allow direct inspection of star images in the field of the telescope (with a magnitude limit of about 14). One is mounted on the gripper assembly to allow pseudo-astrometric mapping of star-fields, while the other 'fixed sky probe' forms the off-axis autoguider. Ten 7-fibre fiducial bundles feed a TV viewing system; they are mainly used for field acquisition and visually monitoring the guiding.
The Vax-based Autofib Observing System allows the astronomer to communicate with the VME-based machine control system that interacts directly with the robot. Among the tasks available are CONFIGURE, which can be used off-line and allocates fibres to target objects, SET-UP, which sets up the fibres for observing, MAP, referred to above, and ACQUIRE, which maps and solves for the required offsets.

5.10.1.2 Fibre feeds

The science fibres and fiducial bundles are terminated at their input ends with SF5 microprisms whose input faces are wide-band coated. Their 92-degree angle provides median compensation for non-telecentricity, which amounts to four degrees at the edge of the field. The residual maximum tilt of two degrees is still enough to produce a field-dependent degradation of focal ratio from f/2.8 to f/2.3 in addition to the intrinsic focal-ratio degradation (FRD) of the fibre. This is one reason why an FRD-insensitive design was chosen for the spectrograph.

Each fibre is equipped with a magnetic button which holds it onto the (flat) field plate. The circular plate and its entourage of radially-disposed fibres are supported in a box from which trail the fibre cables to the spectrograph; the complete assembly constitutes a 'fibre module', which is easily removed from the robot to be interchanged with another. Coded proximity switches tell the Autofib control system which fibre module is in place.

The first fibre module contains 126 high OH^- fibres in 14 individually-cabled bundles of nine fibres, but it will be possible to image only about 120 of these onto the spectrograph detector at any one time. The fibres subtend 2.7 arcsec on the sky, and will be used principally for galaxy observations. Each of the 14 bundles has a nine-way fibre connector some 8.5 metres from the Autofib end to allow the lower part of the feed to remain permanently attached to the telescope.

At their output ends, the fibre bundles are brought together in a slit unit, where each group of nine is disposed in a skewed 3×3 array. The 14 arrays are then lined up in the collimator focus. The spectrograph thus sees three staggered fibre 'slits', an arrangement needed to accommodate the 2-mm diameter sapphire balls that terminate each fibre. These are used in a reverse-Fabry configuration, so that the fibre is imaged accurately onto the collimator while a pupil formed 0.9 mm from the surface of the microlens acts as the entrance slit. The pupil has a nominal diameter of 0.5 mm, but varies with the focal ratio of the beam emerging from the fibre; thus a change in focal ratio alters resolution rather than throughput.

Because the large fibres admit a high level of sky background, and because point images are not well scrambled at fast focal ratios (Watson & Terry, *Gemini*, No. 42 (1993), 32), a smaller second set will be provided (probably late in 1995) for observations of point sources. They will capitalise on the throughput-stability of the spectrograph for accurate sky-subtraction, and will make the best use of the site's sky conditions. For best possible performance, the connectors will be dispensed with and a wide-band hydrogenated low OH^- fibre-type will be considered as an alternative to the current one. It may also be possible to replace the sapphire balls with graded-index lenses.

5.10.1.3 WYFFOS

WYFFOS is built on a dedicated optical table in the GHRIL cabin on one of the WHT Nasmyth platforms. It follows the white-pupil design of Baranne (in *Very Large Telescopes and their Instrumentation*, ESO Conference and Workshop Proceedings **30** (1988), 1195), in which a dioptric collimator is used in double-pass (near-Littrow) mode with a reflection grating to form an intermediate spectrum close to a concave spherical relay-mirror. The Schmidt-type camera works at finite conjugates to re-image the intermediate spectrum onto the detector, while the function of the relay mirror is to image the collimator pupil onto the camera pupil. The configuration offers considerable stability with respect to vignetting, and allows modification of the effective pupil to ease the camera design and reduce the effect of the central obstruction.

The reflection grating can be replaced with an echelle for higher-dispersion work. Introducing a second collimator (with the relay mirror and camera re-positioned) permits the use of a grism for high-throughput low-dispersion work.

The beam emerging from each fibre is matched to the f/8.2 collimator. Immediately beyond the fibre slit is the spectrograph shutter, whose rear surface is used as a reflector for the fibre back-illumination source (an array of IR LEDs). Two filter slides (for colour and ND filters) follow, while the beam is still relatively narrow.

The four-element collimator is wide-band coated, though its twin for use with the grism has a multi-layer coating. Mirrors are overcoated silver, while the doublet Schmidt corrector and field-flattener of the camera are also wide-band coated.

In its reflection-grating mode, WYFFOS will use existing gratings belonging to the ISIS and IDS spectrographs of the William Herschel and Isaac Newton Telescopes. Of the many possible grating configurations, just three are shown in Table 5.10.1.3. They assume the use of the 2.7 arcsec fibres and the Tektronix detector.

Table 5.21: Examples of WYFFOS dispersion options using ISIS gratings

Grating	Wavelength (Å)	Reciprocal Dispersion (Å/mm)	Instrumental Resolution (Å)	CCD Resolution (Å/pixel)	Spectral Range (Å)
R158R	6500	479	39	11	—
R1200B	4000	63.0	5.1	1.5	1540
H2400B	4000	31.5	2.5	0.8	774

WYFFOS is controlled using EPICS/VxWorks on a VME micro. Motor-drives operate slit translation and focus, filter slides and the grating table, while the Hartmann shutters on the camera are operated pneumatically. The spectrograph shutter is under the direct control of the CCD system. The VME communicates with the Observing System on the Vax, and thence with Autofib-2.

For wavelength calibration, it is planned to direct a near-collimated beam from calibration lamps on or near the GHRIL table (adjacent to WYFFOS) *via* the Nasmyth flat to the prime-focus corrector and thence to the fibres. A disadvantage of this is that the beam entering each fibre will have a very slow focal ratio, changing the effective resolution of the spectrograph.

5.10.2 Status (Nov. 1994)

5.10.2.1 Autofib-2

AF2 underwent a rigorous test programme in Durham and Cambridge prior to its shipment to La Palma. There it was commissioned on the telescope in a ten-night run in October, 1994. Although hampered by bad weather, the run demonstrated performance levels comparable with those achieved in the UK tests.

Absolute placement accuracy is 15 microns (0.25 arcsec) with a mean placement time of 10 sec per fibre, the maximum number of permitted iterations being five. Full field set-ups took 20 to 25 minutes.

The emphasis of the commissioning tests was to establish the exact transformation required between sky positions and AF2 *(x,y)* coordinates so that each fibre can be precisely placed on its target. This involves knowledge of the geometry of the prime-focus field as imaged through the corrector. Initially, the information was determined from measurements of prime-focus plates. To refine the transformation as it applies to AF2, the robot itself was used to measure the positions of stars in the field. It can do this very accurately with the two sky-viewing probes. Towards the end of the run this mapping process was providing a fit with rms residuals of only 0.35 arcsec. It was also demonstrated that field acquisition was straightforward and could be done in under a minute.

AF2 performed reliably throughout the run and all aspects of its operation were tested. The daytime jobs of putting it on and taking it off the telescope are quite complex procedures. They went relatively smoothly, however, and no particular difficulties are foreseen in carrying them out routinely. Remaining work on AF2 consists mainly of tidying up a few loose ends in both hardware and software. The instrument will be formally handed over when WYFFOS is commissioned.

5.10.2.2 Fibres

The large-diameter fibre feed was tested at all stages of its fabrication, primarily for focal-ratio degradation and wide-band absolute throughput. The FRD performance of the finished feed is excellent, with 95 percent of the output flux contained within the input focal ratio of f/2.8. Laboratory tests of end-to-end throughput averaged over a bundle gave results in the range 70 to 80 percent at 5440Å, the variation arising principally in the connectors. Minimum connector loss is 6 percent. Data exist to confirm these values from the Autofib commissioning run; they are currently being reduced.

5.10.2.3 WYFFOS

Preliminary optical testing of WYFFOS in its reflection-grating mode has demonstrated that the optical components are within specification, an on-axis point source at the slit projecting to 1.1 pixels at the detector. Control tests using EPICS/VxWorks software have been successful.

The optical components of the WYFFOS transmission mode are currently under test at RGO. The only outstanding mechanical work is the fabrication of alignment jigs and enclosure panels for the WYFFOS optical table in the GHRIL cabin. Electronics and software work is proceeding. Final UK testing will take place with the entire instrument assembled in the RGO optical lab; this is scheduled for January, 1995. Commissioning on the telescope will take place during the first semester of 1995.

5.10.3 Expectations

Even with the larger fibres, the throughput-stability of the design should allow sky-subtraction with an accuracy of better than 1 percent. The smaller fibres will capitalise on the good seeing conditions of the site. Ultimate limiting magnitude for absorption-line spectra is expected to be fainter than B$\sim$21.5.

Autofib-2 and WYFFOS have been designed so that they can be operated independently of one another. A proposal already exists to use WYFFOS for integrated-field spectroscopy by means of a short reformatting fibre-feed from the Nasmyth focus. The modular construction of the Autofib feeds means that scope also exists for Autofib-2 to be used with a multi-object spectrograph other than WYFFOS. In combination or together, it is confidently expected that these two will form a cornerstone of the WHT's suite of instruments into the next millenium.

Chapter 6

Detectors

6.1 Introduction

The two types of electronic detector available on La Palma are a range of Charge Coupled Devices (CCDs) and the Image Photon Counting System (CCD-IPCS). These are described in Sections 6.2 and 6.3 respectively. The CCD-IPCS is available only at the WHT, where it is an option on the UES, the blue arm of ISIS and on TAURUS. A strong case would have to be made for using the IPCS for a particular application, since low noise, thinned, Tektronix CCDs are available at all three telescopes. Section 6.4 discusses how to decide which detector is best suited for a particular application.

6.2 Charge Coupled Devices (CCDs)

6.2.1 Overview

A Charge Coupled Device (CCD) is a 2-dimensional electronic image detector. Its enormous attractions for astronomers are threefold: linearity, with dynamic ranges of 10000 being realized; speed, with quantum efficiencies of up to 80 per cent; and wavelength response, some devices being usable from the near UV (< 300 nm) to the near IR (> 1 μm).
CCDs offer a considerably smaller area than photographic plates, but the improved performance generally outweighs this disadvantage. CCDs suffer from readout noise, which makes them less suitable than an IPCS at very low count rates, in particular while observing faint objects at high dispersion with the UES. CCDs integrate signal during the exposure, and then exhibit a finite read-out time afterwards- this can be many 10s of seconds for the large arrays; in contrast the IPCS has a real-time data collection.
CCDs are used on La Palma for both spectroscopic and imaging observations. This section is a brief description of these detectors. Some useful references for further reading are:

McLean, I.S. 1989. Ellis Horwood.
Electronic and computer-aided astronomy.

ESO-OHP workshop on the Optimization of the Use of CCD detectors

in astronomy.
Editors: Baluteau, J.P. & D'Odorico, S., 1986

Wall, J.V. & Laing, R.A.
User's Guide to the prime focus CCD camera on the INT

Argyle, R.W., Mayer, C.J., Pike, C.D. & Jorden, P.R.
User Guide to the JKT CCD camera, 1988.

Jorden, P.R. & Lupton, W.L.
Spectroscopy with the CCD on the INT, 1984.

Jorden, P.R. *Basic parameters of CCDs in use at La Palma,*
La Palma Technical Note 55, latest version Nov 1990

Jorden, P.R. *CCD Frame size parameters*
ING La Palma Technical Note 79, Dec 1990

Oates, A.P., & Jorden, P.R. *New Large-Format CCDs for the ING*
ING La Palma Technical Note 92, Nov 1993

Jorden, P.R. *Properties of Operational Cameras*
ING La Palma Technical Note 93, Jan 1994

6.2.2 General description

A CCD is a silicon based semiconductor arranged as an array of photosensitive elements, each one of which generates photoelectrons and stores them as a small 'bucket' of charge. Each pixel is typically 15 to 30 μm square. Our first CCDs had formats of about 400 rows by 600 columns, with an area of about 1 square centimetre. Current CCDs have formats of about 1024 $\times$ 1024 pixels, with a size of about 25mm square. We anticipate introducing 2048 $\times$ 2048 pixel CCDs before the end of 1995.
When requested, the elements form a bucket brigade; each row of charges is passed from element to element, a process which is known as clocking, down the columns and horizontally along the final row. The value in each pixel is measured in turn and recorded digitally. To ensure that only positive numbers result from this analog to digital conversion process a fixed offset known as the bias level is introduced. The charge-transfer process is essentially noise-free and almost all of the noise contributed to the signal by the CCD is from the output stage, where the charge content of each bucket is measured. This is called the readout noise.
The dark current of CCDs means that they must be cooled to cryogenic temperatures for use as astronomical detectors. At room temperatures, the dark signal is such that most CCDs would saturate in a few seconds. Cooling via temperature-controlled liquid-nitrogen dewars (or by closed-cycle refrigeration) provides a crucial reduction in dark current. The mobility of

electrons is somewhat impaired by cooling, so that a compromise is required to maintain adequate charge-transfer efficiency. The optimum temperature is about 150 K, depending on specific device type.

6.2.3 Design

CCDs require electronics to generate electrode biases, clocking waveforms, low-noise amplification of weak signals, A/D conversion, buffering, and digital storage. They also require temperature-controlled environments mountable at different telescope foci for direct imaging, and at spectrograph foci for use as spectroscopic detectors. The details of how operational systems meet these demands differ, but the major elements are similar.

The cryostat or dewar provides the cooled environment for the CCD. A liquid-nitrogen cryostat designed at RGO can be used in either downward or upward-looking modes, for example in direct imaging at prime or Cassegrain foci. It has a hold time of some 12 hours so that it only has to be filled once a night. The CCD itself is mounted behind an anti-reflection coated quartz window, on a copper block with which it makes good thermal contact and which has a temperature sensor attached. Resistive heating controlled by a feedback loop maintains the CCD at the optimum operating temperature to within ± 0.05 K. A preamplifier is mounted on the cryostat.

The electronics needed to drive the CCDs is not the same on the WHT as on the INT or JKT. However, the main functions remain the same: analogue signal sampling and CCD control, digitisation of data, telemetry of system voltages, control interfaces and data links to the instrument computer. The systems may be reprogrammed in order to use a wide variety of different chip types or operating modes. Windowed readout of the chip can be used to minimise readout time or data storage. On-chip binning can be used to increase signal to noise at the expense of spatial and spectral resolution. Five different readout speeds (faster readout gives higher readout noise), as opposed to two on the INT and JKT controllers, are available. Two different clearing speeds are also available.

6.2.4 CCD systems on La Palma

The CCD systems on La Palma use a variety of chip types; the earlier RCA-SID501 and GEC-P8603 have now been superseded by larger devices, primarily EEV P88300 and Tektronix 1024 square chips. Table 6.2.4 summarises important general parameters of the types of CCD chip available; La Palma Technical Notes 55 and 93 describe some of the CCDs in rather more detail.

It can be seen that there are a range of formats and performances available. The thinned TEK (and the older GEC7 and RCA) chips have a higher efficiency at most wavelengths, and so are better suited for most imaging applications. The lowest readout noise chips are usually preferred for most spectroscopic applications. The overall high efficiency, and low noise of the TEK CCDs makes them the preferred sensor for most general use. See also section 6.4. for a discussion about choice of detector. It should be noted that we hope to introduce larger, high performance CCDs in the next 2 years- refer to RGO for latest information.

Table 6.1: CCD parameters

Chip	EEV P88300	Tek 1024
Pixel size (μm)	22.5 × 22.5	24 × 24
Format (pixels)	1152 × 1242	1024 × 1024
Format (mm)	25.9 × 27.9	24.6 × 24.6
Readout frame (pixels)	1180 × 1280	1124 × 1124
Frame Readout time (seconds):		
Standard Speed	~130	~105
Turbo Speed	~60	~50
Electrons per ADU	~1	~1
Saturation (ADU)	>60000	>60000
R.Q.E. (per cent)		
Peak	55	75
400 nm	15	40
800 nm	40	60
Noise:		
Readout noise(electrons):		
Standard Speed	~4	~5
Turbo Speed	~5	~7
Dark count (e^-/pix/hr	<1	<1

6.2.5 Performance

6.2.5.1 Efficiency

The major advantage of CCDs over other detectors is their high efficiency. The wavelength response for the types of CCD currently in use on La Palma is shown in Figure 6.1. The best (thinned) devices have a peak efficiency of about 80 per cent, whilst the unthinned ones have a peak efficiency of about 50 per cent.

6.2.5.2 Noise level

The read out noise for the CCD chips used on La Palma is given in Table 6.2.4. This is typically 4-5 electrons per pixel.

Cosmic ray events become important for longer exposures, and are a worse problem with Tektronix chips than EEV. During an exposure cosmic rays hit the CCD. When a pixel is hit, its charge content is vastly increased and the resulting 'spike' in the image needs to be removed during the data reduction stage. This can be done either by numerical filtering techniques using the fact that the appearance of a cosmic ray event is quite distinct

Figure 6.1: Responsive Quantum Efficiency (RQE) as a function of wavelength for the Tektronix and EEV CCD detectors most commonly used on the La Palma Telescopes

from that of an astronomical object, or by combining multiple exposures of the same object.

6.2.5.3 Saturation level and dynamic range

The peak capacity of a CCD pixel is typically 200,000 electrons, and CCDs are demonstrably linear devices up to within a factor of two of this limit. When the limit is exceeded, the arrival of more photons continues to create further photoelectrons, which then spread out along the column of the CCD. In addition to saturating the chip, it is possible to saturate the analogue to digital converter; in fact, for most of our systems this will happen first.
Together with readout noise, the saturation level defines the dynamic range of a CCD, crudely, as (saturation level)/(readout noise)^2.
Where the readout speed can be varied, the "gain" of the CCD is higher (more electrons/ADU) at the faster readout speeds, and, as this is a stronger effect than the change of readout noise with speed, the dynamic range is increased at the faster speeds.

6.2.5.4 Charge transfer efficiency

At low light levels the charge transfer is sometimes imperfect resulting in slightly deformed images, showing a trailing along the rows and/or columns of the CCD. To increase the performance one can preflash the chip with a fixed amount of light. This is, of course, undesirable because it adds shot noise to the data. All the chips in use on La Palma have good charge-transfer characteristics and do not require preflash. The charge transfer characteristics are somewhat worse at faster readout speeds.

6.2.5.5 Cosmetic defects

Cosmetic defects can come in many varieties, and vary from chip to chip. Dark pixels, as a result of local poor charge-transfer inefficiency (traps) are unavoidable, but for most of our grade-1 chips only a small number (<10) should be seen, and then only at low signal levels. Defective areas such as bad columns, bad pixels or hot pixels cannot be cured. Each chip has its "fingerprint" of cosmetic defects and care should be taken to avoid the worst affected areas when positioning an object on the chip. Multiple exposures in which the object of interest is shifted to a different location on the chip between exposures may help to obtain clean images.

6.3 Image Photon Counting System (IPCS)

6.3.1 Overview

The IPCS is a blue-sensitive imaging detector, which counts individual photon events with zero readout noise and a dark current of only 4 counts/s/cm^2, which corresponds typically to 2×10^5 counts/s/pixel. The IPCS is therefore suited to detecting faint signals, which on a CCD would be dominated

by the readout noise. The saturation characteristics of the IPCS mean that it is *not* suitable for observations at high count rates.
The only IPCS detector available is the UCL-RGO CCD-IPCS on the WHT. This has a four stage EMI Image Intensifiet, coupled by a tranfer lens to a thinned GEC CCD. This system is known by the name CCD-IPCS to differentiate it from the old Plumbicon-based system, which was available at the INT but has now been decommissioned. The CCD-IPCS is available as a detector option for the UES, for Taurus, and in exceptional circumstances for the blue arm of ISIS. Potential users must justify in the technical case for their projects their choice of the IPCS as detector..
This section briefly describes how the IPCS works. Useful references for further reading are:

Boksenberg, A., *Proceedings of the ESO-CERN conference on auxiliary*
instrumentation for large telescopes, eds Lausten, S. & Reiz, A., p295, 1972.

Boksenberg , A. & Burgess, A., 1973. *Astronomical observations with television sensors, eds Glaspey, J.W. & Walker, G.A.H., p21, 1973*

Boksenberg A. *Philosophical Transactions of the Royal Society of London A,*
vol 307, p531, 1982

W.L. Martin & P.B. Taylor, *IPCS Users Reference Manual.*
(A detailed description of the INT system)

C.R. Jenkins, *IPCS Cookbook.*
(Spectroscopy with the IPCS on the INT)

C.R. Jenkins, *Monthly Notices of the Royal Astronomical Society, vol 226, p341, 1987.*
(Saturation characteristics of the INT IPCS)

6.3.2 Design

Ultimately, the information contained in an optical image can be expressed as the spatial and temporal variation in the number of photons. The problem of detecting and recording such an image is then essentially one of counting the number of photons in each image element.
The way in which the IPCS does this is shown schematically in Figure 6.2, and can be described in very general terms as follows: individual photon events are detected by means of an image intensifier, on the front of which is mounted a photocathode. Photons incident on the photocathode result in the emission of an electron. Each of these electrons triggers a cascade of electrons through the image intensifier, producing a signal of order 10^7 electrons at the output. This splash of electrons is detected by a TV cam-

era, and passed to a hardwired image processing unit which calculates the centroid of each splash, and hence the position on the photocathode of each photon event. The (x,y) coordinates of each photon event are then passed to the Detector Memory System (also known as the External Memory), which counts the number of photons detected in each pixel by incrementing an appropriate memory location. During the course of an integration, a 2-dimensional image or spectrum is built up in the Detector Memory System. In fact, the image can have more than two dimensions, since in addition to assigning each photon event an (x,y) coordinate, the events can be "tagged" with a third number (e.g. etalon gap for observations with TAURUS, UT for observations with high time resolution, Stokes parameter for polarimetric observations).

The IPCS can be broken down into the following components:

- **Photocathode.** This is an S-20 photocathode. The spectral response of this photocathode determines the spectral response of the IPCS as a whole, and is shown in Figure 6.3. It can be seen that the peak efficiency is about 20 per cent at a wavelength of 4000 Å. The efficency is poorer in the red, falling to about 5 per cent at 6500 Å and less than 1 per cent beyond 8000 Å.

- **Image intensifier**. This is a four-stage, magnetically focussed image intensifier, with a gain of about 10^7. The intensifier is manufactured by EMI, and is frequently referred to as the "EMI-tube". The usable area is about 40 mm in diameter, although the unvignetted area passed by the UES camera is 38.5 $\times$ 18.8 mm. Granularity of the available tubes has been measured at RGO to be 3 per cent rms; granularity due to intermediate photocathodes is diminished to around 1.5 percent rms by magnetically scanning the image inside the EMI-tube to reduce the effects of variations of these photocathodes. The scanning system used is described by Jorden, A.R. & Fordham, J.L.A. *(QJRAS, vol 27, p166, 1986)* The intensifier is protected from variations in the local magnetic field by a mu-metal shield.

- **TV camera.** The output of the EMI tube is lens coupled to a thinned GEC CCD camera. Note that the CCD camera used with the CCD-IPCS should *not* be confused with the CCD camera systems available on La Palma for CCD imaging and spectroscopy. The CCD camera in the CCD-IPCS is used as a rapid-readout TV camera, not as a faint light detector.

- **Data integration.** Once the (x,y) coordinates of each photon event have been calculated, they are passed to an external memory unit, which counts the number of photons detected in each image element. This is known as the the Detector Memory System (DMS). While data are being collated by the DMS, the astronomer can examine them.

Figure 6.2: A schematic representation of how photons are counted by the IPCS

6.3.3 Image size and pixel size

The IPCS can provide a wide range of different image formats. The choice of format is often difficult, especially since it affects the saturation characteristics of the detector. Potential users should consult the references listed above for a more detailed discussion. Briefly, the image format depends on two factors: Firstly, it is possible to vary the format of the image from the TV camera. Secondly, the signal produced at the TV camera by each photon event is strong enough that it is possible to calculate the centroid of the event to within a fraction of a TV pixel. Thus the pixel size of the final image in the Detector Memory System can be much smaller than the pixel size of the TV image, and the number of pixels can be correspondingly greater.
The readout uses a GEC CCD, and each pixel has a size in both directions corresponding to 84μm at the photocathode. These CCD pixels can be subdivided by factors of 1, 2, 4 or 8, producing pixel sizes in X and Y of either 84, 42, 21 or 10.5 microns. A typical setup uses 2560 $\times$ 560 pixels of dimensions 10.5 $\times$ 42 microns, the first figure in each case being in the dispersion direction.

6.3.4 IPCS Performance

6.3.4.1 Efficiency

The efficiency of the S-20 photocathode is shown in Figure 6.3. The probability that an electron emitted by the photocathode is counted (the counting efficiency) is of order 60 per cent. The overall efficiency of the IPCS is the product of these two numbers. It can be seen that the peak efficiency of the IPCS is 11 % at a wavelength of about 4000 Å, falling to 8 % at 5000 Å, and ~2.5 % at 6500 Å.

6.3.4.2 Noise

The EMI image intensifier used in the IPCS has a dark current of about 4 counts/cm^2/s. The noise level per pixel due to the dark current is proportional to the area of each pixel. The pixel size of the CCD-IPCS in standard spectroscopic format is 10.5 $\times$ 42 microns. implying a dark current of only 2 counts per pixel per 10^5 seconds.

6.3.4.3 Saturation characteristics

The time taken to read out the TV camera of the IPCS, and update the Detector Memory System is referred to as the TV frame-time. Clearly, at high light levels, when photons arrive at the same (x,y) coordinate within one frame-time, a system such as the IPCS will suffer from coincidence losses. The result is that the detector becomes non-linear, and the way in which this happens is discussed in detail by Jenkins *(Monthly Notices of the Royal Astronomical Society, vol 226, p341, 1987).* The only solution is to keep the

Figure 6.3: Responsive Quantum Efficiency as a function of wavelength for the S-20 photocathode used in the IPCS. The overall efficiency of the IPCS is equal to the efficiency of the photocathode multiplied by the counting efficiency, which is probably about 60 %

light level below the point at which coincidence losses become important. Rough estimates of acceptable light levels are as follows:
For the CCD-IPCS, coincidence losses of around 10% are anticipated at count rates of about 1 photon per pixel per second from continuum sources in lowest resolution mode with full format.

6.3.4.4 Geometric distortion

The IPCS suffers from a variety of image distortions (e.g. S-distortion, barrel distortion). The worst of these are removed online. However, the distortion gets worse towards the edge of the detector. If data at the edge of the detector is crucial to an observation, the image distortion should be calibrated out using observations of a "comb" dekker.

6.3.4.5 Granularity

The granularity of various components of the IPCS gives pixel to pixel variations in sensitivity of a few per cent. These can be calibrated out using flat fields. See Jenkins *(Monthly Notices of the Royal Astronomical Society, vol 226, p341, 1987)* for a much more detailed discussion.

6.4 Which detector ?

The first part of this chapter described the two types of electronic detector available on La Palma, the CCDs and the IPCS. This section describes how to decide which of these is best suited for a particular observation.

6.4.1 General Signal and Noise considerations

Probably the most important criterion in choosing a detector is the achievement of the required signal to noise ratio in the shortest integration time. The first step is therefore to define what signal to noise ratio is required for the observation to be successful. Having done that, we need to consider how to obtain this signal to noise ratio most efficiently.
The noise level for a typical astronomical observation will consist of three components. The first component is signal independent noise arising from the detector itself, readout noise in the case of a CCD and dark counts in the IPCS. Secondly, we have shot noise in the signal from the object being observed. This follows a Poisson distribution, so its variance is equal to the signal level. Finally, we also have shot noise in any background signal (particularly the sky background). Adding the noise terms in quadrature, the signal to noise ratio (SNR) is given by:

$$SNR = \frac{E \times N_{obj} \times t}{\sqrt{(E \times N_{obj} \times t) + (E \times N_{back} \times t) + \sigma^2}} \tag{6.1}$$

E	=	Responsive quantum efficiency of the detector
N_{obj}	=	Number of photons per resolution element per second incident on detector from object
N_{back}	=	Number of photons per resolution element per second incident on detector from background (e.g. sky)
t	=	Integration time
σ	=	Detector noise (readout noise, dark current)

The signal to noise ratio obtained therefore depends on both the efficiency of the detector and the level of detector noise. The way to choose the optimum detector is therefore to choose the combination of efficiency and detector noise which maximises the signal to noise ratio. The two detector types are complementary in this respect, since the IPCS has the lowest level of detector noise but is also the least efficient, the (thinned) CCDs are the most efficient detector but also have a finite noise level. We now quantify these statements more precisely.
Table 6.2 gives estimates of the efficiencies of some representative detectors at a number of wavelengths, using data taken from Sections 6.2.5.1 and 6.3.4.1.

Table 6.2: Detector efficiencies

Wavelength	Detector efficiencies (%)		
(Å)	IPCS (Tube 1759)	EEV P88300	Tek 1024
3500	10	13	25
4000	11	15	55
4500	9.7	17	63
5000	7.5	22	63
5500	5.5	37	67
6000	3.9	45	68
6500	2.7	46	70

The detector noise of a CCD is dominated by the readout noise. Note however that the number we really need is the readout noise per resolution element, not the readout noise per pixel. The readout noise per resolution element depends on two factors:

- How many CCD pixels are there in a resolution element ? In slit spectroscopy of a point object, the emission typically extends for several pixels along the slit, and we will need to bin these up in order to obtain a spectrum. Similarly, for an experiment to detect a well-resolved emission line, it may be possible to bin up several pixels in the dispersion direction into one resolution element. Note that according to sampling theory, a resolution element must always be at least two pixels in each direction. In order to obtain the effective readout noise per resolution element, the readout noise per pixel must be multiplied by the square root of the number of pixels in a resolution element.

- How many separate CCD exposures are being co-added ? The target object may be so faint that a very long integration time is necessary to obtain the desired signal level. The graphs in Section 6.2.5.1 can be used to estimate the total integration time required for a given telescope and instrument. If the total integration time is greater than about 1 hour, it will be necessary to split the observation into a number of shorter exposures. Each CCD exposure adds in more readout noise, resulting in the effective detector noise being equal to the readout noise per exposure times the square root of the number of exposures.

The detector noise of the IPCS comes from the dark count, which is so small that we can neglect it at all practical light levels.

6.4.2 A comparison between CCD and IPCS

In order to show how the principles outlined above work out in practice, we concentrate on the comparison between spectroscopy with the IPCS and with the TEK-1024. The ideas discussed in this section can be extended to other detectors. In particular, the high efficiency of the CCD make it clearly the best detector for most imaging applications, but its finite readout noise means that it may be unsuitable for high dispersion spectroscopy.

A first relatively straightforward but important case to deal with is where the noise level is dominated by the shot noise of the sky background (sky limited observations). This is usually the case for low resolution spectroscopy or imaging observations. Typical values for the sky brightness on La Palma in a variety of wavebands are given in Section 1.3.2. As far as signal to noise ratio is concerned, it can be seen from Equation 6.1 that the most effective detector for sky limited observations is simply the most efficient. For all optical wavelengths this will be the Tektronix CCD.

We now consider the case where the sky background can be neglected, normally the case for high resolution spectroscopy. As we noted above, observations at high signal levels, where we might expect a high signal to noise ratio, will be best suited for the CCD, whereas observations at very low signal levels, and very low signal to noise ratio, will be best suited for the IPCS. It is interesting to define a break-even signal to noise ratio, equal to the signal to noise ratio which can be reached with the two detectors in the same integration time. Only if the signal-to-noise ratio you require or expect is less than the break-even value will the IPCS acquire it faster.

This is a particularly useful parameter since it is independent of the observed count rate and hence independent of the object being observed and the spectrograph configuration. However, the break-even SNR does depend on the effective CCD readout noise per resolution element and hence on the number of separate exposures required. Table 6.3 tabulates the break-even signal to noise ratio in two extreme cases; 1 CCD exposure with a resolution element of 4 pixels, and 10 exposures with a resolution element of 10 pixels.

Given that exposures of at least half an hour are standard on the Tektronix CCDs, it is clear from table 6.3 that only in the case of very long exposures for low expected signal-to-noise will the IPCS be the preferred detector, and it will never be the preferred detector for useful exposures at wavelengths longer than 5000 Å.

Table 6.3: Break-even signal to noise ratio

Wavelength (Å)	$\frac{\text{IPCS efficiency}}{\text{TEK efficiency}}$	Break-even SNR (1 exposure) (4 pixels)	Break-even SNR (10 exposures) (10 pixels)
3500	0.44	5.9	29
4000	0.22	2.5	12.5
4500	0.16	1.7	8.7
5000	0.11	1.2	5.8
5500	0.075	0.8	3.9
6000	0.053	0.5	2.7
6500	0.036	0.4	1.8

There are a number of factors in addition to the required signal to noise ratio which need to be taken into account when choosing a detector:

6.4.3 Other considerations

6.4.3.1 Detector size

The discussion in the previous section only considered how to maximise the signal to noise ratio per resolution element. For certain types of experiment, it may also be important to note that the detectors offer different choices of format and pixel size. For spectroscopic observations, the WHT IPCS provides 2560 pixels along the dispersion direction, each about 10.5 microns in size. The TEK CCD provides 1024 pixels along the dispersion direction, each 24 microns in size. At present the IPCS does offer smaller pixel sizes than any of our CCDS, and is the only detector capable of realising the full resolution potential of UES. We anticipate that smaller-pixel CCDS (15 micron) will be installed by the end of 1995..

6.4.3.2 Real time data display

One advantage of the IPCS over the CCD is the ability to inspect the data in real time. This makes it possible to terminate an exposure as soon as the required signal to noise ratio is reached, thus using observing time more effectively.

6.4.3.3 Time resolution

The IPCS is much better suited than the CCD to observations which require high time resolution (e.g. TAURUS-2, time resolved spectroscopy).

6.4.3.4 Saturation

One of the main disadvantages of the IPCS is its behaviour at high count rates. At count rates much above 0.1 counts per pixel per second the IPCS starts becoming nonlinear. The way in which it does this is rather complex, depending on both the format of the IPCS and the extent of the emission, and is discussed in some detail by Jenkins *(Monthly Notices of the Royal Astronomical Society, vol 226, p341, 1987)*. The maximum count-rate allowable for a particular observation depends on what degree of nonlinearity is acceptable. A common rule of thumb is that the count-rate should not exceed 0.5 counts per pixel per second. At this count-rate we might expect the deviation from linearity to be between 10 and 20 per cent. For observations which would give a higher count rate than this, it is necessary to reduce the count rate using neutral density filters.

6.4.3.5 Cosmic ray events

These are an important source of additional noise on a CCD. Cosmic rays which strike the detector produce bright and narrow noise spikes in the signal. The effect on the data depends exactly where on the detector the event occurs. The only way to deal with cosmic rays is to break long exposures into several shorter exposures. This has the major disadvantage of increasing the total readout noise.

6.4.3.6 Cosmetic defects

As we noted in Section 6.2.5.5, CCDs can suffer from a wide range of cosmetic defects. This is not a problem with the IPCS.

6.4.3.7 Fringing

Thinned CCDS suffer from fringing, especially for observations with narrow passbands (<20nm) at wavelengths >500nm. This is not a problem for broadband images. Fringing in spectra flatfields out, but it is important to obtain a high signal-to-noise rati flatfield at every grating setting.

6.4.3.8 Geometric distortion

The IPCS suffers from severe geometric distortion, especially towards the edge of the field, although this is stable and can be calibrated

Chapter 7

Instruments for photometry and polarimetry

7.1 Overview

Photometry may always be carried out using the CCD imaging facilities described in Chapter 4, rather than with one of the dedicated photometers. The sky subtraction with a CCD image is better than with the photometers, and it is possible to measure all the stars in the field at once, albeit only in one band. Bright stars will saturate a CCD, but this can be avoided by defocussing the telescope. There is a time overhead in clearing and reading a CCD chip but this can be reduced by windowing the chip so that only a reduced area is used. ADAM procedures exist to allow exposures to be made quasi-continuously. Reducing CCD photometry generally takes much longer than reducing the corresponding amount of material from a photometer but the available reduction packages are continually being improved. If the stars you want to observe are fainter than about twelfth magnitude, you should seriously consider using a CCD camera rather than one of the photometers. For photometry of ultra-high accuracy ($\leq$0.1%) there are additional problems with CCD photometry, caused by undersampling and sub-pixel response variations, which need to be treated carefully.

Currently the only common-user photoelectric photometer supported on La Palma is the Peoples' Photometer (PP), and this is only supported on the JKT. It is described in section 7.2. The Multi-Purpose Fotometer (MPF) is not currently available as a common-user instrument, nevertheless it may be available by arrangement with the instrument provider (Dr. J. Tinbergen at Roden), and is described in section 8.5.

The main characteristics of the PP and MPF instruments are summarised in Table 7.1.

7.2 Peoples' Photometer (PP)

The Peoples' Photometer is a two-channel photoelectric photometer designed to have interchangeable optics so as to be suitable for a variety of

Table 7.1: Comparison of photometers

	Peoples' Photometer	MPF
Acquisition	Using TV at rear of aperture	Visually from the observing floor
Number of channels	1 or 2 simultaneously	Up to 12 simultaneously
Quantum efficiency	20 per cent at peak	20 per cent at peak
Time resolution	Normal: 1 s Continuous: 1 ms - 10 s Pulsar mode: $> 4\ \mu$s	Slow: 700 ms Fast: 10 ms
Polarisation	linear & circular	linear
Polarisation modulation	2 and 4 Hz	100 Hz
Sky chopping	Not available (simultaneous sky subtraction in the other channel)	5mm, 6 Hz (not fully implemented)
Dead time	30 - 90 ns	40 - 60 ns
Maximum count rate	3 MHz	1.3 MHz
Filters	Broad, medium, narrow Band overlap allowed but sometimes awkward	Medium, narrow (broad for polarimetry) Simple band overlap allowed
Scanning slits	72 scans per second	Not available
ND filters	Only as part of band filters	3 - 3000 in steps of 3, can be calibrated
Preferred applications	Broadband standard systems Very fast (2 channels) Scanning slits	Large dynamic range Non-standard filters 12 channels

photometric and polarimetric applications. Figure 7.1 shows a schematic optical layout, indicating the location of the most important components of the system. As can be seen, the two channels are orthogonal; channel 1 (Romeo) is along the optical axis of the telescope, while channel 2 (Juliet) is fed via one of several different 45 degree reflectors.

The aperture slide holds three aperture plates which may be selected from a large set. Plates with double apertures are for use with the star/sky prism, the light through each aperture being directed into a separate channel. The apertures are 12.5 mm apart, corresponding to 172 and 66 arcsec when used on the JKT and INT respectively. Plates with single apertures are intended for use with the beam splitters or with the Foster beam analyser for polarimetry. The intensified TV views the field through these apertures. Thus it is best to leave one of the three aperture positions open for the TV to use for acquisition. Once the target star has been acquired the working aperture can be moved in and the star centred precisely.

The photometer contains a retractable glass wheel with 100 mm wide slits located every 10 degrees, approximately 5 mm apart. This wheel can scan the aperture at a rate of 150 scans per second, and is intended for analysis of strip-brightness distributions. To match the slit width with the Rayleigh disc of the JKT it is necessary to use the magnification box with a $\times 10$ microscope objective. This box is a module which bolts above the Peoples' Photometer and cannot be mounted or dismounted except in daylight, when the telescope can be re-balanced. Microscope objectives of $\times 3$ and $\times 2$ are also available.

Each channel has a dedicated slide holding up to six filters; filters can be square (25.4 mm $\times$ 25.4mm) or circular (25.4 mm in diameter) and up to 25 mm thick. Two sets of ready-loaded filter slides are available, standard UBVRI and Stromgren uvby, Hβ. Several narrow band filters are also available. Users requiring particular narrow-band filters should contact RGO staff.

A removable rotating ring (refer to Figure 7.1) is available for polarimetric work. The ring accepts a quarter-wave or a half- wave retarding plate which intercepts the beam before it reaches the aperture. *The quarter-wave plate is usually mounted in ISIS, and prior arrangement must be made to use it with the photometer.* Only one plate at a time can be mounted on the ring; changing plates is a daytime job carried out by support staff. The wave-plates are "super-achromatic" as supplied by the German firm Halle. No significant departure from 100 per cent modulation efficiency has been found over the UBVRI wave-bands. There are however significant differences in the fast direction of the plates between U and I, and observers should determine the zero point of position angle independently for each wave-band they use.

A dedicated high speed photometry module, "AVG", designed for synchronous photometry, is available. Using a frequency synthesizer, the module cycles the addresses in a CAMAC-resident integrating memory which is external to, but shared by, the processor. The memory can be organised as required with variable resolution (up to 16 k bins per cycle in single-channel use), twin channel options and memory paging. Non-synchronous photometry may also be handled; the maximum photon rate is about 2×10^5 counts

Figure 7.1: Optical layout of the Peoples' Photometer. The top eyepiece is the old TV position (not now used) and the lower eyepiece is the present TV position.

s^{-1}. The module has a substantial degree of autonomy from the processor and may be operated remotely by CAMAC commands. It is intended for use in high resolution pulsar work and in a number of other applications, such as occultation and flicker studies.

The performance of the PP is such that with an EMI 9658 photomultiplier, a star of $m_B = 7$ should give about 8×10^5 counts s^{-1} through the B filter on the JKT and about 5×10^6 counts s^{-1} on the INT. It is *extremely important* to note that stars brighter than $m_B = 6$ should *not* be observed through broad-band filters on the JKT, as this would damage the photomultipliers. The corresponding limit for the INT is $m_B= 8$.

Further details are contained in the *Peoples' Photometer User Manual (La Palma User manual III)*. There is a further manual for the *Peoples' Photometer Acquisition Software (La Palma User manual IX)*. The AVG system is described by Dick and Jones *(Journal of Physics E, vol 21, p853, 1988)*.

Chapter 8

Instruments not supported by ING staff

8.1 General Comments

The instruments described in this chapter are not currently supported by the staff of the Royal Observatories, though they may be available as an "own" instrument (see chapter 9) in collaboration with or supported by the instrument provider. Potential users must contact the instrument provider prior to applying for time with such an instrument. Current principal contacts for the instruments in this category are listed below. Updates to this list will be provided in Spectrum or on the World-Wide-Web.

8.1.1 Principal Contacts

- **JKT Wide Field Camera** - R.W. Argyle (Royal Greenwich Observatory).
- **Manchester Echelle Spectrograph** - Prof. J. Meaburn (Astronomy Department, Manchester University).
- **ISIS fibre system** - Dr. S. Arribas (IAC) or Dr. D. Carter (RGO).
- **Multi-Purpose Fotometer** - Dr. J. Tinbergen (Kapteyn Sterrewacht, Roden) or Dr. R.G.M. Rutten (ING La Palma).

8.2 Photographic Imaging

More information on photography at La Palma is available in the *"1-m Camera Users Manual" (La Pama Users' manual V).*
The WFC is designed for direct imaging with astrometric accuracy over a wide field at the flat focal plane of the f/8.06 Harmer-Wynne optical system. The camera uses 250 mm × 200 mm photographic plates; the unvignetted field is 90 arcmin in diameter and the plate scale is 25.6 arcsec mm^{-1}. Plate limits of $m_B \sim 20$ mag, $m_V \sim 19$ mag and $m_R \sim 18$ mag are reached with 60 minute exposures on hypersensitised plates under normal atmospheric conditions.

- **Acquisition and guidance facilities.** The WFC has a dedicated A&G unit which is described in Section 2.3.6.5.

- **Photographic Plates.** IIIa-J, IIIa-F, IIa-O and IIa-D emulsions are normally available but users are advised to communicate their requirements well in advance so that fresh plates can be ordered. In fact, any plate available from Eastman Kodak can be ordered if requested. Unless explicitely stated IIa-O and IIa-D are provided unhypersensitised; IIIa-J and IIIa-F are provided hypersensitised by a combination of hydrogen and nitrogen gas treatment; IV-N can be hypersensitised by bathing in a weak solution of silver nitrate, by prior arrangements. Further details can be found in the WFC manual.

- **Filters.** The following broad-band filters are available: UG1, GG 385, GG 395, GG 455, GG 495, RG 630 and RG 715. The filters are 250 × 200 × 4 mm and are coated with single-layer broad-band anti-reflection coating. Relevant transmission curves, supplied by the manufacturers for uncoated filters, are collected in Appendix D. Additionally, sub-frame assemblies are provided to hold 100 mm × 100 mm interference filters. Two filters centred at 5007 Å and 6563 Å are currently available.

- **Calibration and Focussing.** Six plate-holders are supplied complete with dark slides. The plate-holders are loaded by means of three spring catches and can be flushed with dry nitrogen prior to and during an exposure. Three fiducial marks are projected on to unexposed areas of the plate at the beginning and the end of each exposure, so as to check that the plate has not moved within the plate-holder. Astrometric positions can be measured from the plates to an accuracy of about 0.2 arcsec. A 25 step spot-sensitometer is used for calibration purposes. During the exposure light is projected continuously through the calibration wedge and the filter onto one corner of the plate. A series of apertures is available to optimize the intensity of the calibration source according to the exposure time and plate-filter combination in use. Each plate is identified by projecting onto an unexposed corner the information carried in the top left-hand corner of the corresponding observing card, consisting of: (i) Telescope identification; (ii) Plate number; (iii) Plate centre coordinates.

A dummy plate holder is provided with two knife edges at right angles to each other at the centre of the field for focussing purposes. A hinged bracket on the knife-edge assembly carries a mount for a Polaroid 4 inch $\times$ 5 inch Land film holder, Model 545.

8.3 The ISIS Fibre System

The ISIS fibre system enables the ISIS spectrograph on the WHT to be fed with fibre optic bundles. The bundles link the auxiliary focus, located on the acquisition and guiding box, with the ISIS slit area (see figure 8.1). Below this position, ISIS can be configured in the same way as for the long-slit unit. Then, both arms and FOS can be used in the usual form. However, several ISIS facilities, including autoguider and comparison lamps, cannot be used.
The ISIS fibres system is composed of the following elements:

- **Auxiliary focus**. As the Cassegrain focus is inaccessible when ISIS is mounted on the telescope, the fibres will be placed at the Auxiliary Port of the A&G box. This focus, with a 15 arcmin field, is fed through the large mirror of the A&G box. *FOCAP* aperture plates are used at this auxiliary port to plug the fibres.

- **Fibre optic bundle**. The ISIS Multi-object fibre optic bundle consists of 61 Polymicro Technologies FHP400/475/510 fibres of 2.6m length each. Figure 8.2 shows their attenuation curves. On the auxiliary focus, the 400 μm diameter fibre core covers an area of 1.8 arcsec in diameter on the sky.

- **Guiding system**. One coherent fibre bundle and two semicoherent fibre bundles allow autoguiding or manual guiding. These bundles also enable the focussing and set up of the telescope.

- **Calibration system**. Wavelength calibration is provided by a box which can be mounted on the opposite side of the A&G box from the Auxiliary port, in which any of Argon, Neon or Mercury lamps can be located. The calibration lamps provide a diffuse illumination over the entire Auxiliary port of the A&G box; no attempt is made to mimic the pupil of the telescope.

8.3.1 Guiding system.

The autoguider system in the Cassegrain A&G box cannot be employed when the fibre system is used with ISIS, due to the size of the LARGEFEED mirror.
The guiding system consists of three fibre bundles - two semicoherent and one coherent - to carry the image of three stars to a CCD camera. The

Figure 8.1: The ISIS Spectrograph and the A&G box with the fibre system

Figure 8.2: Attenuation curves for Polymicro high OF (FH series) optical fibre

image of the guide star, obtained with the coherent bundle, can be use by the TV software to generate error signals for the telescope control computer, in order to improve the tracking of the telescope. This image and the two semi-coherent ones can also be used for the set up of the telescope rotator and for the acquisition of the field.
The guiding system includes:

- A coherent bundle manufactured by ORIEL; it covers a rectangular area of 1.89 X 2.38 mm (8.5 X 10.7 arcsec on the sky). One half has a better packing quality than the other half and, therefore, it is used to monitor the object. The focal plane bundle end is connected to the aperture plate via a connector. This connector has a pin to fix the orientation (North) of the bundle. In order to group together the three guiding bundles, the other end of the coherent bundle was shaped to accommodate the semi-coherent bundles.

- Two semi-coherent bundles 2.35 m long, each containing 15 fibres; the central fibre and 6 ones in the first ring are of type FHP100/110/125 while the 8 fibres in the second ring are of type FHP200/240/270. The 7 central fibres were introduced in a polymide microtube of type PPC406/444. This group covers an area of $\sim$ 1.6 arcsec on the sky. The second ring of fibres was glued surrounding this microtube. In order to protect it, the whole structure was inserted in a stainless steel tube of type 1100/1470. Each of the semi-coherent bundles built this way covers an area of $\sim$ 4 arcsec on the sky. The orientation (North) of each bundle is marked by a pin.

- A piece to group the 3 guiding bundle ends when connected at the CCD camera. This can be rotated and must be mounted at a certain orientation which is clearly marked.

- A Westinghouse ISEC TV camera.
- A lens relay system to produce the image of the guiding bundles on the detector.
- A Melles Griot mechanical system for the manual focussing of the guiding bundles

8.3.2 Aperture plates

For multi-object spectroscopy, the acquisition of the field is performed by means of an aperture plate of type FOCAP. This aperture plate is a 3mm thick brass plate. The plate is drilled at precise locations with holes to accept fibre connectors. The holes must be made for each of the three types of connectors: for the individual fibres, for the two semi-coherent bundles and for the coherent bundle. The characteristics of the holes are specified in the Table 8.1 (it is assumed that the OY+ direction corresponds to the North direction during the observing epoch).

Table 8.1: Specification of the holes to be drilled in the Aperture Plates

	Object Position	Drilling Position	Drill diameter (mm)
Single Fibre	(x1,y1)	(x1,y1)	1.983
Semi-coherent bundle	(x2,y2)	(x2,y2)	1.500
Semi-coherent bundle (pin)		(x2,y2+1.175)	0.650
Coherent bundle	(x3,y3)	(x3,y3-0.590)	6.300
Coherent bundle (pin)		(x3,y3+3.010)	0.650

A high precision (on the order of 20μm) both for the coordinates and the hole diameters is fundamental for accurate field acquisition.
The number of holes to be performed for each type of connector is as follows:

- for individual fibres: – one hole for each target – one for each sky area to be sampled
- for the semi-coherent bundle: – one hole 400” North of the field centre (relative to observing epoch) – one 400” South of the field centre (relative to observing epoch) – one for each guide star for manual guiding (two at least)
- for the coherent bundle: – one hole for the field centre – one for the guide stars chosen for telescope tracking (one at least).

Potential users should make their own arrangements for the manufacture of aperture plates, through one of the principal contacts for this instrument.

8.3.3 Observing coordinate determination.

The (X,Y) coordinates of the targets to be observed with multi-object spectroscopy, can be obtained in two ways:

- From the astrometry of the field. Transformation of the equatorial coordinates of the targets onto the corresponding aperture plate coordinates (X,Y), is performed with the LAPLATE programme, which which is a modification of the APLATE programme of the STARLINK package, for the geographical coordinates of the ORM. LAPLATE takes into account the following parameters: telescope focal plane scale, thermal dilation coefficient of the aperture plate material, astronomical coordinates for the centre of the field, and possible proper motions of the targets. These are all considered by the programme in order to obtain the appropriate corrections of the X,Y coordinates.

- By taking photographic plates of the field in advance. The positions can be measured with a microdensitometer or other coordinate measuring machine.

Several error sources can contribute to the field acquisition, for example poor astrometry (the drilled holes for the stars do not coincide with the apparent positions) or bad centering of the field and rotator adjustment. Taking direct plates eliminates some sources of astrometric error, at the expense of requiring extra observing time.
Besides the coordinates of the targets, at least three other field stars must be chosen for telescope guiding. These stars must fulfil the following requirements:

- They must have magnitude 12 to 13 in V. Brighter stars are close to the Earth and can have large proper motions, so that it is in general difficult to obtain good astrometry of them. Less bright stars are difficult to observe.

- They must have similar brightness. If not, simultaneous observation on the monitor could be prevented as the brightest ones can saturate the camera while the weakest remain unseen.

- They must be as separated from each other as possible in the field, and, preferably along the East-West direction which is free of atmospheric refraction. This helps in obtaining a more precise field acquisition.

Finally, some positions free of stars must also be chosen, in order to perform sky corrections.

8.3.4 Fibre System Performance

Geometrical losses, mainly caused by focal ratio degradation, give a mean efficiency of around 25% of the value when observing directly through the slit. Transmission losses in the 2.5 metre fibre length are small, except

shortward of 4200 Å; between 7200 and 7500 Å; and longward of 8700 Å. However acquisition is critical, and much larger losses can be produced if the astrometry is not better than 0.5 arcsec for any reason. Some on-sky measurements, taken in 1.3 arcsec seeing, show that the total sensitivity of the system, is 1 photon/s/Å at 4500 Å for a star of B=15 with the TEK1 CCD on the blue arm; and 1.7 photon/s/Å at 7000 Å for a star of R=15 with the EEV3 CCD on the red arm. There is a fibre-to-fibre scatter of 30% in each of these values.
The efficiency is very sensitive to the acquisition procedure, a shift of 1 arcsec from the best position loses about 55% of the light, and a shift of 11 arcmin in the Cassegrain rotator position angle loses about 50% of the light, although this latter figure depends upon the radial distribution of objects.

8.4 Manchester Echelle Spectrograph (MES)

8.4.1 Overview

Two versions of the Manchester Echelle Spectrograph (MES) have now been constructed: one has been working successfully since 1983 on the Anglo-Australian Telescope. The second has been used on both INT and WHT, and may be available as a guest instrument in collaboration with the Manchester University Astronomy department.
The primary use of these dedicated echelle spectrographs is for problems which require emission or absorption line profiles, at high signal to noise ratios and reasonably high spectral resolutions. Their use up to now has been on the nuclei of Seyfert galaxies, starburst galaxies, giant extra-galactic and galactic HII regions, giant and supergiant interstellar shells, galactic supernova remnants, HH objects and Wolf-Rayet, planetary and bi-polar nebulae.
Note that the MES is *not* a common-user instrument, though anyone is welcome to apply for time in collaboration with the Manchester group. This point is discused in more detail in Section 8.4.3

8.4.2 Design

The design of the MES is discussed in some detail by Meaburn et al. *(Monthly Notices of the Royal Astronomical Society, vol 210, p463, 1984)* so the description given here is brief. In its most common operating mode, a lens designed by Charles Wynne both collimates the incoming beam from the telescope and refocusses the spectrum after the nearly Littrow dispersion by the echelle grating. No cross-dispersion is employed. The separate echelle orders, each containing one or more nebular emission lines, are isolated with highly efficient, three period interference filters. CCD detectors or the CCD-IPCS on the WHT can be used with the MES, these are described in Chapter 6
The simple optical layout, transmission optics with three layer anti-reflection coatings throughout and the quasi-Littrow configuration of a reflection echelle grating all combine to achieve an exceptionally high efficiency for

the spectrometer. One penalty for this optimization is the restriction to 3900–7500 Å of the operating wavelength range.

The efficiency is enhanced further for particular astrophysical problems by having a variety of options for the entrance slits. Either a single long slit or a multi-slit with up to five long slits transmitting simultaneously are routinely employed. Separate line profiles are obtained for each resolvable element along these slits. Where emission and absorption line sources are distributed randomly within the entrance aperture, multi-image masks, prearranged to accept the light from the separate sources, can be used.

Fibre-optic format changers are also available. Initially, six separate fibre arrays have been assembled for use in this mode (MATADOR). Here the entrance ends of the fibres (with up to 529 being employed in one array) are arranged to match the shapes of various sources in the focal plane of the telescope. The output ends of the fibres are then distributed along up to five entrance slits of the spectrometer.

In its primary mode, the MES fills a distinct niche between more traditional, cross-dispersed, echelle spectrometers, which are primarily useful for small sources over very large wavelength ranges, and the stepped Fabry-Perot devices such as TAURUS-2 which are most usefully applied to very extended sources but over very small wavelength ranges. The fibre-optic format changers extend the MES's application to some extent into TAURUS-2 territory.

The imaging mode of the MES, which was originally introduced as a minor alternative, has also proved very useful in practice. Here the slit assembly is replaced by a clear aperture and the plane mirror is inserted. A deep, filtered IPCS image of any source whose line profiles have been measured, can be obtained at the touch of a button. Moreover, an image of the slits superimposed on a quick-look image of the source, produces a precise positional record of the echelle data.

Two other modes are included but have not been used, since they do not compete very well with conventional echelle and intermediate dispersion spectrometers. In these a grism can produce cross-dispersion or, with the mirror in the beam, a low dispersion spectrum.

8.4.3 Operation

The MES on the WHT is university owned, and its continuing development and astrophysical exploitation are the focus of the activity of the Manchester group. Consequently it should not be regarded as the usual common-user devices encountered by the observing community. However, the Manchester group is committed to making them available to a wide number of workers. All that is necessary is for a potential user to contact John Meaburn, Department of Astronomy, University of Manchester before an application for telescope time to work out the suitability of the instrument for the problem in hand. After the award of time a visit to Manchester for an afternoon is strongly recommended to fix residual instrumental details.

8.5 Multi-Purpose Fotometer (MPF)

MPF's prime field of application is precision multi-channel work on brighter stars, the limit of what is "bright" depending on the bandwidth. ND filters provide it with high dynamic range. Dichroic beam-splitters make it possible to observe in up to 12 channels simultaneously. In addition to being an efficient use of the available light, this allows cancellation of extinction and scintillation noise in many applications. The MPF has a wide spectral range, from about 360 to about 870 nm.

A Users' Manual and a Manual of Exchangeable Optics are available. The latter contains details of filters and beamsplitters available. An overview is given in Table 8.5. MPF is shown schematically in Figure 8.3.

The dark current of the photomultiplier tubes in MPF varies from tube to tube, and is normally between 30 and 200 counts per second, though it may be as high as 1000 counts per second in the summer, when ambient temperatures are around 15°C. The dark current noise is about the same for both red and blue photomultipliers, so that the red and blue channels are well matched. A rough estimate of the limiting magnitude for dark current limited applications can be obtained by assuming a norm for the dark current of 100 counts per second, a total beamsplitting efficiency of 40% , and a detector efficiency of 15%. For a 10 second integration, a signal to noise ratio of about 30 will be obtained on the JKT for stars of the following magnitudes:

Total bandpass (Å)	1	10	100	1000
Limiting m_V	8.5	11	13.5	16

Since, with a 10 arcsec diaphragm, even a dark sky is of magnitude 15, many wider-band observations will be limited by sky background rather than dark current and the limiting magnitude should be estimated on the basis of expected sky conditions (including the likelihood of dust). There is no bright limit in night-time observations: the ND filters can handle Jupiter and the moon.

The linear polarisation modulation exceeds 98% over the whole wavelength range and if one is interested in wide spectral coverage of polarisation, then MPF is currently the best instrument to use. MPF does lose 50% of the light in the analysing polariser compared to PP, so only comes into its own when observations in many bands are required. Polarisation zero-point instabilities, which are as yet imperfectly understood, can be kept below 0.05% by careful (re)centering

A mode only available in MPF is multi-line-index photometry with high precision. This mode combines the freedom from slow drifts of the single-channel line photometer with the freedom from extinction/scintillation noise of the two-channel line photometer, and all of this in up to 6 lines simultaneously. This technique holds great promise for work with the stronger absorption lines, supporting precise, efficient line photometry when large format CCDs become available. Due to its ND filters, MPF can calibrate these indices on the very brightest stars, while applying them to the much

Table 8.2: Overview of MPF

Number of channels:	Up to 6, each with 2 photomultipliers and 3 filters
Modes of operation:	(1) Hβ type photometry in up to 6 channels simultaneously (2) Multi-colour photometry in: a) up to six channels simultaneously b) up to twelve channels simultaneously or up to 36 passbands quasi-simultaneously (using 12 channels) (3) Linear polarimetry (channels as for photometry)
Optical efficiency: (excluding filters)	Modes (1) and (2a): 70 per cent Mode (2b): 35 per cent Mode (3): half the efficiency of photometric modes
System accuracy:	Photometry: 0.1 per cent Polarimetry: 0.01 percent
Dynamic range:	Maximum count rate: $1{\times}10^6$ counts s^{-1} Up to 9 magnitudes of calibrated ND filters available Dark current: about 200 counts s^{-1}
Wavelength range:	3100 to 8700 Å
Optical passbands:	5 Å < m_B < 1000 Å (defined by the temperature stability of interference filters)
Diaphragm sizes:	Single: 0.4–8 mm (nominal) Double: 0.2–3 mm (nominal); 5 mm separation, 6 Hz chopping
Time resolution:	0.7 s at full accuracy; down to 10 ms with some reservations about periodicities in the data
Eyepiece:	40 mm field; crosswires or finding-chart projected in 50 × 50 mm slides

Figure 8.3: The Multi-Purpose Fotometer

fainter ones in the CCD fields. The limiting precision of this mode has not yet been determined; it is certainly better than 0.001 magnitudes in the line index.

Chapter 9

Users' own instruments

9.1 General Comments

This chapter provides a basic summary of the information required to modify and interface instruments to the ING telescopes. Some of this material is covered in more detail in other sections of this manual.

The interfacing of non-standard equipment to unfamiliar telescopes is always a difficult task. Users of such instruments should be prepared to undertake last minute modifications due to the inevitable detail that gets overlooked. The ING has the technical staff and facilities to cope with a limited number of last minute modifications and repairs. They are however often fully occupied with the day to day maintenance and operation of the ING telescopes and instrumentation. Thus every attempt should be made to arrive on the mountain as well prepared and as self sufficient as possible.

One important aspect in the planning of an observing run with your own instrument is that of getting your equipment to the mountain top. Particular attention should be given to this, ensuring that equipment is shipped well ahead of time with an ample margin for the unforseen (strikes, bad weather, etc). See Section 1.7.7 for more information on freighting equipment to La Palma.

Finally it should be stressed that this chapter provides only a *basic* outline of the information required to put a new instrument on a telescope. It is *essential* to obtain more specific, detailed and up–to–date information in advance of an observing run by contacting ING staff. The *Telescope Manager* of the particular telescope should be the initial contact, names and email addresses of Telescope Managers are published regularly in *Spectrum*.

9.2 Optics

9.2.0.1 WHT f/2.8 corrected prime focus

- Focal plane position: 40 mm behind the mounting plane.
- Field size: 40 arcmin unvignetted, 60 arcmin with 45% vignetting.
- Image quality: ≤0.5 arcsec over a 40 arcmin field.
- Image scale: At nominal focus, 17.55 arcsec mm^{-1}.

9.2.0.2 WHT f/11 Cassegrain focus

- Focal plane position: Nominal position 150 mm below A&G mounting face and 800 mm behind instrument rotator. Range of movement possible ±1500 mm about this position.
- Field size: 15 arcmin unvignetted, 19 arcmin with 50% vignetting.
- Image quality: At nominal focus on a flat focal plane, ≤0.5 arcsec over a 10 arcmin field and ≤1 arcsec over a 20 arcmin field.
- Image scale: At nominal focus, 4.51 arcsec mm^{-1}, 222 μm $arcsec^{-1}$.

9.2.0.3 WHT f/11 Nasmyth focus direct

- Focal plane position: Nominal position is 585 mm behind Nasmyth instrument rotator flange. Range of movement possible is ±1500 mm about this position, although a move away from the nominal focus casues image degradation due to spherical abberation (see *La Palma Technical Note no. 9*).
- Field size: Unvignetted 7 arcmin, partial vignetting 23 arcmin. Note that vignetting due to the size of the Nasmyth flat drops slowly to only 70%.
- Image quality : At the nominal focus on a flat focal plane, ≤0.5 arcsec over a 10 arcmin field and ≤1 arcsec over a 20 arcmin field.
- Image scale: At nominal focus, 4.51 arcsec mm^{-1}, 222 μm $arcsec^{-1}$.

9.2.0.4 WHT f/11 Nasmyth focus with optical image derotator

- Focal plane position : The power in the derotator ensures that the focal plane position is close to that of Nasmyth focus direct. The range of focus position is the same as for the Nasmyth focus direct, however the derotator optics causes vignetting on-axis if the telescope focus is moved more than 360 mm beyond the nominal position.

  On the GHRIL optical table, the nominal focal plane is 150 mm from the front edge of the table with the optical axis 300 mm in from the side and at a height of 150 mm above the table.

- Field size: At nominal focus, 2.5 arcmin unvignetted, 5 arcmin with 50% vignetting.
- Image quality: At nominal focus $\leq$0.5 arcsec over the 5 arcmin field.
- Image scale: At nominal focus, 4.44 arcsec/mm, 225 μm arcsec^{-1}.
- Throughput: $\sim$70%; much worse in the K band.

9.2.0.5 WHT f/11 Nasmyth focus with infrared image derotator

- Focal plane position : 16mm onto the GHRIL optical table, and 451mm behind the Nasmyth instrument rotator. 150mm abobe the GHRIL optical table.
- Field size: At nominal focus, 3 arcmin unvignetted.
- Image quality: At nominal focus $\leq$0.5 arcsec over the 5 arcmin field.
- Image scale: At nominal focus, 4.44 arcsec/mm, 225 μm arcsec^{-1}.
- Throughput: Poor in the ultraviolet as it used silvered mirrors, elsewhere $\sim$80%.

9.2.0.6 INT f/3.3 prime focus

- Focal plane position: 56 mm above the D–plate mounting surface, 126.9 mm behind the rear element of the corrector. The range of focus travel is about $\pm$25 mm.
- Field size: 40 arcmin unvignetted, 52 arcmin with 50% vignetting.
- Image quality: On flat focal plane at standard focus, $\leq$0.5 arcsec over a 40 arcmin field, 0.5–2 arcsec at extreme of focus travel.
- Image scale: 24.7 arcsec mm^{-1}, 40 μm arcsec^{-1}.

9.2.0.7 INT f/15 Cassegrain focus

- Focal plane position: Nominal 150 mm below A&G mounting face, shift of $\pm$759 mm possible from this position.
- Field size: 20 arcmin unvignetted, 22 arcmin with 50% vignetting.
- Image quality: At nominal focus on a flat focal plane, $\leq$1 arcsec over a 10 arcmin field and $\leq$1.5 arcsec over a 20 arcmin field. For the maximum shift of 759 mm in the focal plane position, on axis images $\leq$1 arcsec.
- Image scale: 5.41 arcsec mm^{-1}, 185 μm arcsec^{-1}.

9.2.0.8 JKT f/15 Cassegrain focus

- Focal plane position: Nominal 150 mm behind standard A&G mounting, 370 mm behind instrument rotator mounting face. The secondary mirror can be adjusted by ± 20 mm, giving a focal plane shift of ± 241 mm.
- Field size: 34 arcmin unvignetted, 50 arcmin with 50% vignetting.
- Image quality: For a flat focal plane, ≤ 1 arcsec over a 2 arcmin field, ≤ 2 arcsec over a 34 arcmin field.
- Image scale: 13.8 arcsec mm^{-1}, 72 μm arcsec^{-1}.

9.2.0.9 JKT f/8.06 wide field Cassegrain focus

- Focal plane position : Nominal 125 mm behind instrument rotator face (no A&G unit available). Adjustable from 45 mm to 206 mm.
- Field size : 90 arcmin field unvignetted, 93 arcmin with 50% vignetting.
- Image quality : At nominal focus, ≤ 0.5 arcsec on axis, ≤ 1 arcsec at edge of 90 arcmin field. With focal plane shifted by 50 mm, ≤ 1 arcsec on axis, ≤ 3 arcsec at edge of field.
- Image scale : 25.6 arcsec mm^{-1}, 39 μm arcsec^{-1}.

The JKT f/8.06 focus is not normally offered to users, and requirement for this focus should be discussed well in advance with the JKT telescope manager.

9.3 Mechanical Mounting

9.3.0.10 WHT f/2.8 corrected prime focus

- Mounting holes:
- Maximum mass and moments: Maximum mass of an instrument mounted on the instrument platform is 70 kg, maximum moment 70 kg m.
- Clearances:

9.3.0.11 WHT f/11 Cassegrain focus

- Mounting holes : The main mounting point on the WHT Cassegrain A&G unit is the outer flange, with 16 $\times$ 16.5 mm diameter holes on a 1200 mm PCD. The same set of mounting holes are repeated on the instrument rotator flange. In addition, to mount smaller instruments, there are 2 sets of 12 $\times$ M10 tapped holes on PCDs of 457 and 635 mm.

- Maximum mass and moments: For instruments mounted on the A&G unit, the maximum allowed mass is 1000 kg and the maximum moment is 1600 kg m. For instruments mounted directly on the rotator flange, the maximum mass is 1500 kg and maximum moment is 1800 kg m. Note that even small lightweight instruments can cause problems, since the telescope must be rebalanced to compensate and there is, at present, no simple method of doing this.
- Clearances: The allowed size for instruments mounted on the Cassegrain A&G unit is 3500 mm diameter and 2000 mm length.

9.3.0.12 WHT f/11 Nasmyth focus

The drive side Nasmyth focus is occupied by the Utrecht Echelle Spectrograph. This has a dedicated A&G unit permanently mounted, thus access to this Nasmyth focus is limited. The GHRIL side Nasmyth focus can be used, although the positioning of the large optical table makes direct access to the Nasmyth turntable difficult.

- Mounting holes : The Nasmyth instrument rotators have two sets of mounting holes, 12 × M10 on a 362 mm PCD and 12 × M10 on a 457 mm PCD.
- Maximum mass and moments: The instrument rotators are designed for small lightweight instruments and are capable of supporting a maximum mass of 130 kg, a maximum moment of 65 kg m about the mounting face and a maximum out of balance moment about the axis of 10 kg m.
- Clearances and volumes: Access to the GHRIL-side Nasmyth turntable is restricted by the GHRIL table to a distance of 440 mm behind the rotator mounting face. The turntable mounting frame restricts the diameter to less than 560 mm. The optical axis is 150mm above the surface of the GHRIL table.

9.3.0.13 WHT GHRIL Laboratory

- Mounting holes : The GHRIL optical table is 2500 mm long × 1350 mm wide, with an array of M6 holes on 25 mm centres in its SS top surface. The table is mounted on three rigid legs (not vibration isolated) directly to the telescope fork adjacent to the altitude bearing.
- Maximum mass and moments: The table itself is extremely rigid and could support quite heavy instruments. However care should be exercised with point loads as the table top consists of an epoxied SS sheet which dents easily.
- Clearances and volumes: The position of the focal plane/optical axis has already been detailed. The full area of the table is available for instruments, although a major restriction is the position of the focus in the front corner of the table.

9.3.0.14 INT f/3.3 prime focus

- Mounting holes : The instrument mounting at INT prime focus, known as the D“D–plate”, attaches to the top of the corrector cell and has a cutout section to clear the guide probe assembly. There are two existing D–plates, one for use with the standard ING CCD cryostats (3 point kinematic mounting) and another with a simple photographic plateholder. Either of these could be used for user supplied instruments, or alternatively a new D–plate made. Contact RGO staff for more details.

- Maximum mass and moments: No more than a typical cryostat weight of about 15 kg is allowed on the cryostat mounting.

- Clearances and volumes: To avoid vignetting and to ensure clearance with the dome, instruments should be less than the 900 mm diameter of the prime focus assembly. The length should be less than 1500 mm.

9.3.0.15 INT f/15 Cassegrain focus

- Mounting holes : The Cassegrain A&G has two sets of mounting holes. One set consists of four circular patterns of 12 $\times$ M10 tapped holes with PCDs of 362, 457, 508 and 635 mm. In addition there are rectangular sets of 4 $\times$ M16 tapped holes, with spacings 460 mm $\times$ 1072 mm, 600 mm $\times$ 1072 mm and 740 mm $\times$ 1072 mm.

- Maximum mass and moments: For instruments mounted on the A&G unit, the maximum load on the M10 hole set is 200 kg, and on the M16 hole set is 500 kg.

- Clearances and volumes: Instruments must have a length of less than 1300 mm.

9.3.0.16 JKT f/15 & f/8.06 Cassegrain foci

- Mounting holes: On the instrument turntable, 12 $\times$ M10 holes on 457 mm PCD are provided. On the general purpose A&G unit, 12 $\times$ M10 holes on 457 mm PCD are provided plus 12 $\times$ M10 holes on 362 mm PCD. The acquisition TV axis bisects the mounting hole pattern. The CCD A&G unit requires a three point ball ended screw mounting with a PCD of 230 mm.

- Maximum mass and moments: On the instrument turntable, the maximum mass is 270 kg, and the maximum moment is 95 kg m. On the general purpose A&G unit face, the maximum mass is 250 kg and the maximum moment is 90 kg m. The CCD mounting should not be used with anything heavier than a CCD cryostat (i.e. 15 kg).

- Clearances and volumes: Instruments should not exceed a volume defined by the 1200 mm diameter of the mirror cell and a distance of

1200 mm behind the instrument rotator face (to clear the telescope pier).

9.4 Acquisition and guidance

Most of the ING telescope foci are equipped with a dedicated acquisition and guiding unit. In most cases the use of these A&G facilities in conjunction with user supplied instruments is fairly straightforward. In some cases the instruments themselves will have some A&G capability, however it will often be difficult to interface these with the existing telescope operation. For example, it may be necessary to use long ladders to access eyepieces. In some cases it may be possible to modify these facilities, to allow for example a standard ING TV camera to be fitted to an eyepiece holder. The following list summarises the A&G facilities available at each of the ING telescope foci.

- WHT f/11 Cassegrain focus: The WHT Cassegrain A&G unit will provide a comprehensive range of acquisition, guiding and calibration facilities. See Section 2.1.6.2 for a detailed description. The slit-viewing axis bisects the 16 mounting hole pattern (i.e. displaced 11.25° from a hole centreline)

- WHT GHRIL laboratory: Guiding is possible using a Westinghouse TV camera or CCD Autoguider and pellicle (95%/5%) beamsplitter mounted on an aluminium jig. With the derotator it is possible to guide on an off-axis guide star; without the derotator it is necessary to guide on the target. Please contact the GHRIL manager for further details.

- INT f/15 Cassegrain focus: The INT Cassegrain A&G unit provides a wide range of useful facilities. See Section 2.2.6.3 for a detailed description. There is scope for modification and adjustment to cope with some non–standard configurations with user supplied instruments. The slit viewing optics works at the standard 15° angle (7.5° slit tilt) at the nominal 150 mm back focus. The optical axis of the slit viewing system is oriented to bisect the 12 $\times$ M10 instrument mounting hole pattern.

- INT f/3.3 prime focus: The INT prime focus is equipped with its own autoguider which can access half of the avaliable 40 arcmin field. See Section 2.2.6.4 for a more detailed description. The usual method of acquisition at prime is to use the finder telescope, however it is possible to run one of the spare integrating TVs if this is required for a user instrument. The CCD mounting for prime is equipped with a filter wheel and fast shutter which could also be used with a user instrument.

- JKT f/15 Cassegrain focus : Two possible A&G units are available, described in some detail in Sections 2.3.6.3 and 2.3.6.4.

The original general purpose unit provides a TV, direct acquisition and slit viewing optics, and a calibration lamp. This general purpose A&G unit is designed to be used with the standard instrument mounting with 150 mm back focus. The slit viewing optics works at the standard 15° angle (7.5° slit tilt) at the nominal 150 mm back focus. The optical axis of the slit viewing is orientated to bisect the $12 \times$ M10 instrument mounting hole pattern (i.e. displaced 15° from a hole centreline) .

A newer A&G unit is also available, dedicated for use with the CCD camera. This has a three point kinematic mounting to match the standard CCD cryostats. The A&G unit has a standard acquisition TV, offset autoguider, filter wheel and fast shutter, as well as a pair of low dispersion grisms. The disadvantages of this A&G unit are a reduced back focus clearance of only about 16 mm ,a reduced field of view of 270 arcsec (20 mm) and no slit viewing facilities or calibration lamps.

9.5 Electrical and electronic

The mains power supplies to the telescopes can be divided into three catagories.

- Raw mains (nominally 240 V, 50 Hz) as supplied to site from the La Palma grid, or in the event of supply failure by backup diesel generators on site. This supply is subject to voltage fluctuations.
- A "no break" supply for essential equipment which must be left running continuously, but which can tolerate some voltage fluctuations. This system is currently only available in the INT.
- A fully buffered supply for use with sensitive equipment such as computer hardware. This supply is not normally avaliable for user supplied instruments.

The mains connectors used from these supplies are the standard UK pattern. For more detailed information on the specifications of these supplies consult La Palma technical staff.

All the telescopes are provided with an extensive set of general–purpose cabling for data transfer and control. Various types of shielded multi–core and co–axial cables run from the instrument mounting points to the control room. Connector types are standardised between telescopes. At the WHT there is a set of fibre optic cables to transfer data between the various focal stations and the control room. The fibre cable is Optronics H200P with SMA type connectors.

User supplied instruments can be connected through this cabling system with suitable interface connections. Whilst it is possible for this interfacing to be done by the user after liason with La Palma technical staff, it has been found that the most satisfactory and reliable method is to arrange for suitable interface cables to be made by the La Palma technical staff. It is of course essential to provide plenty of advance warning of these requirements. The other alternative is for the user to provide cables of sufficient length to run directly from telescope to control room along a suitable path. This arrangement is most suited to the smaller telescopes such as JKT and INT Cassegrain focus, where the telescope movement permits a cable length which is not excessive. The relatively large movement possible with the altazimuth mounting of the WHT would make this difficult.

9.6 Cooling, cryogenics, vacuum, gas supplies

The ING site has its own plant which supplies liquid nitrogen for the ING telescopes either in large 75 litre pressure vessel cryostats, or in smaller, more portable 25 litre cryostats. The plant has ample capacity to supply liquid nitrogen for most uses. However if a high usage is expected, it is worth warning RGO staff ahead of time. Filling the instrument cryostats is usually done with a self–pressurising or electric pump via a plastic hose.
Liquid helium is difficult to obtain since it has to be supplied from mainland Spain via Tenerife. Users requiring liquid helium should make their own enquiries and arrange shipment.
For cooling instruments with photomultipliers or image tubes there are several Churchill coolers, model 10/CTC HG. The WHT and INT each have two cooling units, the extra one intended as a spare. The spare units are avaliable for user supplied instruments. These coolers use a pumped glycol–water coolant with the temperature adjustable from 0° to 20° C (WHT units) and -20° to 20° C (INT). The coolers have a capacity of 3 kW. The coolant is fed through 16 mm plastic hose with quick connect couplings.
On the INT, there is a standard 80 psi compressed air supply which is fed through a drier and filter before connection to the telescope. The INT also has a bottled supply of dry notrogen. These gas supplies are terminated at the Cassegrain and prime foci in standard type quick connects. The JKT gas supply is similar to the INT, with cleaned compressed air and dry nitrogen avaliable at the Cassegrain focus.
At present the WHT has a dry nitrogen gas supply to the telescope. This supply comes from a pressurised liquid nitrogen cryostat with a backup system of bottled nitrogen. The supply pressure is set at 80 psi (6 bar). The supply outlets at Cassegrain, Nasymth and prime foci are Swagelok Pat DOC4 Key 1 quick connects. The WHT Cassegrain focus also has a pressure regulator multi–outlet manifold with multiple miniature quick connects. This gas supply system has a limited capacity, so care should be taken when using it for purposes such as instrument flushing to avoid excessive consumption.

9.7 Detectors

The ING integrating TV cameras are available for use with user instruments. However there are only a limited number of extra cameras, which are meant as spares, so the use of these TVs should be planned well in advance. These sensitive cameras are vulnerable to over-illumination and great care must be used to avoid damage. Users intending to fit these TVs to their instruments should contact RGO technical staff for details of mounting dimensions, overall size and detector characteristics.

The ING photon–counting and CCD detector systems could also be used with user instruments. These are described in detail in Chapter 6. Prior agreement should be obtained to ensure that these detectors are both suitable and available for use on other instruments. The photon–counting systems in particular are extremely vulnerable to damage from over-illumination, and can only be used on instruments for which special precautions are taken (e.g. the detector shutter and any instrument access hatches should be interlocked).

Appendix A

Documentation

Documentation listed in the Appendix is current at the beginning of 1995, and copies can be obtained from RGO Cambridge. Availability of earlier technical notes cannot be guarenteed.

A.1 User manuals

1. **Spectroscopy with the CCD on the INT – a user guide [version 2.1]**
   E Terlevich, R J Terlevich & P A Charles
   1989 October

2. **INT Faint Object Spectrograph – user guide [version 2]**
   D King, M Breare et al
   1992 May

3. **JKT user guide [version 3.1]**
   R W Argyle, D H P Jones & D Pike
   1989 June

4. **The St Andrews Richardson-Brealey Spectrograph user manual [version 2]**
   R Edwin
   1988 September

5. **Users' guide to the INT prime focus CCD**
   J V Wall, R A Laing, R W Argyle & R E Wallis
   1989 September

6. **WHT Faint Object Spectrograph - interim user manual**
   J Allington-Smith, M Breare, R Ellis, P Gray & S Worswick
   1988 January

7. **A user guide to the JKT CCD camera**
   R W Argyle, C J Mayer, C D Pike & P R Jorden
   1988 February

8. **La Palma data archive users' guide [version 1]**
Ernt Raimond and Ger van Diepen
1989 June

9. **The INT user manual**
E J Zuiderwijk, D H P Jones & B M J Hassall
1991 January

10. **WHT Spectropolarimetry user manual [version 1]**
J Tinbergen & R G M Rutten
1992 July

11. **ISIS astronomers' guide [version 1]**
R Clegg, D Carter, P Charles, J Dick, C Jenkins, D King & R Laing
1992 July

12. **WHT ISIS users' manual**
D Carter, C Benn, R Rutten, J Breare, P Rudd, D King, R Clegg, V Dhillon, S Arribas, J-L Rasilla, A Garcia, C Jenkins & P Charles
1993 October

13. **WHT - LDSS-2 observers' manual**
RGO & Durham
1993 December

A.2 Technical notes

1. **General optical description of the 4.2–m William Herschel Telescope**
R Bingham
1984 September

2. **Hour angle limits of the JKT**
D Jones
1985 May
Gives tables showing limiting hour-angles east and west as a function of declination

3. **CCD cryostat use**
P Jorden
1985 June
Describes the method of liquid nitrogen filling and temperature monitoring

4. **Atmospheric extinction at the Roque de los Muchachos observatory**
D L King
1985 September
A theoretical extinction curve is given, covering the spectral range 3000-11000A.

5. **Spectrum of the copper neon lamp on the IDS**
   D L Harmer & R Collins
   1985 November
   Plots of the spectrum cover the wavelength region 320 to 970 nm, from IPCS and CCD data taken on the INT.

6. **CCD filters for use on La Palma [Version 2]**
   P Jorden
   1988 February
   The specifications and profiles for 24 narrow and broad band filters to be used with the CCD imaging systems on La Palma.

7. **Geology and meteorology of Sahara dust**
   P Murdin
   1986 April

8. **Statistical results from INT observations catalogue 1984–86**
   C R Benn & R Martin
   1987 February
   The analysis relates to 491 nights of observations made at the INT during the period 22 May 1984 to 15 March 1986.

9. **Arc maps for copper-argon lamp on the INT spectrograph**
   D Harmer
   September 1983
   Cu-Ar arc maps for the IDS on the INT are given for the IPCS+500, IPCS+235 and CCD+235 Cameras with various gratings and angles.

10. **Basic parameters of CCDs in use at La Palma**
    P R Jorden

11. **CCD data reduction**
    J E Sinclair
    1988 May
    Describes the corrections that should be applied for CCD photometry and the programmes available at RGO.

12. **The alignment of the JKT optics**
    R E Wallis
    May 1988

13. **Accurate calibration of field distortion of the JKT**
    J E Sinclair
    January 1989

14. **Spectrophotometric standards**
    J E Sinclair and R Wood
    November 1989

15. **La Palma Data Archive primer [version 2]**
    E J Zuiderwijk
    July 1991

16. **IDS Calibration lamp arc maps**
    E J Zuiderwijk & J Knapen
    October 1989

17. **Rising and setting times for observations with an Alt-Azimuth telescope**
    R A Laing
    November 1989

18. **The WHT Harris filter set**
    P Eldridge, D Jackson, J E Sinclair & S W Unger
    January 1990

19. **Transmission curves for WHT interference filters**
    S W Unger, J E Sinclair, D KJackson & P Eldridge
    February 1990

20. **Wood's anomalies in the INT Spectrograph**
    P G Murdin
    March 1990

21. **CCD frame-size parameter**
    P R Jorden
    December 1990

22. **GHRIL user notes**
    M N Devaney
    August 1991

23. **The night-sky spectrum from La Palma**
    C R Jenkins & S W Unger
    October 1991

24. **Maps of the standard arc-lamps for the WHT ISIS**
    J E Sinclair
    July 1992

25. **Standard star lists available at the ING**
    J E Sinclair
    July 1992

26. **Beta-light sources for CCD response calibrations**
    P R Jorden, P Terry & A P Oates
    July 1992

27. **Throughput of the WHT ISIS**
    C R Jenkins, J E Sinclair & R E S Clegg
    July 1992

28. **Direct measurement of the throughput of the WHT ISIS**
    C R Jenkins & P Terry
    July 1992

29. **Transmission curves for more WHT interference filters**
    P Terry, S W Unger & J E Sinclair
    July 1993

30. **UES spectrum of the Thorium-Argon hollow-cathode lamp**
    K Lipman, M Pettini, M Wall & N Walton
    November 1993

31. **New large-format CCDs for the ING**
    A P Oates & P R Jorden
    November 1993

32. **ING CCDs-properties of operational cameras**
    P R Jorden
    January 1994

33. **ING Bibliography, 1993**
    W L Martin
    March 1994

34. **Landolt faint photometric standards**
    J Pilkington, J E Sinclair & R Wood
    July 1994

35. **Update on filter characteristics for ING telescopes**
    R F Peletier
    November 1994

Appendix B

Scheduling aids

This Appendix gives a variety of information useful for scheduling observations.
Table B shows how the Local Sidereal Time (LST) of the start and end of the night varies throughout the year, and should be used to determine which month is best suited for observing a particular object. Figures B to B are plots of declination against hour angle for the latitude of La Palma, showing lines of equal zenith distance, and indicating the telescope limits. These plots can be used to determine for how long either side of transit it is possible to observe an object.
Observations should of course be scheduled so that objects are not observed at large values of the zenith distance. This causes problems both with atmospheric extinction (see Appendix C), and with differential refraction, whereby light at different wavelengths is refracted by different amounts. Differential refraction means that:

- If acquisition and guiding is carried out at a very different wavelength from that of the observation, the object may not be where you think it is.
- For low dispersion slit spectroscopy, the object being observed can only be simultaneously centred in the slit for all wavelengths if the PA of the slit is aligned with the parallactic angle. If the slit is not aligned with the parallactic angle, there are likely to be wavelength dependent slit losses.

Figure B shows the angle of refraction as a funtion of wavelength and airmass. Table C.4 gives the airmass as a function of zenith distance. The parallactic angle for a particular observation can be found from Figure B, which is a plot of parallactic angle against hour angle, showing lines of constant declination. Note that there is a discontinuity at transit of objects with declination equal to the latitude of La Palma.

Figure B.1: Plot of declination against hour angle for the latitude of La Palma, showing lines of equal zenith distance. This plot shows the region within which observations are possible with the WHT.

Figure B.2: Plot of declination against hour angle for the latitude of La Palma, showing lines of equal zenith distance. This plot shows the region within which observations are possible with the INT.

Figure B.3: Plot of declination against hour angle for the latitude of La Palma, showing lines of equal zenith distance. This plot shows the region within which observations are possible with the JKT, with the telescope both east of the pier (a) and west of the pier (b).

Figure B.4: Plot showing how the magnitude of atmospheric refraction varies with wavelength and airmass.

Figure B.5: Plot of parallactic angle against hour angle, showing lines of constant declination. Note the discontinuity at transit (hour angle equal to zero) for objects with a declination equal to the latitude of La Palma.

Table B.1: LST of twilight on La Palma (1989)

Date	Sunset	End of twilight			Start of twilight			Sunrise
		Civil	Nautical	Astronomical	Astronomical	Nautical	Civil	
Jan 1	00:08	00:26	00:55	01:24	12:13	12:42	13:11	13:28
Feb 1	02:35	02:52	03:20	03:48	14:13	14:41	15:10	15:26
Mar 1	04:46	05:02	05:29	05:57	15:43	16:10	16:38	16:54
Apr 1	07:06	07:22	07:50	08:19	17:09	17:37	18:05	18:21
May 1	09:23	09:39	10:09	10:40	18:30	19:01	19:31	19:47
Jun 1	11:44	12:01	12:34	13:08	20:08	20:42	21:14	21:32
Jul 1	13:50	14:09	14:41	15:16	22:08	22:43	23:15	23:24
Aug 1	15:41	15:58	16:29	17:01	00:32	01:04	01:35	01:52
Sep 1	17:13	17:29	17:58	18:27	02:58	03:27	03:55	04:12
Oct 1	18:36	18:51	19:19	18:46	05:14	05:42	06:09	06:25
Nov 1	20:07	20:23	20:51	21:19	07:34	08:02	08:30	08:46
Dec 1	21:53	22:10	22:40	23:08	09:52	10:21	10:50	11:08

Appendix C

Instrumental throughput

C.1 Empirical throughputs

Throughputs have now been measured on-sky for all current ING common-user instruments except WHT TAURUS (Fabry-Perot mode), JKT Richardson-Brealey spectrograph and WHT LDSS imaging. WYFFOS and WHIRCAM are not fully commissioned at the time of writing; only theoretical estimates of throughput are available. Most of the measurements reported below were made in 1994.

C.1.1 Spectroscopy

The tables give the above-atmosphere AB apparent magnitudes which yield 1 detected photon/sec/Å for a wide-slit observation made at the zenith in clear conditions. (Number of photons = number of counts × CCD gain; gain typically ∼ 1.)

Table C.1: WHT ISIS with the 158 lines/mm gratings and the TEK1 (blue arm) or TEK2 (red arm) CCDs

Wavelength:	3500	4000	4500	5000	5500	6000	6500	7000	7500	8000	8500	9000
AB mag (blue arm):	16.9	17.8	17.6	17.5	17.3	17.1	16.8	16.3	15.7	15.3	15.3	15.4
AB mag (red arm):	12.5	16.3	17.1	17.4	17.7	17.9	17.7	17.6	17.4	16.9	16.5	16.1

Table C.2: WHT FOS first-order, with the GEC CCD

Wavelength:	5250	6000	6500	7000	7500	7750	8500	9500
AB mag	17.0	17.8	18.1	18.0	17.9	17.6	16.8	15.1

The throughput of the IDS 500-mm camera has been measured only at 6700 Å; it is similar to that of the 235-mm camera.

Table C.3: WHT UES with the 79 lines/mm grating and the TEK1 CCD and IPCS

Wavelength:	3500	3750	4000	4500	5000	5500	6000	6500	7000	7500	8000	8500
AB mag (TEK1):	16.3	16.8	17.0	17.0	17.0	17.0	17.0	16.9	16.7	16.4	16.0	15.5
AB mag (IPCS):	14.6		15.1	14.9	14.7	14.3						

Table C.4: WHT LDSS with the TEK1 CCD

Wavelength:	3600	3800	4000	4500	5000	5500	6000	6500	7000
AB mag (Med-R grism):				17.4	18.1	18.6	18.6	18.5	18.2
AB mag (Med-B grism):		17.1	17.8	18.4	18.5	18.6	18.5	18.3	17.9
AB mag (High-res. grism):	15.9	17.0	17.9	18.1	18.1	18.0			

Table C.5: INT IDS 235-mm camera with the AgRed collimator, R300V grating, EEV5 CCD and with the AlWide collimator, R150V grating and TEK3 CCD

Wavelength:	3330	3500	4040	4520	5000	5480	6040	6520	7000	7480	8090	9080	9560
AB mag (EEV5 CCD):		13.4	14.3	14.6	15.0	15.4	15.5	15.5	15.6	14.7	14.0		
AB mag (TEK3 CCD):	13.0	13.8	15.8	16.1	16.1	16.0	15.9	15.8	15.8	15.5	15.0	14.2	13.6

Table C.6: INT FOS with the GEC CCD

Wavelength:	3500	4000	4500	5000	5500	6000	6500	7000	7500	8000	8500	9000	9500
AB magnitude:	13.6	15.7	15.7	15.8	15.8	16.4	16.7	16.9	16.8	15.9	15.9	15.2	14.2

C.1.2 Imaging

The tables give the above-atmosphere AB apparent magnitudes which yield 1 detected photon/sec for an observation made at the zenith in clear conditions. (Number of photons = number of counts $\times$ CCD gain; gain typically ~ 1.) The response curves of the Harris filters are given in La Palma technical note 96 (note that the throughput of the Harris B filter is believed to be about 30% lower than that of the older KPNO B filters).

Table C.7: Imaging Instruments with broadband filters

	CCD	Filters	U	B	V	R	I
JKT f/15	TEK4	Harris	21.0	23.1	23.3	23.5	23.0
INT prime-focus	TEK3	Harris	23.1	25.3	25.3	25.4	24.7
WHT prime-focus	TEK2	Harris	24.1	26.2	26.4	26.5	26.0
WHT auxiliary port	TEK	Harris		25.9		26.2	
WHT TAURUS f/2 or f/4	EEV			24.5	25.1	25.5	24.9

Count rates for the JKT Peoples' Photometer were given in *Gemini* 35 (March 1992).

C.1.3 Comparison between theoretical and empirical throughput

The ratios between mean measured instrumental throughputs, and those predicted on the basis of estimated or measured efficiencies of individual optical components (e.g. mirrors, filters, gratings) are given in the table below, for representative wavebands:

Table C.8: Comparison between theoretical and empirical throughput

	U	B	V	R	I
WHT ISIS	0.9	0.6	0.7	0.8	0.4
WHT FOS			0.8	0.7	0.8
WHT UES	0.9	0.5	0.6	0.5	0.6
WHT LDSS (spectroscopy)	1.7	0.7	0.7	0.7	
INT IDS 235	0.4	0.4	0.5	0.4	0.6
INT FOS	0.3	0.5	0.6	0.8	0.8
WHT prime-focus imaging	0.7	0.6	0.8	0.6	1.0
WHT aux-port imaging		0.9		0.6	
WHT TAURUS f/2 imaging		0.7	1.0	0.	0.9
INT prime-focus imaging	0.9	0.8	0.8	0.	0.9
JKT f/15 imaging	0.9	0.7	0.9	0.	1.0

The small scatter of values for each instrument confirms that the error in measuring the instrumental sensitivities is typically 10 - 20%. The INT IDS

235-mm camera has a throughput much less than that predicted; its optical surfaces are visibly dirty, and an overhaul of IDS is planned for late 1995.

C.2 SIGNAL

The measured sensitivities are incorporated in a Fortan program SIGNAL, which can be used to predict the number of object and sky photons which will be detected as a function of above-atmosphere apparent magnitude (or intensity in Jy), wavelength band (U, B, V, R or I), detector, exposure time and sky brightness and, for spectroscopy, diffraction grating and slit width. For the few instruments for which no empirical data are available, the program calculates throughput on the basis of measured or estimated efficiencies for the telescopes, cameras, gratings and detectors. The program can be used before observing to estimate the exposure time needed for a particular experiment, and at the telescope to check that the expected number of photons (counts∗gain) arrives at the CCD. The program may be obtained by email from `crb@lpve.ing.iac.es` or by anonymous ftp via the ING information page on the Cambridge server `ftp://ftp.ast.cam.ac.uk/pub/lpinfo/signal`.

C.3 Theoretical throughputs

For a system with no light losses, it is straightforward to show that the number of photons per second incident in each resolution element is:

$$N = 15080 * A * F * f * \delta\lambda/\lambda$$

where:

A = Geometric aperture of telescope (m^2)
= 0.66 (JKT), 4.41 (INT) or 12.47 (WHT)
F = Monochromatic flux density of object (mJy)
For airmass > 1, a correction must be applied for atmospheric extinction.
An AB magnitude of 15 corresponds approximately to 1.9 (U), 4.4 (B), 3.8 (V), 3.0 (R) or 2.4 (I) mJy
f = Fraction of total flux density of object in each spatial resolution element.
Note that for slit spectroscopy, the spatial resolution perpendicular to the direction of the slit is set by the width of the slit. For many observations, the slit width will be comparable to the size of the seeing disc, and so even for sources which are intrinsically unresolved, a significant fraction of the light will not enter the spectrograph.
$\delta\lambda$ = Observing bandpass (Å). For imaging observations, this is the FWHM of the filter used. For spectroscopy, it is equal to the wavelength resolution of the observations.
λ = Observing wavelength (Å)

To find the number of photons *detected*, N must be multiplied by the product of the efficiencies with which the various optical components in the light

path reflect and transmit light, and by the efficiency of the detector. For observations at prime focus, Cassegrain and Nasmyth (or WHT auxiliary port), there will be respectively 1, 2 or 3 mirror reflections. Typical reflectivity of a freshly-aluminised mirror surface is 0.85, and this figure probably decreases $\sim$ 10 - 20% before the next aluminising. Efficiencies of diffraction gratings were given in chapter 5. Filters are listed in Appendix D. Glass-air surfaces transmit 0.98 of the incident light, and the many surfaces within cameras result in them having typical throughputs $\sim$ 0.4 - 0.8 e.g. 0.3 for UES (including echelle), 0.4 for IDS, 0.6 for TAURUS, 0.7 (peak) for FOS-2. The throughput of the correctors at WHT and INT prime focus is believed to be $\approx$ 0.9. The WHT Nasmyth optical derotators have a throughput of 0.75. The throughput of the IR derotator has not yet been measured. CCD detector quantum efficiencies are given in Fig. 6.1. The throughput of WYFFOS (including fibres and grating) is expected to be $\approx$ 0.36.
Total throughputs for spectroscopy (telescope + camera + detector) range from 18% for WHT FOS and 11% for ISIS with R300V grating and TEK CCD to 0.5% for WHT UES with IPCS. Throughputs for imaging are higher.

C.4 Atmospheric extinction

La Palma Technical Note 31 discusses the atmospheric extinction on La Palma in some detail. Briefly, it is possible to separate the extinction into a wavelength dependent component, due to Rayleigh scattering by air molecules and absorption by ozone, and a wavelength independent component due to dust scattering. The wavelength dependent component is plotted as a function of wavelength and airmass in Figure C.1. The extinction at the zenith on a clear night with low aerosol content is tabulated as a function of wavelength in Table C.9. Table C.4 gives the airmass as a function of zenith distance. It can be seen that this component of the atmospheric extinction is much more important in the blue than in the red, varying from 3.7 magnitudes per unit airmass at 3000 Å to 0.007 magnitudes per unit airmass at 10000 Å.
The extinction due to dust scattering varies from night to night, but is usually less than a few tenths of a magnitude per unit airmass (see Table 1.3.2). The total vertical extinction in V band (i.e. the sum of the wavelength independent and wavelength dependent components) is measured each night by the Carlsberg Automatic Meridian Circle, and these values are placed on the ING information pages of the World-Wide Web.

Figure C.1: Theoretical atmospheric extinction on La Palma as a function of wavelength and airmass

Table C.9: La Palma Standard Extinction Curve

λ	m	λ	m	λ	m
3000	3.7150	5700	0.1001	8400	0.0143
3100	1.5961	5800	0.0950	8500	0.0136
3200	0.9908	5900	0.0887	8600	0.0130
3300	0.6967	6000	0.0891	8700	0.0124
3400	0.5934	6100	0.0844	8800	0.0118
3500	0.5146	6200	0.0770	8900	0.0113
3600	0.4554	6300	0.0702	9000	0.0108
3700	0.4061	6400	0.0638	9100	0.0103
3800	0.3633	6500	0.0575	9200	0.0099
3900	0.3260	6600	0.0524	9300	0.0095
4000	0.2935	6700	0.0473	9400	0.0091
4100	0.2649	6800	0.0428	9500	0.0087
4200	0.2397	6900	0.0389	9600	0.0083
4300	0.2175	7000	0.0356	9700	0.0080
4400	0.1986	7100	0.0330	9800	0.0077
4500	0.1811	7200	0.0307	9900	0.0074
4600	0.1664	7300	0.0282	10000	0.0071
4700	0.1529	7400	0.0268	10100	0.0068
4800	0.1424	7500	0.0254	10200	0.0065
4900	0.1320	7600	0.0213	10300	0.0063
5000	0.1244	7700	0.0202	10400	0.0060
5100	0.1179	7800	0.0192	10500	0.0058
5200	0.1120	7900	0.0183	10600	0.0056
5300	0.1087	8000	0.0174	10700	0.0054
5400	0.1046	8100	0.0165	10800	0.0052
5500	0.1020	8200	0.0157	10900	0.0050
5600	0.0991	8300	0.0150	11000	0.0048

Table C.10: Airmass as a function of zenith distance

Zenith distance (degrees)	Airmass	Zenith distance (degrees)	Airmass
0	1.000	55	1.740
10	1.015	60	1.995
20	1.064	65	2.357
30	1.154	70	2.904
40	1.304	75	3.816
45	1.413	80	5.60
50	1.553	85	10.40

Appendix D

FILTERS

This appendix summarises the filters available for use with the ING telescopes. Tables D.1.4.1 and D.1.4.1 list the filters available for CCD imaging. All of these are 50 mm square, except where otherwise noted, and can be used at all the imaging instruments: JKT Cass, INT Prime, WHT Prime and WHT AUX port. Apart from the filter characteristics we also give some telescope specific information. At the end of this appendix we list in Tables D.3 and D.3 the larger, circular, filters available for imaging and for Fabry-Perot spectroscopy with TAURUS-2 on the WHT, and in Table D.2 the filters available for CCD imaging at WHT prime focus, which are 125mm in diameter. The information in this document comes from various sources: the La Palma Technical Notes 45, 73, 75 and 90, the INT Prime Focus manual, and a List of Optical Components compiled by Chris Benn. Filter transmission curves can be found in graphical and tabular form on the ING Information pages of the Cambridge World-Wide Web server, and on the La Palma World-Wide Web server.
Filter transmission curves for ING filters

D.1 Imaging filters

Our collection consists of broad band and narrow band filters. For broad band imaging we have several sets of BVRI filters, which are not meant to leave their telescope. Our set of narrow band filters at the moment is still rather limited, except for (redshifted) Hα filters, of which we have more than 15. All filters are square, and have a length and width of more or less 50mm. Some of the larger filters do not fit into every filterwheel. There are however filterwheels to accomodate each filter.

D.1.1 Broad band filters - the Kitt Peak Interference Filters (BVRI)

These were purchased from Kitt Peak, as originally specified by J Mould. They have flat-topped profiles and are intended for use with CCD detectors (unlike earlier filter systems). Three sets exist, all are normally kept in the INT filter store cupboard. The original specifications are given below:

All filters to be 5cm × 5cm, 3mm thick, blocked to 1.1 micron, better than 75% peak transmission (except B 70%), MgF_2 coated, no pinholes, optical quality glass.

R: *Filter 7200Å= short-pass hard-coated on 3mm OG590, blocked to 1.1 micron, 75% or better peak transmission, MgF_2 coated on glass side.*

I: *Filter 9000Å= Short-pass hard-coated on 3mm RG-M9, blocked 1.1 micron, 75% or better peak transmission, MgF_2 coated on glass side.*

V: *Filter 6000Å= Short-pass hard-coated on 3mm GG 495 blocked to 1.1 micron, 75% or better peak transmission, MgF_2 coated on glass side.*

B: *Filter 4900Å= Short-pass, hard-coated on the glass substrate indicated below, blocked to 1.1 micron, 65% or better peak transmission, MgF2 Coated on glass side. Glass substrate to be cemented combination of Schott GG 385 and either Hoya GM-500 or Hoya C-500 (whichever will adequately suppress the red leak). Total thickness to be 3mm as with the other items.*

D.1.2 Broad band filters - The RGO Glass Broad Band Filters (UBVRIZ)

These filters have been made at RGO from various cemented combinations of Schott glass. R W Argyle specified the combinations which are similar to those in use at the AAT, SAAO and elsewhere. Table D.1.2 shows details of these filters. Two sets exist, and an extra spare of some of the filters.

Table D.1: **RGO Glass Filters**

Filter	**Materials**
U	1mm UG1 + 5mm $CuSO_4$ (Solid)
B	1mm GG385 +1mm BG12 + 1mm BG18 + 2mm KG3 + 2mm WG280
V	2mm GG495 + 2mm BG 18 + 2mm KG3 +1mm WG280
R	2mm KG3 + 2mm OG570 + 3mm WG280
I	3mm RG9 + 4mm WG280
Z	4mm RG850 + 3mm WG280

The WG280 is used to give uniform thickness of all filters (except U). For Z, and to some extent I, the longwave cutoff is determined by the CCD response.

D.1.3 Broadband filters - the Harris set

To replace a deteriorating set of Kitt Peak filters, 3 sets of large BVR glass colour filters were purchased in 1990 for CCD imaging.
The filters consist of cemented stacks of Schott glass, following the following recipe (see also NOAO newsletter 11,12 and 14:
B: 2mm BG12 + 2mm BG39
V: 2mm OG570 + 2mm KG3

R: 1mm BG12 + 2mm BG39 + 1mm GG385

An I band filter of the same thickness has been added to all of the Harris sets, this is refereed to as a "Harris I", although it was not defined as such by Harris. The recipe is:
I: 4mm RG9

It is thought that

- When the filter response curves are convolved with a typical CCD response, the glass filters provide a closer match to the standard Johnson B and V and the Kron-Cousins R bandpass.
- The transmission of the glass filters is comparable to that of the interference filters, and does not deteriorate with time.
- Glass filters are significantly cheaper than interference filters of the same size.

Note that the transmission in B is significantly (about 30%) lower than in Kitt Peak B.

D.1.4 Narrow band filters

At present, we have 31 narrow band filters, mostly of 50Å bandwidth, comprising a set of emission line filters and a set of redshifted Hα redshifted filters. Only one set exists and therefore the filters are shared between the telescopes. These filters were specified for a focal ratio of 4.5 which explains the difference in wavelength between the actual peak wavelength and the required peak wavelength. The original specification for the emission line filters is given below:

D.1.4.1 Specification of the narrow band filters

Unless otherwise specified the effects of an f/4.5 converging beam of light has been taken into account and the central wavelength duly reddened. A correction of +2 Angstroms has also been made to correct the central wavelength for operation at +10 degrees Celsius on the assumption that the filters will be made, tested and specified at +20 degrees Celsius.
In all cases the thickness of the filter including blocking filters should not exceed 9mm and should be the same for all filters wherever possible. Blocking in all cases should be 3000-12000 Angstroms and the tolerance on the central wavelength should be ± 3 Angstroms. The tolerance on the dimensions of each filter should be ± 0.5mm. Filters should be free from pinholes greater than 0.03mm diameter in the central 25mm diameter circle and free from pinholes greater than 0.1mm diameter elsewhere.

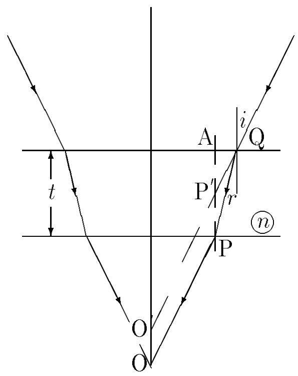

Figure 1:

The angle $\widehat{APQ}$ is the angle of refraction r,

so $sin r = \frac{AQ}{PQ}$

The angle $\widehat{AP'Q}$ is the angle of incidence i.

so $sin i = \frac{AQ}{P'Q}$

herefore $n = \frac{AQ}{P'Q} / \frac{PQ}{AQ} = \frac{PQ}{P'Q}$

If i, r are small,

$n = AP/AP'$

Figure D.1: The light path of INT or WHT prime focus near the filter

D.1.5 General Remarks

The filters marked with an asterix in Tables D.1.4.1 and D.1.4.1 have been scanned in October, 1994. No lightleaks were found, except for the [OI] λ 6306 filter. We plan to scan the rest of the interference filters in the first half of 1995, and the scans will be made available as they are done. Many filters are already old, which means that especially their edges are not as smooth as they could possibly be. To prevent stray light coming in through the edges, especially on INT-PF, some blocking off of the edges before observing is advisable.

D.1.6 Calculating of Focus Offsets

Focus offsets for a filter of thickness t can be calculated as follows:
Consider the light from a converging beam falling on a translucent plate of thickness t and refractive index n as shown in Figure D.1.

Now the change in focus $OO' = PP' = AP - AP' = AP(1 - \frac{1}{n}) = t(1 - \frac{1}{n})$
For the glass broad-band filters, the refractive index is 1.6, so the focus offset $= 0.38\,t$
For the interference filters, the values for the refractive indices are approximately 1.45 for the OII(3727Å), SII(4070Å), HeII, Hβ, OIII, HeI(5876Å), OI and NII filters, and 1.48 for the Hα, SII(6724Å), OII(7325Å), SIII(9069Åand 9532Å) and HeI(10830Å) filters. (N.B. Do not use the refractive index of the substrate, which, although of large refractive index ($\sim$2.1), is thin and enclosed in thick glass.
In practise you have to multiply the correction calulated above by $(f/f')^2$, where f is the focal length without corrector lens, and f' the focal length of

the whole system. For INT prime these values are 2.94 and 3.29, and the change in focus is $t \times (1 - \frac{1}{n}) \times 0.799$. For WHT prime these values are 2.498 and 2.81, and the change in focus is $t \times (1 - \frac{1}{n}) \times 0.790$.

D.1.7 Calculation of Central Wavelength

When interference filters are used at angles other than normal incidence, the optical path difference between the direct transmitted beam and the multiple order reflections within the cavity decreases, causing a corresponding decrease in the wavelength of peak transmission. Changes in the bandwidth and transmission characteristics are generally small (for the relatively wide passbands used here).
For angular tilts of less than 30°, the central wavelength can be calculated from the expression

$$\lambda_\theta = \frac{\lambda_0 \sqrt{n^2 - sin^2\theta}}{n}$$

where λ_0 = Central wavelength at normal incidence

λ_θ = Central wavelength at the off-normal angle, θ

and n = Effective refractive index of the total filter.

D.1.7.1 Change due to uncollimated light

Utilising the filter in uncollimated (i.e. convergent or divergent) light involves slightly more complex considerations. Here, light enters the filter at a range of angles, so that different rays undergo unequal wavelength shifts. This results in not only a central wavelength shift, but a broadening of the bandwidth and lower peak transmission.
As a rough approximation, relatively uniform beams (with full cone angles less than 20°) will undergo peak shifts of aproximately one half of that which would be predicted for a collimated beam at the maximum angle of incidence of the cone.

$$\text{Therefore, } \lambda_\theta - \lambda_0 = \frac{\lambda_0}{2}\left(\frac{\sqrt{n^2 - sin^2\theta}}{n} - 1\right)$$

The filters were specified for a focal ratio of 4.5, having a maximum angle of incidence of the cone of 6°.34, and of effective refractive index 1.6.
Substituting these values in the equation,

$$\lambda_\theta - \lambda_0 = -0.0012\lambda_0$$

The focal ratio of the INT prime focus is 3.29, which gives a maximum angle of incidence of the cone of 8°.64, so, substituting again into the equation,

$$\lambda_\theta - \lambda_0 = -0.0013\lambda_0$$

Therefore, at the INT prime focus, the central wavelength (i.e. the wavelength of peak transmission) is shifted towards shorter wavelengths by 0.06% from the specified central wavelengths. For example, for an H_α filter with specified central wavelength 6560Å, the effective central wavelength will be 6556.1Å.
Similarly for the WHT prime focus the maximum angle of incidence is $10^\circ.08$ and the central wavelength is shifted towards shorter wavelengths by 0.08%.

D.1.8 Change due to temperature

Temperature changes affect a filter's performance due to thermal expansion and contraction of the materials used to construct them. Most filters are designed and specified for operating at 23°C, and deviations from this value in the range of -60°C to +60°C will produce peak wavelength shifts approximately linear with temperature. The exact shift coefficient will depend on the particular design wavelength of the filter, and, typically, ranges between 0.2Å and 0.3Å per °C at 4000Å and 6500Å respectively. Bandwidth and peak transmission changes observed are relatively minor, of the order of 0.01Å per °C and 0.013Å per °C respectively.
The interference filters were specified for working at 10°C, so temperatures significantly different from this will affect the effective central wavelength of the filters.
For example, at an ambient temperature of 0°C, an $H\alpha$ filter with specified central wavelength 6556Åwill have an effective central wavelength of 6553Å.

D.2 125 mm diameter filters for WHT prime focus

There is one set, plus some spares, of 125mm diameter filters for use with the WHT prime focus filter wheel. These are all glass filters, and the prescriptions follow those for Harris B,V,R and I; RGO Z filters given above, plus a U prescription (1mm UG1 + 3mm BG39). This last filter has very low peak throughput (∼30%), and its use is not recommended. These filters are listed in Table D.2.

D.3 Special Purpose Filters

Tables D.3 and D.3 present a list of interference filters for use at the WHT, either for narrow-band imaging, or as order-sorting filters for instruments such as TAURUS or UES.
The filters have been scanned using the Guildford Spectrometer at RGO. Results are not presented here, but ara available on the World-Wide Web servers at Cambridge and La Palma, where they will be updated when necessary. The measurements covered a region of about 5mm in diameter close to the center of the filters. The measurements were taken with the filters

at room temperature. Note that temperature changes will affect the transmission; the central wavelength of an interference filter shifts to the red with increasing temperature, with a temperature coefficient of about 0.2 Å/degree C.

The transmission of an interference filter also depends on the angle of incidence of the light on it. This has the advantage that it is possible to fine-tune the central wavelength by tilting the filter; the central wavelength shifts to the blue with increasing tilt angle. For small tilt angles ($\theta < 10^{o}$) the effective wavelength is given by:

$$\lambda_{eff} \ = \ \lambda \times (1 - \frac{\theta^2}{28954})$$

It should however be noted that tilting an interference filter also affects the bandpass and the peak transmission; the bandpass increases and the peak transmission decreases with increasing tilt angle.

Table D.2: Summary of 50 mm filters for CCD imaging

Type	Central wavelength (nm)	Bandpass (nm)	Peak transmission (per cent)	Thickness (mm)	#	Comments
Kitt Peak broad-band glass/interference filters:						
B	440	110	80	3	3	
V	547	94	80	3	2	
V	547*	94	80	5	1	
R	646*	126	87	3	3	
I	809*	184	85	3	3	
U-band filters:						
U	360*	62	60	7	1	25mm square
U	360*	62	60	7	1	38mm square
U	360*	62	60	6	4	50mm square 1 damaged
Glass broad-band filters (Harris set):						
B	436*	107	67	4	3	
V	545*	105	88	4	3	
R	659*	149	84	4	3	
I	780	$\sim$280	95	4	3	
Glass broad-band filters (RGO set):						
B	435	106	52	7.3	2	
V	535	94	70	7.2	2	
R	645	150	81	7.2	2	
I	$\sim$840	$\sim$200	94	7.0	2	
Z	$\sim$930	$\sim$150	80	7.1	3	
Emission line interference filters:						
[OII]	373.1*	5.2	43	9	1	
[SII]	407.5	3.0	33	9	1	
HeII	469.1*	4.9	61	9	1	
Hβ	486.6*	5.1	60	9	1	
[OIII]	501.2*	5.0	61	9	1	
HeII	588.1	4.6	62	9	1	
[OI]	630.6*	5.3	70	9	1	Red leak
Hα	655.6*	6.0	70	8.2	1	Ghost
[NII]	659.0*	1.6	60	9	1	
[SII]	673.0	4.8	68	9	1	
[OII]	733.1	4.6	67	9	1	
[SIII]	907.5*	5.4	74	9	1	
[SIII]	953.9*	5.2	74	9	1	
HeII	1083.7*	11.4	52	9	1	

Table D.3: Summary of 50 mm filters for CCD imaging (continued)

Type	Central wavelength (nm)	Bandpass (nm)	Peak transmission (per cent)	Thickness (mm)	#	Comments
Redshifted Hα interference filters: - old set						
	656.3	5.3	50	6.0	1	
	660.7	5.3	54	6.0	1	
	665.2	4.9	55	7.5	1	
	670.0	5.3	58	7.5	1	
	674.2	4.7	54	7.5	1	
	678.9	5.3	60	7.5	1	
	683.5	5.0	55	6.0	1	
	687.7	5.3	58	6.0	1	
	692.5	5.0	59	6.5	1	
	697.0	5.1	57	6.0	1	
Redshifted Hα interference filters: - new set						
	656.5	4.5	56	7	1	
	656.5	6.0	53	7	1	
	659.5	4.5	51	7	1	
	662.5	4.5	56	7	1	
	665.5	4.5	56	7	1	
	668.5	4.5	56	7	1	
	671.5	4.5	56	7	1	

Table D.4: Summary of 125 mm filters for CCD imaging

Type	Central wavelength (nm)	Bandpass (nm)	Peak transmission (per cent)	Thickness (mm)	#	Comments
Glass broad-band filters (125 mm set):						
U	360	62	~30	4	1	
B	436*	107	67	4	2	
V	545*	105	88	4	2	
R	659*	149	84	4	2	
I	780	~280	95	4	2	
Z	~930	~ 150	80	7	1	

Table D.5: **TAURUS-2 filters**

Central wavelength (Å)	Bandpass (Å)	Diameter (mm)	Thickness of filter (mm)	Thickness of cell (mm)	Comments
3721	28	76			
3737	50	50	8.5		
3742	40	76			
3760	34	76			
3769	30	76			
3770	15	50	9.0		
4550	100	76.2	4.0		
4550	300	63.5	6.1	7.0	
4770	320	63.5	5.9	7.0	
4868	15	63.5	6.1		
4880	100	76.2	10.5		
4883	15	63.5	7.0		
4898	15	63.5	7.0		
4912	15	63.5	6.1		
4962	15	76.2	6.1	6.7	
4974	15	76.2	6.0	7.0	
5000	350	63.5	7.0		
5009	15	76.2	13.0		
5010	100	76.2	10.0		
5012	20	50.7	9.1	10.0	
5021	15	76.2	13.0		
5032	20	50.8	9.2	10.1	
5033	15	76.2	13.0		
5046	15	76.2	12.2		(Missing)
5052	20	50.8	9.2	10.1	
5065	15	76.2	7.0		
5072	20	50.7	10.0		
5092	20	50	10.6		(Missing)
5108	16	76			
5124	16	76			
5145	15	76.2	6.1	7.0	
5164	16	76			
5175	15	76.2	5.9	7.0	
5194	16	76			
5216	16	76			
5220	380	63.5	6.0	7.0	
5232	16	76			
5247	17	76			
5267	15	76			
5340	15	76.2	5.1	7.0	
5450	410	63.5	6.1	7.0	(Broken)

Table D.6: **TAURUS-2 filters (continued)**

Central wavelength (Å)	Bandpass (Å)	Diameter (mm)	Thickness of filter (mm)	Thickness of cell (mm)	Comments
5700	450	63.5	6.0		
5905	10	76.2	7.0		
5960	490	63.5	6.1	7.0	
6240	540	63.5	5.9	7.0	
6303	15	63.5	10.0		
6345	18	50.7	6.0		
6565	15	76.2	13.0		
6568	17	50.7	6.0		
6577	15	76.2	13.0		
6589	15	76.2	14.0		
6589	16	50.8	5.1	6.0	
6590	130	76.2	10.3		
6601	15	76.2	13.0		
6610	16	50.7	6.0		
6613	15	76.2	13.0		
6631	17	50.8	7.0		
6639	18	76			
6652	17	50.8	7.0		
6667	15	76			
6673	17	50.8	7.0		
6676	15	76			
6689	15	63.5	6.1	7.0	
6692	18	76			
6702	17	76			
6714	18	76			
6726	18	76			
6730	50	50.8	6.1	7.0	
6741	19	76			
6754	19	76			
6765	18	76			
6770	50	50.8	6.1	7.0	
6778	18	76			
6792	18	76			
6803	19	76			
6816	18	76			
6826	17	76			
6838	17	76			
6851	19	76			
6859	16	76			
6872	16	76			
6884	18	76			